Non-coding RNAs in eccentric cardiac remodeling and heart failure

Non-coding RNAs in eccentric cardiac remodeling and heart failure

“Imagination is more important than knowledge. For knowledge is limited to all we now know and understand, while imagination embraces the entire world, and all there ever will be to know and understand.”

— Albert Einstein

Cover Design: Nelleke Philippen-Odekerken
Published by: Datawyse, Universitaire Pers Maastricht
ISBN: 978 94 6159 606 2

Non-coding RNAs in eccentric cardiac remodeling and heart failure

PROEFSCHRIFT

ter verkrijging van de graad van doctor
aan de Universiteit Maastricht
op gezag van de Rector Magnificus,
Prof. dr. Rianne M. Letschert
het besluit van het College van Decanen,
in het openbaar te verdedigen
op woensdag 23 november 2016 om 10.00 uur

door

Leonne Elisabeth Philippen

Geboren te Valkenburg op 17 januari 1986

Promotor

Prof. Dr. Leon J. de Windt

Co-promotors

Dr. Paula A. Da Costa Martins
Dr. Ellen Dirkx

Assessment Committee

Prof. Dr. Marc Vooijs (chairman)
Prof. Dr. Ir. Erik Biessen
Prof. Dr. Jan de Boer
Prof. Dr. Thomas Thum, Hannover
Prof. Dr. Xander Wehrens, Houston, USA

Financial support by the Dutch Heart Foundation for the publication of this thesis is gratefully acknowledged.

The research described in this thesis was supported by a grant of the Dutch Heart Foundation (DHF1-CVON-ARENA 2011-11)

CONTENTS

CHAPTER 1

General introduction

Pathological hypertrophy is a principal risk factor for the development of heart failure and lethal arrhythmias. This has been indicated by the Framingham Heart study that demonstrated that left ventricular hypertrophy is the strongest predictor of heart failure and cardiovascular morbidity.[1] Left ventricular hypertrophy is caused by chronic pressure overload, as observed in long-standing systemic arterial hypertension or LV outflow tract obstruction. With time pressure overload causes exhaustion of the preload reserve and basal contractility becomes mismatched to the level of afterload, provoking a lower extent and speed of shortening of the LV chamber. The reduced systolic fractional shortening is associated with an inadequate cardiac output. Although the pathophysiology of pressure overload-induced hypertrophy is well-recognized in heart failure patients, current treatment heart failure regimens fail to address the underlying genetic and molecular mechanisms of this pathological condition.

Current pharmacological treatment strategies using e.g. β-blockers and ACE-inhibitors primarily addresses the symptoms of heart failure, while the prognosis of affected individuals still remains poor. As such, there is a dire need for new diagnostic as well as therapeutic approaches for treatment of this disease. More molecular, mechanistic insights will lead to the development of tailored diagnostics as well as personalized therapeutics, which would decrease the morbidity and increase life quality of heart failure patients.

Molecular mechanisms and signaling pathways underlying cardiac hypertrophy

Pathological cardiac hypertrophy as a result of pathophysiological stress signals (such as neurohormonal activation, hypertension, aortic stenosis, inflammation or cardiac injury) may be initially compensatory in terms of decreasing ventricular wall stress and maintaining pump function, but can proceed to decompensation and heart failure. Pathological remodeling is associated with fibrotic remodeling, increased rates of cardiomyocyte death, and ventricular chamber dilatation. The defining features of maladaptive hypertrophy include increased cardiomyocyte size, enhanced protein synthesis, and a higher organization of the sarcomere. At the molecular level, these changes are characterized by the activation of the fetal gene program, so called since expression patterns resemble those observed during embryonic stage. Still, the molecular mechanisms responsible for long-standing hypertrophy eventually proceeding to overt heart failure are poorly understood.

Two distinct hypertrophic phenotypes can be distinguished based on the geometry of the heart and individual cardiomyocytes: concentric cardiac hypertrophy and eccentric cardiac growth. Concentric pathological hypertrophy is characterized by a decrease in left ventricular chamber dimension and thickening of the left ventricular free wall and septum. At the cellular level, individual cardiomyocytes typically increase in size in lateral direction by adding sarcomeres in parallel. Concentric pathological hypertrophy is usually due to pressure overload (hypertension, aortic stenosis). On the other hand, eccentric pathological hypertrophy (associated with myocardial infarction, dilated cardiomyopathy) is characterized by longitudinal growth of individual cardiomyocytes with sarcomeres added in series, and can lead to ventricular wall dilatation.[2] Concentric hypertrophy can progress to eccentric hypertrophy and dilation with associated systolic heart failure, as observed in animal models with long-term pressure overload stress due to aortic banding. However, the underlying mechanisms of this transition remain poorly understood. Furthermore, whether left ventricular hypertrophy is adaptive or maladaptive remains highly controversial.[3]

A growing number of signaling mechanisms have been characterized as important pathways in the development of pathological cardiac hypertrophy. The circulating peptides Angiotensin II, Endothelin-1 (ET-1) and several Cathecholamines are able to bind to myocardial G protein Coupled Receptors (GPCRs) and play a fundamental role in cardiac hypertrophy. GPCRs are coupled to and activate three principal classes of heterotrimeric GTP-binding proteins: $G_{\alpha s}$, $G_{\alpha i}$, and $G_{\alpha q}/G_{\alpha 11}$. All G proteins consist of G_{α} and $G_{\beta\gamma}$ subunits that dissociate upon receptor activation and independently modulate the activity of downstream signaling effectors, typically Adenyl Cyclase (AC) or Phospholipase-C (PLC). The cardiac β_1-adrenergic receptors couple primarily to downstream effector $G_{\alpha s}$ and initially increase myocardial contractility and heart rate after epinephrine or nor-epinephrine stimulation, but eventually lead to cardiomyocyte hypertrophy, fibrosis and progressive impaired cardiac function.[4] The cardiac cholinergic receptors are typically coupled to $G_{\alpha i}$ and are activated by acetylcholine. The third class of receptors coupled to $G_{\alpha q}/G_{\alpha 11}$, include Angiotensin II receptor, Endothelin receptor type A, and alpha-adrenergic receptors. Activation of $G_{\alpha q}/G_{\alpha 11}$ is also a potent inducer of MAPK signaling in cardiac myocytes.[5] MAPK pathways are initiated in cardiomyocytes by GPCRs, Receptor Tyrosine Kinases (IGF-1 and fibroblast growth factor receptors), PKC, TGF-β, Cardiotrophin-1 (gp130 receptor), and by stress stimuli such as ischemia or cytotoxic agents. $G_{\alpha q}/G_{\alpha 11}$ signaling activates PLC. PLC then catalyzes the generation of diacylglycerol (DAG), which leads to PKC activation and synthesis of inositol 1,4,5-triphosphate.[6] $Ins(1,4,5)P_3$ accumulation induces intracellular Ca^{2+} release to then

activate calcineurin–NFAT or calmodulin- dependent protein kinase (CaMK), which mediate cardiomyocyte growth. Calcineurin is a calcium-dependent protein phosphatase that dephosphorylates transcription factors of the NFAT (nuclear factor of activated T cells) family. This leads to their translocation to the nucleus where NFAT forms complexes with cofactors such as GATA4 and MEF2 to activate hypertrophic target genes including ANF (Atrial Natriuretic Factor), Alpha-actinin, Beta-myosin, and TNF-α (Tumor Necrosis Factor-Alpha). The Calcineurin-NFAT pathway is one of the most well established pathways involved in pathological hypertrophy and heart failure.[7]

IL-6 family cytokine signaling via the glycoprotein 130 (gp130) co-receptor is reported to involve at least four major pathways: the janus kinase/signal transducer and activator of transcription (JAK/STAT) pathway[8], p42/44 MEK/ERK1/2 pathway[9], MEK5/ERK5[10,11], and the phosphatidylinositol 3-OH kinase (PI3K)/Akt pathway[12]. All four pathways are involved in hypertrophic and/or protective signaling in the heart in vitro and in vivo. JNK and p38 are mainly activated by stress type stimuli.[13] ERK1 and ERK2 are directly activated by the MAPK kinases MEK1 and MEK2, whereas ERK5 is activated by MEK5. JNKs are directly activated by MKK4 and MKK7, and p38 kinases are activated by MKK3 and MKK6. Cardiac-specific overexpression of MEK1 in transgenic mice resulted in specific activation of ERK1/2 and concentric hypertrophy without signs of cardiomyopathy.[14] Constitutively active MEK5 specifically activated ERK5 and induced an elongated morphology in vitro where sarcomeres were assembled in series. Stimulation with the cytokine leukemia inhibitory factor (LIF), which activates MEK5, led to a similar response. Cardiac-specific MEK5 transgenic mice showed eccentric cardiac hypertrophy that progressed to dilated cardiomyopathy and sudden death.[10] Although different IL-6 cytokines can exert similar cardioprotective effects, they induce distinct activation patterns of gp130 downstream signaling. The IL-6 family member Cardiotrophin-1 (CT-1) can induce eccentric hypertrophy in cardiomyocytes via MEK/ERK signaling, whereas Leukemia Inhibitory Factor (LIF) induces hypertrophy and protection via gp130-mediated JAK/STAT activation. It is highly likely that IL-6 family cytokines achieve their effects via a combination of these downstream signaling pathways.
Although a growing number of pathways have been unraveled, we still do not fully understand the molecular mechanisms underlying pathological hypertrophy leading to heart failure. The past decade it has become increasingly clear that not only protein-coding genes play an important role in the development of (pathological) cardiac hypertrophy, but that also non-coding RNAs (ncRNAs) are playing an interesting role in these phenomena.

The non-coding part of the genome

Today, there is a myriad of publications showing that the actual list of RNAs encoded in the genome (the transcriptome) is more complex and widespread than previously thought.[15] Up to 98% of the human genome encodes for RNA transcripts and the majority of those do not encode proteins.[16] Among these RNAs are thousands of ncRNAs, which contain regulatory information. Classification of ncRNAs is based on their length, function, biogenesis, polarity (sense or antisense), and protein-binding partners.[17]

Long ncRNAs or lncRNAs (>200 nucleotides) are relatively stable and do not undergo major processing before carrying out their normal functions.[18] On the other hand, short ncRNAs (<200 nucleotides) are processed from longer precursors.[19]

LncRNAs

LncRNAs can interact with proteins, DNA and RNA. They can be expressed in the nucleus or cytoplasmic fraction of the cell. Nuclear lncRNAs can modulate chromatin architecture by interacting with chromatin remodeling complexes to regulate the expression of genes located on the same chromosome (cis-acting) or on a distant chromosome (trans-acting). LncRNAs can be classified into four categories based on their mechanism of action: guide, scaffold, decoy, and signal.[20] Guide lncRNAs bind proteins such as chromatin modifiers and direct ribonucleoprotein complexes to specific chromatin targets.[21] This activity can cause changes in gene expression either in cis or in trans by lncRNA binding to target DNA as a RNA:DNA heteroduplex, as RNA:DNA:DNA triplex, or RNA recognition of complex surface of specific chromatin features, which cannot easily be predicted by just the lncRNA sequence itself.[22] Scaffold lncRNAs serve as central platforms for assembly of complex protein components and bind multiple effector interaction partners that could each regulate transcription positively or negatively when acting alone and lead to either transcriptional repression or activation[20]. For example, the lncRNA HOTAIR binds the Polycomb Repressive Complex 2 (PRC2), which methylates histone H3 on K27 of HOXD locus to promote gene repression.[23] This same lncRNA was later found to also bind to a second complex containing LSD1/CoREST/REST, indicating HOTAIR serves as a scaffold for at least two distinct histone modification complexes.[24] Decoy lncRNAs can serve as RNA-binding decoys or competing endogenous RNAs (ceRNAs) for microRNA target sites.[25] Signal lncRNAs are transcribed in a spatiotemporal manner to integrate developmental cues, cellular context and other diverse stimuli, thereby influencing downstream signaling in a

tissue-specific and stage-dependent manner. Several lncRNAs are able to exert more than one mechanism of action that all together are critical for their biological function.

LncRNAs in cardiovascular disease

A variety of lncRNAs have demonstrated to play a key role in cardiac development and disease (described in Chapter 2). The lncRNA Braveheart (Bvht) is a key regulator of cardiovascular lineage commitment and cardiac gene regulatory networks expression. Silencing of Bvht in mouse neonatal cardiomyocytes altered cardiac-specific gene expression and blocked their differentiation into mature cardiomyocytes. In cardiac progenitor cells, Bvht promotes expression of mesoderm progenitor 1 (Mesp1), a master gene of cardiovascular lineage commitment, by sequestering PRC2 (a writer of the repressive histone modification H3K27me3).[26] Another study showed that the lateral mesoderm-specific lncRNA Fendrr is also a regulator of heart development in the mouse. Loss of function of Fendrr caused embryonic lethality due to defective heart morphology and function. Fendrr, regulates its neighboring gene *Foxf1* by interacting with the polycomb repressive complex 2 (PRC2) and the resulting complex binds to the promoter region of *Foxf1* and Paired-like homeodomain transcription factor 2 (*Pitx2*), thereby leading to the silencing of these two genes.[27] The lncRNA MALAT1 was shown to regulate endothelial cell function and vessel growth, since silencing of MALAT1 reduces vessel growth in vivo and in vitro.[28] The lncRNA cardiac hypertrophy related factor (CHRF) functions as a sponge for miR-489, which protects against heart failure development by targeting MYD88. The overexpression of CHRF resulted in the upregulation of Myd88 expression and the activation of NF-κB system, inducing hypertrophy with sarcomere organization and increase in cell surface area.[29] Furthermore, a cluster of lncRNAs transcribed from the myosin heavy chain 7 (Myh7) locus was identified that showed transcriptional changes during cardiac development. These myosin heavy-chain-associated RNA transcripts (Myheart, or Mhrt) are abundant in the adult heart and specific to cardiac tissue.[30] Mhrt binds to the helicase domain of Brg1, a domain that is crucial for tethering Brg1 to chromatinized DNA targets, thereby preventing the interaction of Brg1 with chromatin and impairing its ability to regulate chromatin remodeling and gene expression. The Brg1– HDAC–PARP complex is activated by pathological stress and cooperatively controls the change in the α/β- MHC ratio in failing hearts. Cardiac stress in mice induced by pressure overload lead to a progressive loss of Mhrt expression in cardiomyocytes along with the development of pathological hypertrophy. Restoring Mhrt expression to the prestress level attenuated

pathological hypertrophic responses and restored cardiac function, demonstrating the cardioprotective role of Mhrt in vivo. The Mhrt-Brg1 feedback circuit is thus crucial for heart function.[30]

MicroRNAs

Short ncRNAs regulate gene expression by playing crucial roles during mRNA transcription, translation, splicing, and export.[31] Many different ncRNAs exhibit cell type specific expression[32] and localize within specific subcellular domains.[33,34] The fact that ncRNAs are regulated during development,[35] and even associated with human diseases such as cancer, diabetes, neurodegenerative and cardiovascular diseases,[36] underlines the biological relevance of these transcripts. The major classes of short ncRNAs are small interfering RNAs (siRNAs), Piwi-interacting RNAs (piRNAs), small nucleolar RNAs (snoRNAs), and microRNAs. Each class binds to proteins of the Argonaute family to regulate their targets,[37] except for snoRNAs. The siRNAs and microRNAs are generated from dsRNA precursors by RNase III ribonuclease Dicer. SiRNAs (~21 nt) are named after their ability to efficiently reconstitute silencing complexes. It was shown that antisense RNA induced sequence-specific gene silencing by base pairing with complimentary mRNA species and preventing protein translation.[38] Duplexes of siRNA are perfectly matched, unlike microRNA duplexes, which contain mismatches in the middle. In contrast, piRNAs (24-30 nt in length) are produced by a Dicer-independent mechanism and interact with a subset of Argonaute proteins related to Piwi.[39] Another class of small ncRNAs are snoRNAs (60-300 nt), which reside in the nucleolus of the cell, were synthesis and processing of cytoplasmic ribosomal RNAs (rRNAs) occurs. The main function is to guide site-specific rRNA modification.[40]

MicroRNAs are endogenous, single-stranded small RNA molecules consisting of 20-23 nucleotides, generated from endogenous hairpin transcripts. MicroRNAs are transcribed as parts of longer molecules (primary microRNAs or pri-microRNAs) by RNA polymerase II or III. The pri-microRNA is processed in the nucleus by the RNase III endonuclease Drosha and its cofactor, DiGeorge syndrome critical region 8 (DGCR8), to release an approximately 70 nucleotide long stem-loop intermediate known as precursor microRNA (pre-microRNA) (Fig 1).[41,42] The pre-microRNA is subsequently exported to the cytoplasm by the protein exportin-5 (Exp5, member of the nuclear transport receptor family), where it is further cleaved by a second RNase III enzyme, Dicer, to produce a double-stranded RNA duplex comprising the microRNA and its antisense strand microRNA*.[43] The miR maturation is completed by loading the microRNA strand of the duplex onto a protein of the Argonaute family (Ago), to generate the RNA-induced silencing complex (RISC). The microRNA

guide strand, which is complementary to the target, remains in Ago as the mature microRNA, whereas the passenger strand (microRNA*) is degraded.[44] Subsequently, the microRNA directs the RISC complex to its target mRNA and inhibits target gene expression by imperfect base pairing with sequences mainly in the 3' untranslated region (3' UTR) of the mRNA.[45] A key element in this recognition process is a perfect match in the seed sequence, nucleotides 2-8, at the 5' end of the microRNA. Interaction of microRNA with mRNA usually leads to degradation or translational inhibition with subsequent protein expression downregulation.[42] Many microRNAs are represented as families, defined by the conservation of their seed regions with many being highly conserved from nematodes to humans, whereas others are primate-specific (see miRBase).

MicroRNAs in cardiovascular disease

A number of reports have described a role for microRNAs in the developing, but also the diseased, cardiovascular system. MicroRNAs regulate embryogenesis and cell fate determination,[46] play a role in cardiovascular structure and function,[47] and are involved in cardiac development.[48] Interestingly, a hallmark in cardiac failure, is the re-expression of the fetal gene program, with an upregulation of b-type natriuretic peptide (BNP), atrial natriuretic factor (ANF), skeletal α-actin and β-myosin heavy chain (βMyHC).[49] Furthermore, microRNAs regulate genes that are important for ventricular hypertrophy and fibrosis and therefore, play a key role in congestive heart failure.[50,51] Several microRNAs, including miR-1, miR-29, miR-30, miR-133, and miR-150 are often downregulated, while others (miR-21, miR-23a, miR-125, miR-195, miR-199b, and miR-214) are upregulated in cardiac hypertrophy. This microRNA expression pattern dictates the disease state.[50,52] Knockdown of miR-133 alone is sufficient to induce significant cardiac hypertrophy, whereas miR-133 overexpression inhibits experimentally-induced hypertrophy,[53] suggesting an active role for this microRNA in inhibition of hypertrophy and making it a possible target for modulating this process.

Myocardial fibrosis leads to abnormal mechanical stiffness contributing to contractile dysfunction and progression to heart failure.[54]. MiR-21 is enriched in cardiac fibroblasts during later stages of heart failure.[55] MiR-21 targets SPRY1, leading to increased MAPK signaling, and subsequent increased fibroblast proliferation and fibrosis.

Angiogenesis prevents the myocardium from becoming hypoxic and is essential for cardiac repair after a myocardial infarction. This process requires angiogenic growth factors, such as vascular endothelial growth factor (VEGF) and fibroblast growth factor (FGF).[56] The endothelial cell-specific miR-126 regulates the response

of endothelial cells to VEGF, and plays an essential role in neoangiogenesis following myocardial infarction. This occurs through inhibition of SPRED1 and PIK3R2, which are negative regulators of the VEGF pathway.[57]

Aim of thesis

Heart failure is a complex disease, with different underlying molecular mechanisms and pathways that are not yet fully understood. NcRNAs are rapidly emerging as crucial regulators in all different kinds of disease, including heart failure. Focusing on ncRNAs in pathological cardiac hypertrophy, a well-established predictor of heart failure, the aim of this thesis is to identify novel molecular processes underlying heart failure. In this context, the aim is to identify cardiac molecular mechanisms responsible for the transition from pathological cardiac hypertrophy to heart failure.

To this aim, **Chapter 2** describes the role of ncRNAs in gene regulatory programs in cardiac development and disease. **Chapter 3** gives an overview of the current state of microRNA antisense therapeutics in cardiovascular diseases. In **Chapter 4** we describe an intriguing novel mechanism of a microRNA (miR-148a) that represents a switch between concentric and eccentric hypertrophic remodeling. In **Chapter 5** we use high throughput screens of a whole genome microRNA LNA library to identify microRNAs involved in eccentric cardiac hypertrophic remodeling. Finally, **Chapter 6** focuses on the differential expression pattern of lncRNAs in heart failure that were identified by an array on healthy mouse heart tissue and heart tissue from two different mouse models of cardiac disease. All the results and concluding remarks are discussed briefly in **Chapter 7**.

References

[*] World Health Organization, June 2014

[**] European Cardiovascular Disease Statistics 2012, June 2014

1 Levy, D., Garrison, R. J., Savage, D. D., Kannel, W. B. & Castelli, W. P. Prognostic implications of echocardiographically determined left ventricular mass in the Framingham Heart Study. The New England journal of medicine 322, 1561-1566 (1990).

2 Dorn, G. W., 2nd, Robbins, J. & Sugden, P. H. Phenotyping hypertrophy: eschew obfuscation. Circulation research 92, 1171-1175 (2003).

3 Opie, L. H., Commerford, P. J., Gersh, B. J. & Pfeffer, M. A. Controversies in ventricular remodelling. Lancet 367, 356-367 (2006).

4 Engelhardt, S., Hein, L., Wiesmann, F. & Lohse, M. J. Progressive hypertrophy and heart failure in beta1-adrenergic receptor transgenic mice. Proceedings of the National Academy of Sciences of the United States of America 96, 7059-7064 (1999).

5 Clerk, A. & Sugden, P. H. Activation of protein kinase cascades in the heart by hypertrophic G protein-coupled receptor agonists. The American journal of cardiology 83, 64H-69H (1999).

6 Rockman, H. A., Koch, W. J. & Lefkowitz, R. J. Seven-transmembrane-spanning receptors and heart function. Nature 415, 206-212 (2002).

7 Molkentin, J. D. et al. A calcineurin-dependent transcriptional pathway for cardiac hypertrophy. Cell 93, 215-228 (1998).

8 Kunisada, K. et al. Activation of gp130 transduces hypertrophic signals via STAT3 in cardiac myocytes. Circulation 98, 346-352 (1998).

9 Kodama, H. et al. Significance of ERK cascade compared with JAK/STAT and PI3-K pathway in gp130-mediated cardiac hypertrophy. American journal of physiology. Heart and circulatory physiology 279, H1635-1644 (2000).

10 Nicol, R. L. et al. Activated MEK5 induces serial assembly of sarcomeres and eccentric cardiac hypertrophy. The EMBO journal 20, 2757-2767 (2001).

11 Takahashi, N. et al. Hypertrophic responses to cardiotrophin-1 are not mediated by STAT3, but via a MEK5-ERK5 pathway in cultured cardiomyocytes. Journal of molecular and cellular cardiology 38, 185-192 (2005).

12 Kuwahara, K. et al. Cardiotrophin-1 phosphorylates akt and BAD, and prolongs cell survival via a PI3K-dependent pathway in cardiac myocytes. Journal of molecular and cellular cardiology 32, 1385-1394 (2000).

13 Sugden, P. H. & Clerk, A. "Stress-responsive" mitogen-activated protein kinases (c-Jun N-terminal kinases and p38 mitogen-activated protein kinases) in the myocardium. Circulation research 83, 345-352 (1998).

14 Bueno, O. F. et al. The MEK1-ERK1/2 signaling pathway promotes compensated cardiac hypertrophy in transgenic mice. The EMBO journal 19, 6341-6350 2000).

15 Frith, M. C., Pheasant, M. & Mattick, J. S. The amazing complexity of the human transcriptome. Eur J Hum Genet 13, 894-897 (2005).

16 Mattick, J. S. The functional genomics of noncoding RNA. Science 309, 1527-1528 (2005).

17 Farazi, T. A., Juranek, S. A. & Tuschl, T. The growing catalog of small RNAs and their association with distinct Argonaute/Piwi family members. Development 135, 1201-1214 (2008).

18 Ponting, C. P., Oliver, P. L. & Reik, W. Evolution and functions of long noncoding RNAs. Cell 136, 629-641 (2009).

19 Brosnan, C. A. & Voinnet, O. The long and the short of noncoding RNAs. Curr Opin Cell Biol 21, 416-425 (2009).

20 Wang, K. C. & Chang, H. Y. Molecular mechanisms of long noncoding RNAs. Mol Cell 43, 904-914 (2011).

21 Lee, J. T. Lessons from X-chromosome inactivation: long ncRNA as guides and tethers to the epigenome. Genes & development 23, 1831-1842 (2009).
22 Hung, T. & Chang, H. Y. Long noncoding RNA in genome regulation: prospects and mechanisms. RNA biology 7, 582-585 (2010).
23 Rinn, J. L. et al. Functional demarcation of active and silent chromatin domains in human HOX loci by noncoding RNAs. Cell 129, 1311-1323 (2007).
24 Tsai, M. C. et al. Long noncoding RNA as modular scaffold of histone modification complexes. Science 329, 689-693 (2010).
25 Cesana, M. et al. A long noncoding RNA controls muscle differentiation by functioning as a competing endogenous RNA. Cell 147, 358-369 (2011).
26 Klattenhoff, C. A. et al. Braveheart, a long noncoding RNA required for cardiovascular lineage commitment. Cell 152, 570-583 (2013).
27 Grote, P. et al. The tissue-specific lncRNA Fendrr is an essential regulator of heart and body wall development in the mouse. Developmental cell 24, 206-214 (2013).
28 Michalik, K. M. et al. Long noncoding RNA MALAT1 regulates endothelial cell function and vessel growth. Circulation research 114, 1389-1397 (2014).
29 Wang, K. et al. The long noncoding RNA CHRF regulates cardiac hypertrophy by targeting miR-489. Circulation research 114, 1377-1388 (2014).
30 Han, P. et al. A long noncoding RNA protects the heart from pathological hypertrophy. Nature 514, 102-106 (2014).
31 Mattick, J. S. The genetic signatures of noncoding RNAs. PLoS Genet 5, e1000459 (2009).
32 Ravasi, T. et al. Experimental validation of the regulated expression of large numbers of non-coding RNAs from the mouse genome. Genome Res 16, 11-19 (2006).
33 Hutchinson, J. N. et al. A screen for nuclear transcripts identifies two linked noncoding RNAs associated with SC35 splicing domains. BMC Genomics 8, 39 (2007).
34 Sunwoo, H. et al. MEN epsilon/beta nuclear-retained non-coding RNAs are up-regulated upon muscle differentiation and are essential components of paraspeckles. Genome Res 19, 347-359 (2009).
35 Dinger, M. E. et al. Long noncoding RNAs in mouse embryonic stem cell pluripotency and differentiation. Genome Res 18, 1433-1445 (2008).
36 Szymanski, M., Barciszewska, M. Z., Erdmann, V. A. & Barciszewski, J. A new frontier for molecular medicine: noncoding RNAs. Biochim Biophys Acta 1756, 65-75 (2005).
37 Hutvagner, G. & Simard, M. J. Argonaute proteins: key players in RNA silencing. Nat Rev Mol Cell Biol 9, 22-32 (2008).
38 Fire, A. et al. Potent and specific genetic interference by double-stranded RNA in Caenorhabditis elegans. Nature 391, 806-811 (1998).
39 Girard, A., Sachidanandam, R., Hannon, G. J. & Carmell, M. A. A germline-specific class of small RNAs binds mammalian Piwi proteins. Nature 442, 199-202 (2006).
40 Kiss, T. Small nucleolar RNAs: an abundant group of noncoding RNAs with diverse cellular functions. Cell 109, 145-148 (2002).
41 Gregory, R. I. et al. The Microprocessor complex mediates the genesis of microRNAs. Nature 432, 235-240 (2004).
42 Kim, V. N. MicroRNA biogenesis: coordinated cropping and dicing. Nat Rev Mol Cell Biol 6, 376-385 (2005).
43 Lund, E., Guttinger, S., Calado, A., Dahlberg, J. E. & Kutay, U. Nuclear export of microRNA precursors. Science 303, 95-98 (2004).
44 Lee, Y., Jeon, K., Lee, J. T., Kim, S. & Kim, V. N. MicroRNA maturation: stepwise processing and subcellular localization. EMBO J 21, 4663-4670 (2002).
45 Ambros, V. The functions of animal microRNAs. Nature 431, 350-355 (2004).
46 Rosa, A. & Brivanlou, A. H. microRNAs in early vertebrate development. Cell Cycle 8 (2009).

47 Elia, L. et al. Reciprocal regulation of microRNA-1 and insulin-like growth factor-1 signal transduction cascade in cardiac and skeletal muscle in physiological and pathological conditions. Circulation 120, 2377-2385 (2009).
48 Fazi, F. & Nervi, C. MicroRNA: basic mechanisms and transcriptional regulatory networks for cell fate determination. Cardiovasc Res 79, 553-561 (2008).
49 Sucharov, C., Bristow, M. R. & Port, J. D. miRNA expression in the failing human heart: functional correlates. J Mol Cell Cardiol 45, 185-192 (2008).
50 Ikeda, S. et al. Altered microRNA expression in human heart disease. Physiol Genomics 31, 367-373 (2007).
51 Thum, T., Catalucci, D. & Bauersachs, J. MicroRNAs: novel regulators in cardiac development and disease. Cardiovasc Res 79, 562-570 (2008).
52 van Rooij, E., Marshall, W. S. & Olson, E. N. Toward microRNA-based therapeutics for heart disease: the sense in antisense. Circ Res 103, 919-928 (2008).
53 Care, A. et al. MicroRNA-133 controls cardiac hypertrophy. Nat Med 13, 613-618 (2007).
54 Berk, B. C., Fujiwara, K. & Lehoux, S. ECM remodeling in hypertensive heart disease. J Clin Invest 117, 568-575 (2007).
55 Thum, T. et al. MicroRNA-21 contributes to myocardial disease by stimulating MAP kinase signalling in fibroblasts. Nature 456, 980-984 (2008).
56 Syed, I. S., Sanborn, T. A. & Rosengart, T. K. Therapeutic angiogenesis: a biologic bypass. Cardiology 101, 131-143 (2004).
57 Fish, J. E. *et al.* miR-126 regulates angiogenic signaling and vascular integrity. *Dev Cell* **15**, 272-284 (2008).

CHAPTER 2

Non-coding RNAs in control of gene regulatory programs in cardiac development and disease

Leonne E. Philippen[1], Ellen Dirkx[1,2], Paula A. da Costa-Martins[1], Leon J. De Windt[1]

[1]Department of Cardiology, CARIM School for Cardiovascular Diseases, Maastricht University, 6229 ER Maastricht, The Netherlands

[2]Department of Molecular Medicine, International Centre of Engineering and Biotechnology (ICGEB), 34149 Trieste, Italy

Published in Journal of Molecular and Cellular Cardiology, as:

Philippen LE, Dirkx E, da Costa-Martins PA, De Windt LJ. Non-coding RNA in control of gene regulatory programs in cardiac development and disease. J Mol Cell Cardiol. 89 (2015) 51–58

Abstract

Organogenesis of the vertebrate heart is a highly specialized process involving progressive specification and differentiation of distinct embryonic cardiac progenitor cell populations driven by specialized gene programming events. Likewise, the onset of pathologies in the adult heart, including cardiac hypertrophy, involves the reactivation of embryonic gene programs. In both cases, these intricate genomic events are temporally and spatially regulated by complex signaling networks and gene regulatory networks. Apart from well-established transcriptional mechanisms, increasing evidence indicates that gene programming in both the developing and the dis- eased myocardium are under epigenetic control by non-coding RNAs (ncRNAs). MicroRNAs regulate gene expression at the post-transcriptional level, and numerous studies have now established critical roles for this species of tiny RNAs in a broad range of aspects from cardiogenesis towards adult heart failure. Recent reports now also implicate the larger family of long non-coding RNAs (lncRNAs) in these processes as well. Here we discuss the involvement of these two ncRNA classes in proper cardiac development and hypertrophic disease processes of the adult myocardium.

Introduction

For decades, cardiovascular scientists have been studying the molecular processes involved in pathological hypertrophy and observed how these resemble the molecular changes during fetal cardiac development.[1] During mammalian embryogenesis, the heart is the first organ to form, and it starts when a population of mesodermal stem cells commits to the cardiogenic fate. These mesodermal progenitors form the primary heart field in the anterior mesoderm and migrate ventromedially to shape a linear heart tube.[2,3] A second population of mesodermal cardiac progenitors, known as the secondary heart field, is derived from the pharyngeal mesoderm located medial and anterior to the primary heart field. These cells migrate from behind the heart tube into the anterior and posterior poles of the heart tube as it begins to undergo rightward looping as a result of uneven growth and remodeling, leading to the formation of primitive ventricles and atria.[2,3] Maturation of the heart in higher organisms includes septation, leading to the formation of ventricles and atria, as well as valve formation and outflow vessel development. The cells in the primary heart field contribute to most of the left ventricle and part of the right and left atria. The secondary heart field contributes to the right ventricle, most of the outflow tract and part of the atria.[2,3] Cardiac neural crest cells migrating from the dorsal neural tube into the outflow tract participate in separation of the outflow tract.[4] Cardiogenesis in mammals requires exquisite control of gene expression as their distinct patterns define each region of the heart, including individual chambers and valves. Uninterrupted cardiac development is integral to organismal survival.

Studies of cardiogenesis in the simple model organism Drosophila melanogaster have defined many of the essential regulators of cardiac specification and differentiation and revealed that the cardiac gene regulatory network shows a remarkable evolutionary conservation over hundreds of millions of years. These studies, combined with many studies in vertebrate systems, have shown that the gene regulatory events and cellular movements that control cardiogenesis are temporally and spatially regulated by complex signaling networks. The formation of the vertebrate heart is controlled by intrinsic and extrinsic signals, and crosstalk occurs between myogenic transcription factors, their down- stream target genes, and upstream signaling pathways that direct cardiac cell fate, myocyte differentiation, and cardiac morphogenesis in the primary heart field and secondary heart field. Inductive signals such as bone morphogenetic protein (BMP), Notch, WNT and sonic hedgehog (SHH) in vertebrates activate a set of genes encoding transcriptional activators that are expressed in the primary and secondary heart fields. Core groups of transcription factors required for cardiogenesis include NK class of homeodomain proteins, GATA zinc-finger transcription factors, the MADS

domain transcription factor MEF2, T-box and Forkhead transcription factors, and the Hand class of basic helix–loop– helix (bHLH) factors.[5] Nkx2-5 plays a crucial role during embryonic heart development. Mice with a ventricular-restricted deletion of Nkx2-5 display no structural defects but have progressive complete heart block, and progressive cardiomyopathy.[6] Also, the calcineurin-regulated NFATc1 transcription factor is expressed in the murine endocardium and second heart field during cardiogenesis and is required for proper valve elongation and semilunar valve development.[7]

The molecular fingerprints observed during the process of heart failure resemble those observed during cardiogenesis, and therefore adult heart failure is often described as being accompanied by the reactivation of a "fetal gene program".[8] The results of the Encyclopedia of DNA Elements (ENCODE) project have widened our understanding of genomics at an unprecedented level and indicate that at least 80% of the genome is functional and is transcribed into the well-studied coding RNAs as well as a much larger quantity of non-coding, regulatory RNAs.[9-11] Roughly speaking, non-coding RNAs (ncRNAs) can be classified according to their transcript length into either small or long ncRNAs (lncRNAs), with lncRNAs arbitrarily defined as being larger than 200 nucleotides in length. The discovery of the epigenetic control of gene regulatory processes by non-coding RNAs has added a new layer of complexity to our understanding of heart function both during embryonic development and disease. Especially, microRNAs and lncRNAs have been shown to play an essential role in normal heart development and as regulators of the stress response in the adult heart (Fig. 1).

Here, we will provide an overview of ncRNA-mediated control of gene regulation of the cardiac fetal gene program in the developing embryo and how it is reiterated in the processes that contribute to hyper- trophic heart disease of the adult myocardium (Fig. 2).

MicroRNAs as regulators of the cardiac regulatory network

MicroRNAs are a class of evolutionary conserved small (18–24 nucleotide) single-stranded RNAs, encoded by the genome and affect gene expression by repressing mRNA translation and/or stability. In re- cent years, around 1000 microRNAs have been identified and function- ally characterized to certain detail. The importance of microRNA gene regulation for normal heart development and function was first underscored by generating loss of function mutations of Dicer, Drosha, Ago2 and DGCR8, four enzymes essential for microRNA biogenesis.[12-15] Cardiac specific deletion of Dicer, the enzyme required to process microRNAs into their active mature forms, resulted in embryonic lethality in mice due to cardiac failure at day E12.5.

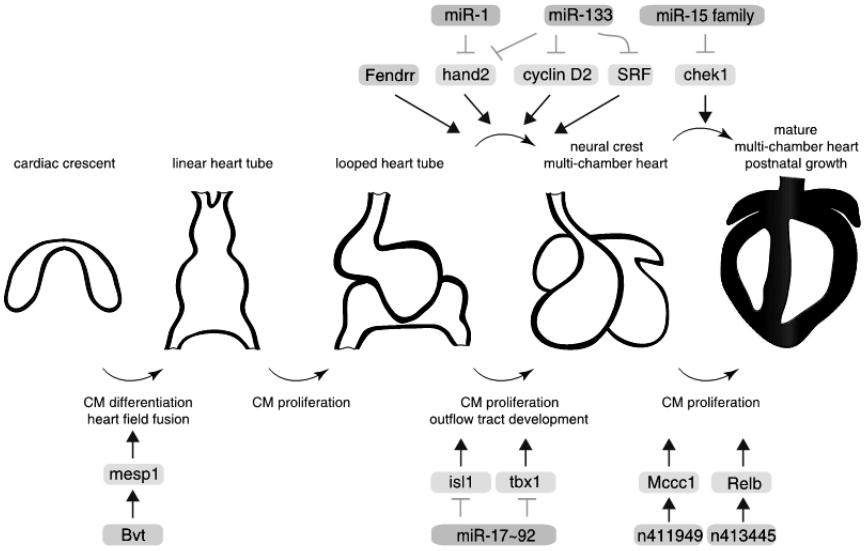

Fig. 1. Non-coding RNAs having a functional role during embryonic development. Already at early developmental stages, lncRNA Braveheart (Bvt) becomes expressed in mouse embryonic stem cells. Bvht is required for expression of core gene regulatory networks involved in defining cardiovascular cell fate and acts upstream of mesoderm posterior (MesP1), a master gene of cardiovascular lineage commitment. After cardiac looping, the miR-1-2/miR-133a-1 cluster becomes expressed, which plays a role in ventricular cardiomyocyte expansion. MiR-1 di- rectly targets Hand2, a bHLH transcription factor involved in ventricular cardiomyocyte expansion, while miR-133 directly regulates expression of serum response factor (SRF) and cyclin D2. The miR-17~92 cluster is involved in myocardial differentiation of cardiac progenitors in the secondary heart field, which is required for normal cardiac outflow tract (OFT) formation by repressing the expression of cardiac progenitor genes Isl1 and Tbx1. Fendrr is specifically expressed in nascent lateral plate mesoderm and is required for proper development of the heart and body wall in the mouse. The lncRNA n413445 regulates Relb mRNA levels, a transcription factor that is an essential component in the NFκB pathway that is important during fetal cardiac growth. Also, increased expression of the lncRNA n411949-regulated mRNA Mccc1 is of importance during embryonic growth. After birth, the miR-15 family becomes important during the neonatal period governing cardiomyocyte cell cycle withdrawal and binucleation by directly targeting chek1.

Embryos lacking Dicer in the developing heart showed pericardial edema and a poorly developed ventricular myocardium, indicating an essential role for microRNA function in cardiogenesis.[16] DGCR8 inactivation in neural crest cells using a Wnt1-Cre-mediated deletion of the floxed DGCR8 allele resulted in major cardiovascular defects at E18.5, including arteriosus, persistent truncus interrupted aortic arch, cervical aortic arch and aberrant origin of the right subclavian artery.[17] Likewise, Dicer activity is also required for normal functioning of the postnatal heart, as targeted Dicer deletion in adult mice resulted in a high incidence of sudden

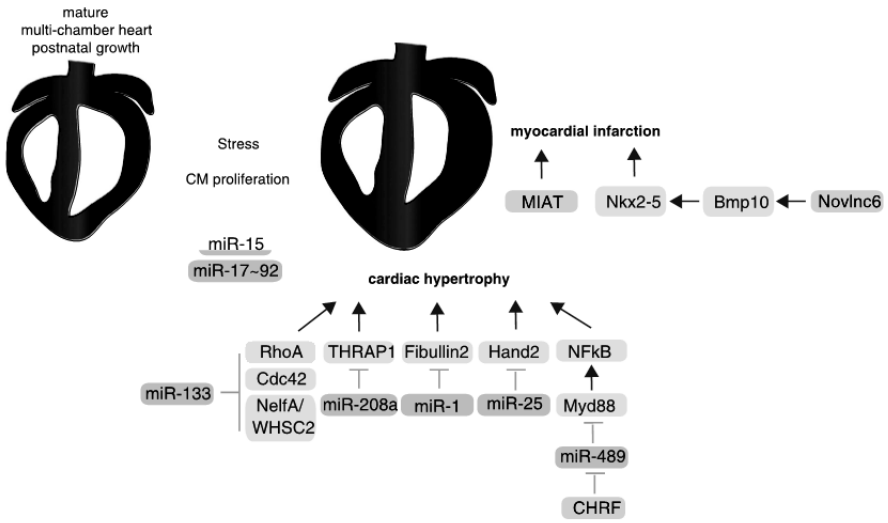

Fig. 2. The role of non-coding RNAs in adult heart disease. During processes leading to adult cardiac hypertrophy, the miR-1–133 cluster becomes downregulated. miR-1 directly targets Fibullin-2, while miR-133 repressing leads to direct derepression of RhoA, a GDP-GTP exchange protein regulating cardiac hypertrophy, Cdc42, a signal transduction kinase implicated in hypertrophy, and Nelf-A/WHSC2, a nuclear factor involved in cardiogenesis. Also, repression of miR-25 by the calcineurin/NFAT pathway leads to derepression of the transcription factor Hand2, leading to pathological cardiac remodeling. In response to cardiac stress stimuli, miR-208a expression leads to the upregulation of β-MyHC expression, thereby inducing myosin isoform switching, which is at least in part due to direct inhibition of the thyroid receptor-associated protein THRAP1, a transcriptional coregulator of the thyroid receptor, leading to increased thyroid hormone signaling. The lncRNA cardiac hypertrophy related factor (CHRF) regulates cardiac hypertrophy by directly binding to miR-489, which on its turn targets myeloid differentiation primary response gene 88 (Myd88). Overexpression of CHRF results in the upregulation of Myd88 expression and the activation of NF-κB signaling, leading to hypertrophy. Furthermore, variants in myocardial infarction associated transcript (MIAT, also known as Gomafu/RNCR2) and Novlinc6 were identified by GWAS as a risk factor for myocardial infarction and cardiac disease. Novlnc6 regulates expression of BMP10, a key signaling ligand for cardiogenesis, which maintains Nkx2.5 expression.

death, pronounced cardiac hypertrophy, ventricular fibrosis and reactivation of the fetal cardiac gene program.[18] Combined, these studies demonstrate that modification of microRNA biogenesis at specific developmental windows impacts embryonic and adult myocardial morphology and function (Table 1).

Bicistronic miR-1/miR-133 families

Among the most abundantly expressed microRNAs in the heart is miR-1. In vertebrates, members of the miR-1 (miR-1-1, miR1-2, miR- 206) and miR-133 (miR-133a-1, miR-133a-2, miR-133b) families are co-transcribed from the same bicistronic transcripts. MiR-1-1/miR- 133a-2 are clustered in an intergenic region of

Table 1
MicroRNAs regulating cardiac genes.

microRNA	Target	Function	Reference
miR-1	Hand2	Ventricular cardiomyocyte expansion	[20]
miR-1	Fibullin-2	Extracellular matrix remodeling	[24]
miR-1	IGF-1,	IGF-1 signal transduction, cardiac muscle tropism and function	[27]
miR-133a	IGF-1 receptor	Cardiomyocyte proliferation, ectopic expression of smooth muscle genes in the heart	[22]
miR-133	SRF,	Cardiac hypertrophy	[23]
miR-133	Cyclin D2	Cardiac hypertrophy	[26]
	RhoA	Cardiogenesis	
	Cdc42	β_1AR-signaling, β_1AR-induced	
	Nelf-A/WHSC2	apoptosis	
	β_1-receptor,		
	AC_{VI},		
	PKA C-β		
miR-208a	THRAP1	Thyroid hormone signaling	[31]
miR-17, miR-20a	Isl1, Tbx1	Cardiac progenitors	[34]
miR-25	Hand2	Cardiogenesis (second heart field formation)	[36]
miR-25	SERCA2	Sarcoplasmic reticulum calcium uptake	[37]
miR-195	Check1	Cell cycle checkpoint	[38]

human chromosome 20, whereas the miR-1-2/miR-133a-1 cluster is located in the antisense orientation within an intron of the Mind bomb1 (Mib1) gene on human chromosome 18. The expression of miR-1 and miR-133a is cardiac and skeletal-muscle specific, whereas the related miR-206 and miR-133b genes are restricted to skeletal muscle.[19,20] Transcription of the miR-1/miR-133 bicistronic precursors is directly regulated by serum response factor (SRF) in cardiac muscle, and by MyoD/Mef2 in skeletal muscles. In cardiomyocytes, SRF binds the enhancer regions of the miR-1/miR-133 cluster and regulates microRNA expression.[20] Gain- and loss-of function studies revealed that miR-1/miR-133 family members play crucial roles in the developing heart. Overexpression of miR-1 specifically in the developing heart resulted in decreased ventricular cardiomyocyte proliferation, ventricular wall thinning, heart failure and subsequent embryonic lethality at E13.5.[20] In line, introduction of miR-1 into developing Xenopus embryos interfered with heart development and injection of miR-133 in embryos resulted in highly disorganized cardiac tissue, absence of cardiac looping or chamber formation, revealing that correct temporal expression and amounts of both miR-1 and miR-133 are required for proper skeletal muscle and heart development.[19]

One of the validated targets of miR-1 is Hand2, a bHLH transcription factor involved in ventricular cardiomyocyte expansion.[20] Interestingly, targeted gene deletion of Hand2 in mouse embryos resulted in embryonic lethality at embryonic day 10.5 from heart failure, similarly to miR-1 transgenic mice.[21] Furthermore, targeted deletion of miR-1-2 revealed that miR-1-2 regulates cardiac morphogenesis, electrical conduction, and cardiac cell-cycle control.[16] Mice lacking either miR-133a-1 or miR- 133a-2 do not display any overt developmental phenotype, whereas deletion of both microRNAs causes lethal ventricular–septal defects in approximately half of double-mutant embryos or neonates. The miR-133a double-mutant mice that survive to adulthood succumb to dilated cardio- myopathy by 5–6 months of age and heart failure. The absence of miR- 133a expression is associated with aberrant cardiomyocyte proliferation and ectopic expression of smooth muscle

Table 2
LncRNAs in cardiac gene regulatory networks.

LncRNA	Target	Function	Reference
Braveheart	Mesp1	Cardiovascular lineage commitment	[42]
Fendrr	PRC2 and TrxG/MLL complexes	Histone modification	[43]
SRA	MyoD	Skeletal myogenesis	[45]
Myheart	Brg1	Chromatin remodeling, α/β-MHC ratio control	[47]
Novlnc6	Bmp10	Cardiogenesis, regulating Nkx2.5 expression	[50]
MIAT	Unknown	Myocardial infarction	[51]
n413445	Relb	Cardiogenesis (transcription factor in NFκB pathway)	[52]
n411949	Mccc1	Sensor of free leucine levels	
CHRF	miR-489	Cardiac hypertrophy (via regulation of Myd88 and NFκB)	[56]

genes in the heart. These abnormalities were proposed to be due to direct targeting of SRF and cyclin D2, both of which contain functional binding sites for miR-133a in their 3'- UTRs. These findings have established critical and redundant roles for miR-133a-1 and miR-133a-2 in orchestrating cardiac development, gene expression, and function.[22]

Also in the adult heart, these microRNA clusters fulfill a critical role since altered expression of miR-1 and miR-133 is associated with heart failure both in rodents and humans.[23] Sequestering endogenous miR-133 with a targeted 3'UTR decoy resulted in marked myocyte hyper- trophy, significantly increased protein synthesis, increased fetal gene expression, and perinuclear expression of atrial natriuretic factor. In cultured neonatal cardiomyocytes, overexpression of miR-1 or miR-133 inhibited phenylephrine and endothelin-1-induced cardiomyocyte hypertrophy. In line, in vivo inhibition of miR-133, using an antagomir treatment, caused marked cardiac hypertrophy by means of derepressing RhoA, a GDP-GTP exchange protein regulating cardiac hypertrophy, Cdc42, a signal transduction kinase implicated in hypertrophy, and Nelf-A/WHSC2, a nuclear factor involved in cardiogenesis. This significant myocardial hypertrophy was associated with re-induction of the fetal gene program.[23] Cardiac delivery of AAV9-miR-1 in male Sprague-Dawley rats subjected to aortic stenosis, reversed hypertrophic remodeling, reduced cardiac fibrosis and apoptosis and improved calcium handling. One of the validated targets in this study was Fibullin-2, a secreted protein implicated in extracellular matrix remodeling.[24] In line, SERCA2a gene therapy, which improves cardiac function both in animals and humans with heart failure, was shown to restore cardiac miR-1 expression via an Akt/Foxo3-dependent pathway, indicating that miR-1 expression is critical for proper cardiac function.[25] Recently, miR-133 was shown to target multiple components of the β_1AR-signaling cascade, thereby protecting cardiomyocytes from β_1AR-induced apoptosis. Among the direct targets of miR-133 are the β_1-receptor itself and its downstream effectors adenylate cyclase VI (AC_{VI}) and PKA C-β, a key modulator of the β_1AR-mediated accumulation of the second messenger cAMP. Using a cardiac-specific TetON-miR-133 inducible transgenic mouse model, the authors showed that after pressure overload TetON-miR-133 inducible transgenic mice maintained cardiac performance and displayed attenuated apoptosis and decreased fibrosis compared to control mice.[26] Another

receptor pathway that is targeted by members of this cluster is the insulin-like growth factor 1 (IGF-1)/insulin-like growth factor 1 receptor signal transduction pathway, a key regulator of cardiac muscle tropism and function. Both IGF-1 and IGF-1 receptor are direct targets of miR-1. Moreover, Foxo3a, a component of the IGF-1 signaling pathway, transcriptionally regulates miR-1 expression levels, providing a feedback loop between miR-1 expression and IGF-1 signaling. In line, miR-1 expression levels in myocardial biopsies from acromegalic patients, where IGF-1 is overproduced after aberrant synthesis of growth hormone, are inversely correlated with cardiac mass and wall thickness.[27]

MyomiRs: miR-208a, miR-208b and miR-499 In the rodent heart, α-MyHC (encoded by the Myh6 gene), a fast

ATPase, is highly expressed in adulthood, whereas β-MyHC (encoded by the adjacent Myh7 gene), a slow ATPase, is the predominant myosin isoform in cardiomyocytes in the embryonic stage.[28] The relative expression of these two myosin isoforms is correlated with the contractile velocity of cardiac muscle. Several pathologic stimuli can cause a shift in the MyHC composition of the rodent ventricle from α-MyHC to β-MyHC. The opposite holds true in humans, where β-MyHC is the pre- dominant cardiac myosin isoform expressed.[29] Interestingly, these muscle-specific myosin genes harbor a family of microRNAs, called myomiRs, within their introns. MyomiRs consist of miR-208a, miR- 208b, and miR-499, encoded within the introns of Myh6, Myh7 and Myh7b genes, respectively. The myomiRs are highly conserved and share similar sequence identity, and the expression of the myomiRs parallels the expression of their respective host genes during development.[30] Targeted deletion of miR-208a resulted in ectopic activation of the fast skeletal muscle gene expression within the heart, and mice were protected against cardiac hypertrophy and myocardial fibrosis. Mice lacking miR-208a fail to upregulate β-MyHC expression in response to cardiac stress stimuli, at least in part due to direct inhibition of the thyroid receptor–associated protein THRAP1, a transcriptional coregulator of the thyroid receptor, leading to increased thyroid hormone signaling, thereby regulating myosin isoform switching. Given that miR-208a null mice are viable, it indicates that miR-208a is not required for development of the heart and embryogenesis.[31] Inhibition of miR-208a in adult mouse hearts by systemic administration of an antimir against miR-208a prevented pathological myosin switches and cardiac remodeling upon stress, resulting in improved cardiac function and survival.[32] Furthermore, miR-208a regulates the expression of the two slow myosins and their intronic microRNAs, Myh7/miR-208b and Myh7b/miR-499, as deletion of miR-208a abolishes the expression of miR-208b and miR-499. MiR-208b and miR-499 display functional redundancy, and have crucial roles in specifying muscle fiber identity by activating slow and repressing fast myofiber gene programs.[30]

The miR-17~92 cluster The miR-17~92 cluster consists of six microRNAs: miR-17, miR-18a,

miR-19a, miR-20a, miR-19b, and miR-92a. These six microRNAs belong to four microRNA families and are generated from a common primary transcript. The miR-17~92 cluster was initially reported as a human oncogene, named Oncomir-1 and is located on human chromosome 13. This microRNA cluster has two paralogs, the miR-106b~25 cluster and the miR-106a~363 cluster. The two paralogs are located at different genetic loci, which provide an extra layer of redundancy among the four microRNA families. The miR-106b~25 cluster consists of miR-106b, miR-93 and miR-25 and is located in the 13th intron of the human MCM7 gene. On the other hand, the miR-106a~363 cluster maps to chromosome X in both humans and mice. The miR-106a~363 and miR-106b~25 clusters contain microRNAs that are highly similar, and in some cases even identical, to those encoded by the miR-17~92 cluster. This indicates that they probably have overlapping functions by regulating a similar set of direct downstream targets[33] and most likely originated from a series of ancient evolutionary genetic duplication events. The broad conservation of sequence across species implies the importance of those microRNAs during vertebrate development.[33]

Loss of function studies revealed a critical role for the miR-17~92 cluster in heart development. MiR-17~92 mutants die shortly after birth and display ventricular septal defects and lung hypoplasia. In contrast, loss of the paralogous miR-106a~93 and miR-106b~25 clusters does not affect organismal viability and these mutants do not display an obvious phenotype. This is most likely due to functional redundancy with the miR-17~92 cluster. However, miR-17~92/miR-106b~25 double null embryos and miR-17~92/miR-106b~25/miR-106a~363 triple null embryos die at mid-gestation, before E15, and exhibit a much more severe phenotype compared to embryos lacking miR-17~92 alone. At E13.5 and E14.5 in the developing mouse embryo, miR-17~92/miR-106b~25 double null embryos showed edema and vascular congestion associated with severe cardiac developmental abnormalities including defective ventricular and atrial septation and thinning of the ventricles.[33]
Furthermore, the miR-17~92 cluster is involved in myocardial differentiation of cardiac progenitors in the secondary heart field, which is required for normal cardiac outflow tract (OFT) formation. The cardiac OFT is a developmentally complex structure that is often defective in patients with congenital heart disease. The bone morphogenetic proteins Bmp2 and Bmp4, direct OFT myocardial differentiation via regulation of the miR-17~92 cluster. The miR-17~92 cluster in its turn represses the expression of cardiac progenitor genes Isl1 and Tbx1.[34]
Gain-of-function studies have revealed a role for the miR-17~92 cluster in organ size regulation. Global miR-17 overexpression leads to organ growth retardation,

including the heart. In contrast, overexpression of the entire miR-17~92 cluster provokes cardiomyocyte hypertrophy and hyperplasia. Recently, transgenic overexpression of the miR-17~92 cluster in cardiomyocytes was shown to be sufficient to induce cardiomyocyte proliferation in embryonic, postnatal, and adult hearts. Moreover, miR-17~92 cluster overexpression in adult cardiomyocytes protects the heart from myocardial infarction-induced injury.[35]

Inhibition of miR-25 in vivo by 4 weeks of antagomir treatment in adult mice induced cardiac dilatation accompanied by decreased cardiac function.[36] This phenotype was even more severe in a pressure overload-induced heart failure model, due to the miR-25 mediated derepression of the transcription factor, Hand2. Hand2 is involved in the formation of the second heart field of the developing heart, and becomes re-activated in the adult failing heart by this microRNA mechanism. In line, Hand2 overexpression in mice leads to decreased cardiac function and dilatation, while conditional Hand2 gene deletion proved protective against pressure overload-induced heart failure.[36] A contrasting publication found that inhibition of miR-25 by antagomir treatment in a five-month long pressure overload study in mice increased cardiac function by derepression of SERCA2a. Further research is needed to clarify this contradiction and obtain a more integrative understanding of the functional role of the miR-106b~25 and miR-106a~363 clusters in the adult heart.[37]

The miR-15 family

By comparing microRNA expression profiles in mouse cardiac ventricles at P1 and P10, multiple miR-15 family members were identified as regulators of postnatal cardiomyocyte mitotic arrest. The miR-15 family consists of miR-15a, miR-15b, miR-16, miR-195, and miR-497. Family member miR-195 displayed a 6-fold increase in expression at P10 compared to P1. Overexpression of miR-195 in the developing heart using a transgenic mouse model caused congenital heart abnormalities associated with premature cell cycle arrest. The miR-15 family member miR-195 directly targets cell cycle gene checkpoint kinase 1 (Chek1). Inhibition of the miR-15 family in neonatal mice with locked nucleic acid-modified anti-microRNAs was associated with an increased number of mitotic cardiomyocytes and derepression of Chek1. These results suggest that the miR-15 family is important during the neonatal period governing cardiomyocyte cell cycle withdrawal and binucleation.[38] The neonatal mammalian heart still has regenerative capacity after myocardial infarction through proliferation of preexisting cardiomyocytes. The miR-15 family modulates neonatal heart regeneration by inhibiting postnatal cardiomyocyte proliferation. Inhibition of the miR-15 family from an early postnatal age until adulthood increased myocyte proliferation in the adult heart and improved left ventricular systolic function after adult myocardial infarction in mice.[39]

LncRNAs: adding layers of complexity to cardiac gene regulation

Most lncRNAs are RNA polymerase II transcribed, 5'-capped, alternatively spliced and polyadenylated. They are less conserved than microRNAs and only a small subset show evolutionary conservation of the primary sequence. Yet, lncRNAs do show tissue and cell type-specific expression, indicating that their expression must be tightly controlled. LncRNAs are distinguished by a diversity of molecular functions derived from their ability to act as scaffolds for protein–protein interactions and/or chaperones that direct protein complexes to specific RNA or DNA sequences. One of the first identified mechanisms for lncRNA action is imprinting. For imprinted genes, the expression occurs from only one allele, instead of both parental alleles being expressed equally. Secondly, LncRNAs can act both as transcriptional activators and repressors by interacting with epigenetic modifying protein complexes, regulate expression of genes located in close proximity (cis-acting) or target distant transcriptional activators or repressors (trans-acting). LncRNAs can also act as molecular decoys. In this case, the lncRNA can 'sponge' protein-based factors such as transcription factors away from chromatin or sponge tiny RNA species.[40] Finally, lncRNAs can act as molecular guides by directing ribonucleoprotein complexes to specific chromatin targets.[41] LncRNAs may serve as central platforms for assembly of complex protein components. Some lncRNAs possess distinct domains that bind different protein factors, bringing transcriptional activators or repressors together in both time and space (Table 2).

Since many cardiac diseases are heritable, series of genome-wide association studies (GWAS) have been performed to identify new disease loci for cardiovascular diseases. Remarkably, 93% of the identified disease loci fall outside protein-coding regions and could influence the expression or function of non-coding RNAs. In line, single nucleotide polymorphisms (SNPs) associated with cardiac disease have been identified to locate within lncRNA encoding genes[42], suggesting that lncRNAs may have more causal roles in disease, which justifies an in-depth analysis of individual lncRNA function.

The more detailed characterization of individual lncRNAs in development and disease of the cardiovascular system is only starting to emerge. In 2013, a hallmark publication demonstrated that lncRNA Braveheart (Bvht, AK143260) is required for cardiovascular lineage commitment. Bvht is expressed at early developmental stages in mouse embryonic stem cells (mESCs) and is also highly expressed in the adult mouse heart. Depletion of Bvht in mESCs impaired formation of cardiomyocytes in multiple in vitro differentiation assays. Bvht depletion in primary murine neonatal ventricular cardiomyocyte cultures resulted in unevenly distributed and irregularly bundled myofibrils after 5 days in culture compared to control cells and significantly smaller overall cardiomyocyte cell surface area, indicating that neonatal cardiomyocyte structure is disrupted in Bvht-depleted cells. Bvht is required for expression of core gene regulatory networks involved in defining cardiovascular cell fate and acts upstream of mesoderm posterior (MesP1), a master

gene of cardiovascular lineage commitment.[43] Furthermore, the authors show that also the downstream targets of MesP1 require upstream Bvht activation, including the core cardiac transcription factors Gata4, Gata6, Hand1, Hand2, Tbx2, and Nkx2.5, among others.

Another lncRNA, Fendrr (Foxf1 adjacent non-coding developmental regulatory RNA; ENSMUSG00000097336), is specifically expressed in nascent lateral plate mesoderm and is required for proper development of the heart and body wall in the mouse. Fendrr-deficient mice die around E13.5 due to abnormal functioning of the heart. Fendrr acts by modifying the chromatin signatures of genes involved in the formation and differentiation of the lateral mesoderm lineage through binding to both the PRC2 and TrxG/MLL complexes.[44] Expression of the transcription factors Nkx2.5 and Gata6 was increased upon cardiac Fendrr deletion, accompanied by corresponding H3K4me3 changes in their promoter regions, while expression of other core transcription factors, such as Gata4 or Tbx5 was not affected.

A third example of lncRNAs involved in cardiac development is the lncRNA SRA. The steroid receptor RNA activator 1 (SRA1) gene generates both steroid receptor RNA activator protein (SRAP) as well as several non-coding SRA transcripts, depending on alternative transcription start site usage and alternative splicing.[45] The lncRNA SRA binds to MyoD, which regulates skeletal myogenesis. In vitro and in vivo experiments showed that SRA is a coactivator of MyoD.[46] SRA is present in a 600-kb region of linkage disequilibrium (LD) associated with human dilated cardiomyopathy on 5q31.2-3, harboring multiple genes, in three independent Caucasian populations. Knockdown of SRA1 by Morpholino antisense in zebrafish resulted in impaired cardiac function phenotypes, with impaired contractility predominantly in ventricular heart chambers at 72 h post fertilization.[47]

Recently, a cluster of cardiac-specific lncRNA transcripts from Myh7 loci was identified and named myosin heavy-chain-associated RNA transcripts (Myheart, or Mhrt). Mhrt antagonizes the function of Brg1, a chromatin-remodeling factor that is activated by stress to trigger aberrant gene expression and cardiac myopathy.[48] The ATP-dependent Brg1– HDAC–PARP complex cooperatively controls the change in the α/β- MHC ratio in failing hearts.[49] These lncRNAs, which are splice isoforms of Mhrt, have a tight correlation with the Myh6/Myh7 ratio during cardiac development and in hypertrophic hearts. Cardiac stress in mice induced by pressure overload lead to a progressive loss of Mhrt expression in cardiomyocytes along with the development of pathological hypertrophy. Restoring Mhrt expression to the prestress level attenuated pathological hypertrophic responses and restored cardiac function, demonstrating the cardioprotective role of Mhrt in vivo. Mhrt directly binds to the helicase domain of Brg1, a domain that is crucial for tethering Brg1 to chromatinized DNA targets, enabling a competitive inhibition mechanism by which Mhrt sequesters Brg1 from its genomic DNA targets to prevent chromatin remodeling and gene regulation by Brg1. This negative feedback circuit between a lncRNA and the Brg1 chromatin remodeling complex is thus crucial for heart function.[48]

Likewise, lncRNA profiling of the cardiac transcriptome after myocardial infarction was performed to identify novel heart-specific lncRNAs with potential roles in both cardiac development and pathological cardiac remodeling. These novel lncRNAs also have human orthologues, which are dysregulated during disease. The novel lncRNA Novlnc6 was significantly downregulated in human dilated cardiomyopathy. Novlnc6 is associated with a bonafide cardiac developmental enhancer and modulates the expression of Nkx2.5, a master cardiac transcription factor, critical for the modulation of gene programs involved in cardiogenic differentiation, maturation, and homeostasis. Furthermore, knockdown of Novlnc6 by GapmeRs in cardiomyocytes resulted in concomitant downregulation of BMP10, a key signaling ligand for cardiogenesis, which maintains Nkx2.5 expression.[50]

Additionally, variants in myocardial infarction associated transcript (MIAT, also known as Gomafu/RNCR2) were identified by GWAS as a risk factor for myocardial infarction. Six single nucleotide polymorphisms (SNPs) in MIAT showed markedly significant association with myocardial infarction.[51] To date, the molecular mechanism by which MIAT causes cardiac disease is still unknown.

By RNA sequencing of embryonic (E14), normal adult and hypertrophied adult hearts, Matkovich et al. identified 157 lncRNAs that were differentially expressed in embryonic hearts compared with adults, but relatively few fetal lncRNAs that showed altered expression in adult-onset cardiac hypertrophy. Only 17 lncRNAs were differentially expressed in hypertrophied hearts, 13 of which observed in embryonic hearts. By analyzing neighboring mRNAs within 10 kb of dynamically expressed lncRNAs, the authors revealed that 22 mRNAs were concordantly and 11 were reciprocally regulated. Using lncRNA knockdown in C2C12 myoblasts, the functional reciprocal interactions between mRNAs Mccc1 and Relb, and lncRNAs n411949 and n413445, respectively, were validated. LncRNA n413445 and n411949 are highly expressed in the embryonic heart but show quite low expression in adult hearts, with no apparent change in the pressure overloaded heart. The lncRNA n413445 regulates Relb mRNA levels, a transcription factor that is an essential component in the NFκB pathway that is important during fetal cardiac growth. An increase of the lncRNA n411949-regulated mRNA Mccc1 during embryonic growth may be of key importance for sensing free leucine levels and thus the availability of branched-chain amino acids for anabolic signaling in muscle.[52]

In order to determine the expression profile of myocardial lncRNAs and their potential role in early stage reperfusion, Liu and colleagues performed microarray analysis and validated the results using polymerase chain reaction (PCR). They identified 64 lncRNAs that were up-regulated and 87 that were down-regulated, while 50 mRNAs were up-regulated and 60 down-regulated in infarct region at all reperfusion sampled. Target gene-related pathway analysis showed significant changes in cytokine–cytokine receptor interaction, the chemokine signaling pathway and nucleotide oligomerization domain (NOD)-like receptor signaling pathway which have a close relationship with myocardial ischemia/reperfusion

injury (MI/RI). The co-expressed network of 10 highly-dysregulated lncRNAs showed that ENSMUST00000166777 and AK156124 are in closest relation with coding RNAs (mRNAs). However, ENSMUST00000170410 and uc007prv.1 have the slightest relevance to coding RNAs (mRNAs). Six mRNAs (CXCL1, CCL9, CXCL12, EDA, TNFAIP3 and BIRC3) were targeted by corresponding lncRNAs, all of which have been linked to ischemia/reperfusion injury.[53]

Deep sequencing of RNA isolated from paired nonischemic (NICM; n = 8) and ischemic (ICM; n = 8) human failing LV samples collected before and after LVAD and from nonfailing human LV (n = 8) revealed high abundance of mRNA (37%) and lncRNA (71%) of mitochondrial origin. The analysis identified 18,480 lncRNAs in human LV. Among the 679 (ICM) and 570 (NICM) lncRNAs differentially expressed with heart failure, ≈10% are improved or normalized with LVAD. Furthermore, the expression signature of lncRNAs, but not microRNAs or mRNAs, distinguished ICM from NICM in this study, suggesting a predominant role for lncRNAs in the pathogenesis of heart failure and in reverse remodeling by mechanical support.[54]
Recently, it was shown that the lncRNA cardiac hypertrophy related factor (CHRF) regulates cardiac hypertrophy by directly binding to miR-489, acting as a functional sponge to regulate anti-hypertrophic miR-489 expression and activity. The responsible downstream target of miR-489 appeared to be myeloid differentiation primary response gene 88 (Myd88). The overexpression of CHRF resulted in the upregulation of Myd88 expression and the activation of NF-κB signaling, leading to hypertrophy.[55]

Conclusions and perspectives

Studies on two major species of ncRNAs, microRNAs and lncRNAs, have changed our understanding about the epigenetic control of gene regulatory programs and reveal a vast overlap between the regulation of gene programs in the developing heart and adult-onset heart disease. As such, the emerging picture also demonstrates that the heart seems sensitive to relatively subtle changes in gene modifier effects. The ability of microRNAs to fine-tune gene expression programs and act as powerful stress regulators suggests their central role in many facets of cardiac biology. Since one single microRNA could possibly modulate dozens of target genes at once, and one gene could be targeted by multiple microRNAs, methods aimed to better understand the integration of microRNA control within gene regulatory networks are clearly necessary for the field. Our collective understanding of how these tiny post-transcriptional gene regulators function in cellular networks provides new molecular horizons for cures or therapies to a variety of human heart diseases, and the first examples of microRNA-based proof-of-concept therapies in small and larger animal models are well underway. Manipulation of individual microRNAs by

chemically modified oligonucleotides or adeno-associated viral vectors have therapeutic potential in animal models for cardiovascular diseases. A major translational challenge will remain in understanding the pharmacology/toxicology aspects, correct dosing and correct delivery to the site of action of these fundamentally new therapeutic entities. As for lncRNAs, literally thousands of putative lncRNAs have been identified in mammalian species including humans, but only dozens have been experimentally studied in sufficient detail so far. The relatively poor evolutionary conservation of lncRNAs still poses a barrier to translate their function from animal models to humans. Likely, the identification of evolutionary conserved functional domains in lncRNAs will provide relief to latter obstacle and possibly allow therapeutic manipulation by antisense oligonucleotide-based cardiac therapy. Eventually, the detailed characterization of ncRNAs with essential roles in the developing or the diseased heart will undoubtedly lead to a richer understanding of the complex gene regulatory networks that drive proper cardiac development and maintain healthy myocardial function.

Conflict of interest disclosures

L.E.P.: none. E.D.: none. P.D.C.M.: none. L.J.D.W.: none.

Acknowledgments

E.D. was supported by a Long Term Fellowship of the EMBO Organization (ALTF 848-2013), Marie Curie actions Intra-European fellowship (PIEF-GA-2013-627539) and VENI fellowship (016.156.016) from the Netherlands Organization for Health Research and Development (ZonMW). P.D.C.M. was supported by a Leducq Career Development Award, the Dutch Heart Foundation grant NHS2010B261 and a NWO MEERVOUD grant. L.D.W. acknowledges support from the Netherlands CardioVascular Research Initiative: the Dutch Heart Foundation, Dutch Federation of University Medical Centers, the Netherlands Organization for Health Research and Development (ZonMW) and the Royal Netherlands Academy of Sciences. L.D.W. was further supported by grant 311549 from the European Research Council (ERC).

References

1 Thum, T. *et al.* MicroRNAs in the human heart: a clue to fetal gene reprogramming in heart failure. *Circulation* **116**, 258-267 (2007).

2 Srivastava, D. Making or breaking the heart: from lineage determination to morphogenesis. *Cell* **126**, 1037-1048 (2006).

3 Buckingham, M., Meilhac, S. & Zaffran, S. Building the mammalian heart from two sources of myocardial cells. *Nat Rev Genet* **6**, 826-835 (2005).

4 Kirby, M. L. & Waldo, K. L. Neural crest and cardiovascular patterning. *Circ Res* **77**, 211-215 (1995).

5 Olson, E. N. Gene regulatory networks in the evolution and development of the heart. *Science* **313**, 1922-1927 (2006).

6 Pashmforoush, M. *et al.* Nkx2-5 pathways and congenital heart disease; loss of ventricular myocyte lineage specification leads to progressive cardiomyopathy and complete heart block. *Cell* **117**, 373-386 (2004).

7 Lin, C. Y. *et al.* The secondary heart field is a new site of calcineurin/Nfatc1 signaling for semilunar valve development. *J Mol Cell Cardiol* **52**, 1096-1102 (2012).

8 Dirkx, E., da Costa Martins, P. A. & De Windt, L. J. Regulation of fetal gene expression in heart failure. *Biochim Biophys Acta* **1832**, 2414-2424 (2013).

9 Carninci, P. *et al.* The transcriptional landscape of the mammalian genome. *Science* **309**, 1559-1563 (2005).

10 Kapranov, P. *et al.* RNA maps reveal new RNA classes and a possible function for pervasive transcription. *Science* **316**, 1484-1488 (2007).

11 Consortium, E. P. An integrated encyclopedia of DNA elements in the human genome. *Nature* **489**, 57-74 (2012).

12 Bernstein, E. *et al.* Dicer is essential for mouse development. *Nat Genet* **35**, 215-217 (2003).

13 Wang, Y., Medvid, R., Melton, C., Jaenisch, R. & Blelloch, R. DGCR8 is essential for microRNA biogenesis and silencing of embryonic stem cell self-renewal. *Nat Genet* **39**, 380-385 (2007).

14 Fukuda, T. *et al.* DEAD-box RNA helicase subunits of the Drosha complex are required for processing of rRNA and a subset of microRNAs. *Nat Cell Biol* **9**, 604-611 (2007).

15 Morita, S. *et al.* One Argonaute family member, Eif2c2 (Ago2), is essential for development and appears not to be involved in DNA methylation. *Genomics* **89**, 687-696 (2007).

16 Zhao, Y. *et al.* Dysregulation of cardiogenesis, cardiac conduction, and cell cycle in mice lacking miRNA-1-2. *Cell* **129**, 303-317 (2007).

17 Chapnik, E., Sasson, V., Blelloch, R. & Hornstein, E. Dgcr8 controls neural crest cells survival in cardiovascular development. *Dev Biol* **362**, 50-56 (2012).

18 da Costa Martins, P. A. *et al.* Conditional dicer gene deletion in the postnatal myocardium provokes spontaneous cardiac remodeling. *Circulation* **118**, 1567-1576 (2008).

19 Chen, J. F. *et al.* The role of microRNA-1 and microRNA-133 in skeletal muscle proliferation and differentiation. *Nat Genet* **38**, 228-233 (2006).

20 Zhao, Y., Samal, E. & Srivastava, D. Serum response factor regulates a muscle-specific microRNA that targets Hand2 during cardiogenesis. *Nature* **436**, 214-220 (2005).

21 Srivastava, D. *et al.* Regulation of cardiac mesodermal and neural crest development by the bHLH transcription factor, dHAND. *Nat Genet* **16**, 154-160 (1997).

22 Liu, N. *et al.* microRNA-133a regulates cardiomyocyte proliferation and suppresses smooth muscle gene expression in the heart. *Genes Dev* **22**, 3242-3254 (2008).

23 Care, A. *et al.* MicroRNA-133 controls cardiac hypertrophy. *Nat Med* **13**, 613-618 (2007).

24 Karakikes, I. *et al.* Therapeutic cardiac-targeted delivery of miR-1 reverses pressure overload-induced cardiac hypertrophy and attenuates pathological remodeling. *J Am Heart Assoc* **2**, e000078 (2013).

25 Kumarswamy, R. *et al.* SERCA2a gene therapy restores microRNA-1 expression in heart failure via an Akt/FoxO3A-dependent pathway. *Eur Heart J* **33**, 1067-1075 (2012).

26 Castaldi, A. *et al.* MicroRNA-133 modulates the beta1-adrenergic receptor transduction cascade. *Circ Res* **115**, 273-283 (2014).
27 Elia, L. *et al.* Reciprocal regulation of microRNA-1 and insulin-like growth factor-1 signal transduction cascade in cardiac and skeletal muscle in physiological and pathological conditions. *Circulation* **120**, 2377-2385 (2009).
28 Lompre, A. M., Nadal-Ginard, B. & Mahdavi, V. Expression of the cardiac ventricular alpha- and beta-myosin heavy chain genes is developmentally and hormonally regulated. *J Biol Chem* **259**, 6437-6446 (1984).
29 Weiss, A. & Leinwand, L. A. The mammalian myosin heavy chain gene family. *Annu Rev Cell Dev Biol* **12**, 417-439 (1996).
30 van Rooij, E. *et al.* A family of microRNAs encoded by myosin genes governs myosin expression and muscle performance. *Dev Cell* **17**, 662-673 (2009).
31 van Rooij, E. *et al.* Control of stress-dependent cardiac growth and gene expression by a microRNA. *Science* **316**, 575-579 (2007).
32 Montgomery, R. L. *et al.* Therapeutic inhibition of miR-208a improves cardiac function and survival during heart failure. *Circulation* **124**, 1537-1547 (2011).
33 Ventura, A. *et al.* Targeted deletion reveals essential and overlapping functions of the miR-17 through 92 family of miRNA clusters. *Cell* **132**, 875-886 (2008).
34 Wang, J. *et al.* Bmp signaling regulates myocardial differentiation from cardiac progenitors through a MicroRNA-mediated mechanism. *Dev Cell* **19**, 903-912 (2010).
35 Chen, J. *et al.* mir-17-92 cluster is required for and sufficient to induce cardiomyocyte proliferation in postnatal and adult hearts. *Circ Res* **112**, 1557-1566 (2013).
36 Dirkx, E. *et al.* Nfat and miR-25 cooperate to reactivate the transcription factor Hand2 in heart failure. *Nat Cell Biol* **15**, 1282-1293 (2013).
37 Wahlquist, C. *et al.* Inhibition of miR-25 improves cardiac contractility in the failing heart. *Nature* **508**, 531-535 (2014).
38 Porrello, E. R. *et al.* MiR-15 family regulates postnatal mitotic arrest of cardiomyocytes. *Circ Res* **109**, 670-679 (2011).
39 Porrello, E. R. *et al.* Regulation of neonatal and adult mammalian heart regeneration by the miR-15 family. *Proc Natl Acad Sci U S A* **110**, 187-192 (2013).
40 Cesana, M. *et al.* A long noncoding RNA controls muscle differentiation by functioning as a competing endogenous RNA. *Cell* **147**, 358-369 (2011).
41 Lee, J. T. Lessons from X-chromosome inactivation: long ncRNA as guides and tethers to the epigenome. *Genes Dev* **23**, 1831-1842 (2009).
42 Maurano, M. T. *et al.* Systematic localization of common disease-associated variation in regulatory DNA. *Science* **337**, 1190-1195 (2012).
43 Klattenhoff, C. A. *et al.* Braveheart, a long noncoding RNA required for cardiovascular lineage commitment. *Cell* **152**, 570-583 (2013).
44 Grote, P. *et al.* The tissue-specific lncRNA Fendrr is an essential regulator of heart and body wall development in the mouse. *Dev Cell* **24**, 206-214 (2013).
45 Colley, S. M. & Leedman, P. J. Steroid Receptor RNA Activator - A nuclear receptor coregulator with multiple partners: Insights and challenges. *Biochimie* **93**, 1966-1972 (2011).
46 Caretti, G. *et al.* The RNA helicases p68/p72 and the noncoding RNA SRA are coregulators of MyoD and skeletal muscle differentiation. *Dev Cell* **11**, 547-560 (2006).
47 Friedrichs, F. *et al.* HBEGF, SRA1, and IK: Three cosegregating genes as determinants of cardiomyopathy. *Genome Res* **19**, 395-403 (2009).
48 Han, P. *et al.* A long noncoding RNA protects the heart from pathological hypertrophy. *Nature* **514**, 102-106 (2014).
49 Hang, C. T. *et al.* Chromatin regulation by Brg1 underlies heart muscle development and disease. *Nature* **466**, 62-67 (2010).

50 Ounzain, S. *et al.* Genome-wide profiling of the cardiac transcriptome after myocardial infarction identifies novel heart-specific long non-coding RNAs. *Eur Heart J* **36**, 353-368a (2015).
51 Ishii, N. *et al.* Identification of a novel non-coding RNA, MIAT, that confers risk of myocardial infarction. *J Hum Genet* **51**, 1087-1099 (2006).
52 Matkovich, S. J., Edwards, J. R., Grossenheider, T. C., de Guzman Strong, C. & Dorn, G. W., 2nd. Epigenetic coordination of embryonic heart transcription by dynamically regulated long noncoding RNAs. *Proc Natl Acad Sci U S A* **111**, 12264-12269 (2014).
53 Liu, Y. *et al.* Expression profiling and ontology analysis of long noncoding RNAs in post-ischemic heart and their implied roles in ischemia/reperfusion injury. *Gene* **543**, 15-21 (2014).
54 Yang, K. C. *et al.* Deep RNA sequencing reveals dynamic regulation of myocardial noncoding RNAs in failing human heart and remodeling with mechanical circulatory support. *Circulation* **129**, 1009-1021 (2014).
55 Wang, K. *et al.* The long noncoding RNA CHRF regulates cardiac hypertrophy by targeting miR-489. *Circ Res* **114**, 1377-1388 (2014).

CHAPTER 3

Antisense MicroRNA Therapeutics in Cardiovascular Disease: Quo Vadis?

[1]Leonne E. Philippen, [1]Ellen Dirkx, [2]Jan B. M. Wit, [3]J. Burggraaf, [1]Leon J. de Windt, [1]P. A. da Costa Martins

[1] Department of Cardiology, CARIM School for Cardiovascular Diseases, Faculty of Health, Medicine and Life Sciences, Maastricht University, Maastricht, Netherlands
[2] Cristal Therapeutics BV, Maastricht, The Netherlands
[3] Centre for Human Drug Research, Leiden University Medical Center, Leiden, The Netherlands

Published in Molecular Therapy, as:

Philippen LE, Dirkx E, Wit JB, Burggraaf K, de Windt LJ, da Costa Martins PA. Antisense MicroRNA Therapeutics in Cardiovascular Disease: Quo Vadis? Molecular Therapy (2015); 23 12, 1810–1818

Abstract

Heart failure (HF) is the end result of a diverse set of causes such as genetic cardiomyopathies, coronary artery disease, and hypertension and represents the primary cause of hospitalization in Europe. This serious clinical disorder is mostly associated with pathological remodeling of the myocardium, pump failure, and sudden death. While the survival of HF patients can be prolonged with conventional pharmacological therapies, the prognosis remains poor. New therapeutic modalities are thus needed that will target the underlying causes and not only the symptoms of the disease. Under chronic cardiac stress, small noncoding RNAs, in particular microRNAs, act as critical regulators of cardiac tissue remodeling and represent a new class of therapeutic targets in patients suffering from HF. Here, we focus on the potential use of microRNA inhibitors as a new treatment paradigm for HF.

Introduction

MicroRNAs (miRs) are a family of small (19–25 nucleotide) single-stranded noncoding RNA molecules that regulate gene expression at the post-transcriptional level. Inhibition of gene expression occurs through complementary base pairing with sequences mainly located in the 3′ untranslated region (3′ UTR) of the target mRNA,[1] leading to translational repression or mRNA degradation (**Figure 1**). Key recognition elements comprise nucleotides 2–8 at the 5′ end of the microRNA and are known as seed sequences.[2] MicroRNAs can be represented as families, defined by conservation of their seed region, with conservation of sequences from nematodes through to humans, implying importance of function during evolution. Between 10–40% of human mRNAs are regulated by microRNAs whereby single microRNA species can regulate multiple mRNA targets and single microRNAs may contain several microRNA recognition sites in their 3′UTR.[3] Such complex regulatory networks can control key biological functions and alterations in microRNA expression are associated with numerous human pathologies such as cancer,[4, 5] neurodegenerative,[6, 7] metabolic,[8, 9] and cardiovascular diseases.[10, 11] In recent years, research has been aimed at targeting dysregulated microRNA expression as a novel way to modulate biological processes for benefit. Such modulation of microRNAs has proven successful *in vivo* through the use of antisense oligonucleotides (ASOs) or modified microRNA mimics such as plasmid or lentiviral vectors that carry microRNA sequences designed to deliver microRNAs to cells and tissues (**Figure 1**). Since available heart failure (HF) pharmacotherapy has only a marginal impact on long-term prognosis of the disease, there is both room and a need for the development of innovative bio-therapeutics. This review focuses on the current status of microRNA-based therapies in HF and highlights the potential use of ASOs as microRNA inhibitors for the treatment of cardiovascular diseases.

MicroRNAs and cardiovascular diseases

A distinct set of differentially expressed microRNAs exists in the failing as compared to normal heart. miR-1, miR-25, miR-29, miR-30, miR-133, and miR-150 show downregulated expression, while miR-21, miR-23a, miR-125, miR-195, miR-199a/b, and miR-214 show increased expression in experimental and human HF. This altered expression pattern is associated with underlying mechanisms that lead to the disease state.[12-14]

A hallmark of HF development is pathological hypertrophy.[15, 16] Several microRNAs are reported to regulate prohypertrophic genes, including hypertrophy-associated

calmodulin, NFAT, Mef2a, Gata4, and Hand2 and are thought to be key regulators in HF development.[12, 17, 18] Therapeutic cardiac-targeted delivery of one such

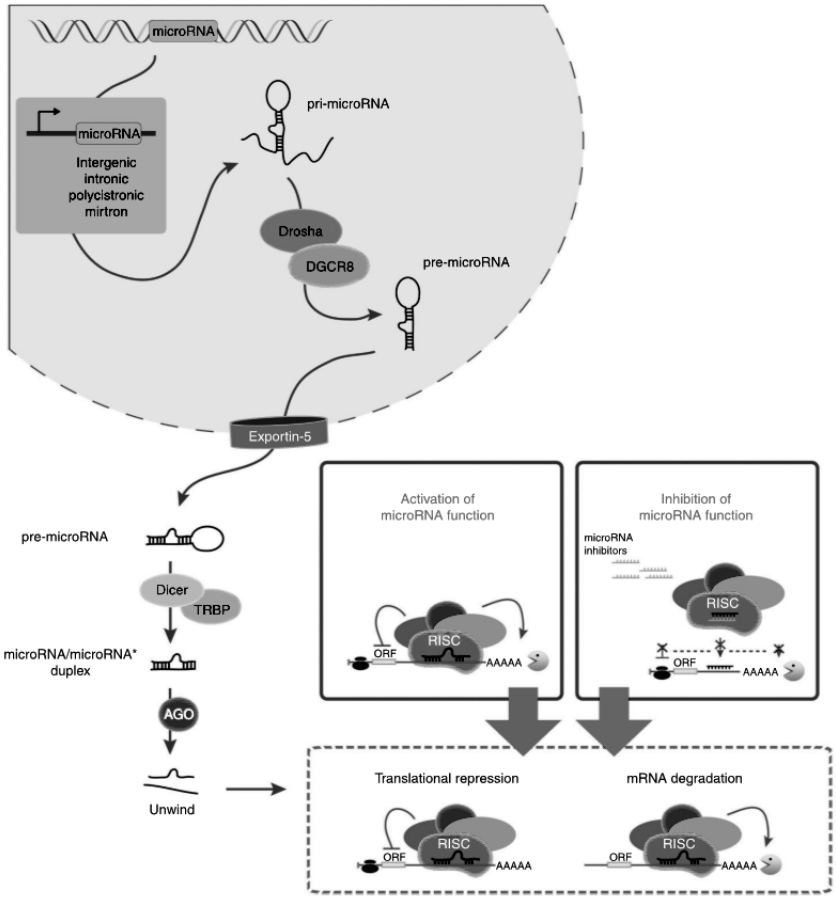

Figure 1 MicroRNA processing and modulation of activity by antisense oligonucleotides and microRNA mimics. MicroRNA maturation is a complex process where any step is subject to tight molecular regulation. MicroRNAs are initially transcribed by RNA polymerase II from intergenic, intronic, or polycistronic loci into long primary transcripts (pri-microRNAs) that can encode one or more miRNAs. Hereafter, multiple 60–100 bp long microRNA precursor hairpin-like structures (pre-microRNA) are released by the action of the Drosha-DGCR8 complex. Export of these precursor stem-loop structures from the nucleus occurs in a Ran/GTP/Exportin-5-dependent manner and once in the cytoplasm, pre-miRNAs are cleaved by the Dicer-TRBP complex and processed to generate microRNA duplexes. These will be incorporated into the Argonaute-containing microRNA-induced silencing complex (RISC) and after unwinding of the duplex occurs the mature microRNA strand will be kept in the RISC while the complementary strand will be freed and degraded. The mature microRNA in the RISC will direct it to mRNAs with partially complementary sites and lead to translational repression and/or degradation. MicroRNA activity can be modulated either by restoring function via double stranded microRNA mimics or by inhibition using single-stranded antisense oligonucleotides.

microRNA, miR-1, reversed pressure over- load-induced cardiac hypertrophy and attenuated pathological remodeling.[19] miR-133, clustered with miR-1, is also repressed during HF and its repression suffices to induce cardiac hyper- trophy and increase expression of target mRNAs such as RhoA (GDP-GTP exchange protein regulating cardiac hypertrophy), Cdc42 (kinase implicated in hypertrophy), and Nelf-A/WHSC2 (nuclear factor involved in cardiogenesis).[20] In line, miR-133 overexpression inhibits experimentally induced hypertrophy. Likewise miR-199b, a direct target of the calcineurin/NFAT pathway, is increased in mouse and human HF, and *in vivo* inhibition of miR-199b with a specific antagomir reduced nuclear NFAT activity and caused marked inhibition of hypertrophy and fibrosis.[21]
An important feature in the process of myocardial infarction (MI) and subsequent systolic HF is myocardial fibrosis leading to abnormal mechanical stiffness and contractile dysfunction.[22] Members of the miR-29 family are implicated in this process as they show marked downregulation in the border zone surrounding the infarcted area.[23] Downstream targets of miR-29 include proteins associated with the fibrotic response such as; extracellular matrix-related genes such as elastin (ELN), collagenase type 1 alpha 1–3 (COL1A1-3) and fibrillin 1 (FBN1). miR-21 is also related to a fibrogenic phenotype as it controls cardiac fibroblast proliferation by facilitating MAPK signaling through induction of Sprouty homolog 1 (SPRY1).[24] MicroRNAs also regulate the repair response after MI, another key aspect of HF. This process prevents hypoxic damage through the induction of angiogenesis driven by the cytokines vascular endothelial growth factor and fibroblast growth factor.[25] The endothelial cell-specific miR-126 can regulate this response following MI by inhibition of negative regulators of the vascular endothelial growth factor pathway such as SPRED1 and PIK3R2[26] and, therefore, positively impact neo-angiogenesis and counteract hypoxia.

MicroRNAs also play a pathophysiological role during atherosclerotic plaque progression. In this context, downregulation of miR-24 induces plaque stability by promoting the invasion of macrophages with matrix metalloproteinase-14 proteolytic activity.[27] In contrast, miR-126-null mice have reduced endothelial cell proliferation and exacerbated atherosclerosis and reconstitution of miR-126-5p was able to rescue endothelial cell proliferation and limit atherosclerosis.[28]

Together, these studies establish microRNAs as key regulators of cardiovascular disease and identify them as potential therapeutic targets to treat human disease.

MicroRNA activity modulation: therapeutic approaches

To date, the regulatory role of specific microRNAs in cardiovascular disease has primarily been elucidated from loss- or gain-of- function studies in mouse models of disease.[17] ASOs have been the main pharmacological tools used to inhibit microRNA function in mouse disease models. Here, we speculate on the potential use of antimirs and their therapeutic potential for cardiovascular disease.

ASOs: mechanism of action

ASOs were first discovered in 1987 and can be described as short, single-stranded chains of nucleotides that hybridize with complementary RNA sequences.[29] In the last 10 years, ASOs have also been used as tools to inhibit microRNA function (anti-microRNA oligonucleotides (AMOs)), based on Watson-Crick base pairing.[30] AMOs exert their activity through several mechanisms including RNase H-mediated RNA degradation where recognition of the RNA-AMO duplex by RNase H leads to cleavage of the RNA strand[31] or sterically blocking access to pre-mRNA and mRNA without degrading the RNA[32] (**Figure 1**).
Despite several publications analyzing decreased microRNA expression level as measure of effectiveness of AMO treatment, the question remains whether this is the most reliable evaluation method to determine efficacy of microRNA inhibition. For example, binding of an AMO to its target microRNA may interfere with its detection but, depending on the chemistry of the AMO used, be able to inhibit microRNA function without also inducing its degradation. An example of this is LNA and 2'-fluoro/2'-methoxyethyl modified AMOs, which can inhibit microRNA activity without decreasing mature microRNA expression levels.[33]

In such cases, evaluating microRNA target derepression as a secondary endpoint may also provide a valuable measure of AMO efficacy.

Chemical modifications

Because AMOs must bind specific nucleotide sequences the rational design of high affinity antagonists is relatively straightforward. However, since several enzymes present in the organism rapidly recognize RNA-like structures, premature degradation of AMOs can limit their bioavailibility. In this context, chemical modifications of AMOs can be employed to alter their pharmacokinetic properties and enhance cellular uptake without loss of binding (**Figure 2**). Indeed, differently modified antisense microRNAs have been shown to directly inhibit microRNA

function *in vivo* and the examples detailed herein clearly show the potential of antisense microRNAs to treat cardiovascular diseases.

2'-OMe modifications

Theoretically, systemically delivered oligonucleotides are susceptible to enzymatic degradation by nucleases present in the bloodstream by the same mechanisms that regulate native RNA. Methylation of the hydroxyl group at the 2′ position of the ribose unit is a relatively simple and attractive approach to increase resistance to nuclease attack. The 2′-O-methyl (2′-OMe) AMOs have been increasingly used in the

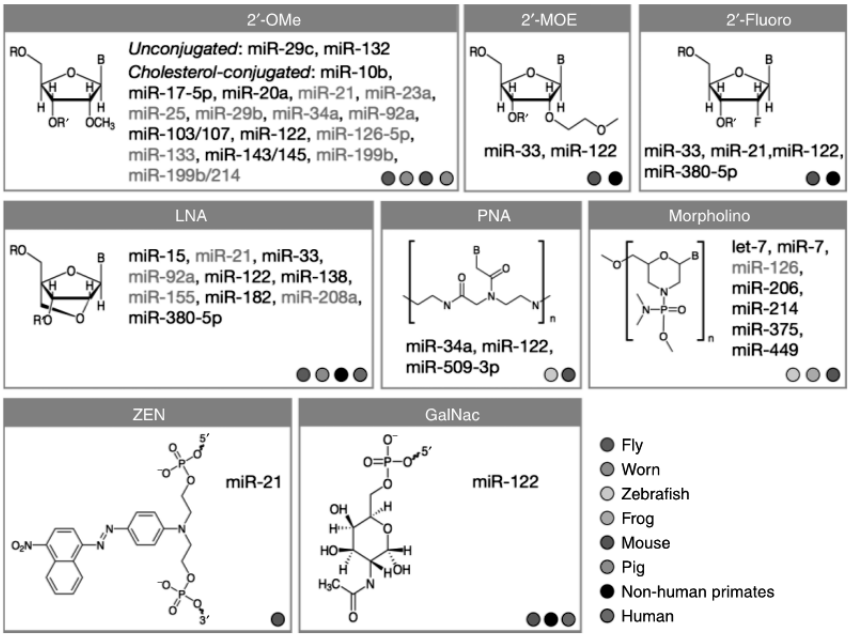

Figure 2 Chemical modifications of anti-microRNA oligonucleotides. Structures of the most commonly used chemical modifications in antisense oligonucleotides to modulate microRNA activity (AMOs). The 2′-O-methyl (2′-OMe), 2′-O-methoxyethyl (2′-MOE), and the 2′-fluoro (2′-F) nucleo- tides are modified at the 2′ position of the ribose moiety. Locked nucleic acid (LNA) is a bicyclic RNA analogue in which the ribose is locked in a C3′- endo conformation by introduction of a 2′-O,4′-C methylene bridge. PNA oligomers are uncharged oligonucleotide analogues where a peptide-like backbone consisting of N-(2-aminoethyl)-glycine units replace the sugar-phosphate backbone. In the morpholino oligomers, the sugar moiety is replaced by a morpholine ring. In the ZEN modification, a (N,N-diethyl-4-((4-nitronaphtalen-1-yl) diazenyl) aniline) unit is placed at several locations in the phosphate backbone, reducing susceptibility to nuclease attack. The GalNac modifier includes a *N*-acetylgalactosamine (GalNAc) conjugate as a ligand to target delivery to the liver. Many microRNAs have been modulated with different AMOs, in different disease settings and different animal models (colored circles). MicroRNAs that were targeted by different chemically modified AMOs in the context of cardiovascular diseases are marked in red. PNA, peptide nucleic acid.

past decade and have proven *in vivo* efficacy. Besides enhanced resistance to nuclease attack, 2′-OMe ASOs show improved binding affinity to their corresponding microRNA sequence as compared to unmodified AMOs.[28, 33, 34] Let-7 was the first microRNA to be success- fully silenced using this method in the nematode *C. elegans.*[35] To further enhance resistance to nuclease attack conferred by 2′-OMe modification, phosphorothioate moieties in the linking backbone have also been introduced. These sulphur analogues of phosphate can be incorporated near either the 5′ or 3′ and show, in combination with a 3′-cholesterol unit, enhanced AMO stability in cell cultures.[36] Krützfeldt *et al*.[37] explored the potential of 2′-OMe modification to modulate microRNA *in vivo* using regulation of miR-122, a microRNA involved in cholesterol synthesis in the liver, as a model system. Unmodified single- stranded AMO-122 had no effect on miR-122 expression levels, whereas unconjugated chemically altered RNA analogues, partially or fully modified with a phosphorothioate backbone and 2′-OMe modifications, had a partial effect.[37] Additional cholesterol-conjugation of the altered synthetic AMO (antagomir) was able to completely abolish endogenous miR-122 levels suggesting that the partial decrease in miR-122 expression by the unconjugated modified RNA analogues was due to microRNA- 122-RNA duplex formation, whereas silencing miR-122 by the antagomir was the result of complete microRNA degradation.[37] High sequence specificity was demonstrated by introducing position specific mismatches. The use of fluorescently labeled antagomirs further showed that antagomir-microRNA interaction took place in the cytoplasmic compartment, upstream of the processing bodies (P-bodies),[37] sites that act as scaffolding centers for microRNA function. Administration of a miR-122-specific antagomir at a dose of 80 mg/kg for 3 consecutive days effectively reduced miR-122 expression levels in mice for a period of 23 days.[37] Moreover, antagomirs successfully abolished microRNA expression in a few cardiovascular studies (**Figure 2**). Antagomirs exhibit a broad biodistribution and can efficiently silence their target microRNAs in all tissues tested. Although they cannot cross the placental and blood–brain barriers, injection of antagomirs directly into the cortex efficiently reduced microRNA levels in the brain.[37]

2′(F)-MOE modifications

Another approach to increase the stability of AMOs is the combination of 2′-MOE (2′-O-methoxyethyl) with phosphorothioate modifications in the linking backbone. This method is similar to 2′-OMe modifications albeit using $CH_2CH_2OCH_3$ protective groups rather than a simple CH_3. The use of a library of 2′-MOE AMOs to investigate the biological importance of microRNAs identified several microRNAs involved in adipocyte differentiation. Effective silencing of miR-143, a microRNA that is

upregulated in differentiating adipocytes,[38] reversed adipocyte differentiation in the liver. The same group also showed that silencing miR-122 in mice with a specific 2'-MOE RNA antagonist efficiently reduced plasma cholesterol levels, increased hepatic fatty-acid oxidation and decreased hepatic fatty acid and cholesterol synthesis rates.[39] Interestingly, the results obtained by Esau *et al*.[39] suggest that each AMO may have different affinity for their corresponding microRNA, with some specific targets being maximally affected at very low doses and others being less responsive. Besides the 2'OMe and 2'MOE variations of RNA analogues, other RNA analogues containing substitutions at the same location within the ribose unit have been described. One such example is the 2'Fluoro modification, which has proven to be a potent inhibitor of both miR-122 and miR-21 in mice.[33, 40] However, ASOs containing 2'-fluoro modifications require further modification to make them resistant to nuclease attack by making single strand antagonists with a full phosphorothioate backbone or additional 2' protective groups like 2'MOE.[33, 34, 41]

LNA

The pharmacokinetics of AMOs can also be modified by locked nucleic acid (LNA) modifications where the 2'-hydroxyl group is linked to the 4' carbon atom of the sugar ring thereby forming a bicyclic sugar moiety. The linkage is preferably a methylene $[CH_2]_n$ group bridging the 2' oxygen atom with the 4' carbon atom wherein n is 1 or 2. LNA-protected antisense RNAs exhibit extremely high thermal stability when hybridized with their corresponding RNA target molecules. In addition, LNA oligonucleotides display low toxicity at low doses, are highly soluble[42] and show excellent activity in targeting microRNAs. An LNA targeting miR-122 was the first of its kind to be validated in nonhuman primates causing a meaningful reduction in plasma cholesterol. Systemic delivery of an LNA in a physiological buffer resulted in a dose-dependent long-lasting and reversible decrease in total plasma cholesterol levels in African green monkeys, without any observed toxicities or histopathological changes.[43] Empirically, LNAs possess the thermodynamically strongest duplex formation with complementary target RNA of all the AMOs. As a result, biological activity is often obtained with very short (8–15 nt) LNA-protected RNA sequences. Another advantage of LNA-modified oligonucleotides is their high metabolic stability (partly explained by enhanced nuclease resistance), their small size, excellent mismatch discrimination, and lack of toxicity in nonhuman primates.[43, 44] However, LNAs may also form tight double strand binding which can lead to off-target microRNA engagement with subsequent inhibition of nontargeted microRNAs or precursor microRNAs. Indeed, a large animal model study using an LNA against miR-92a also inhibited the very closely resembling miR-25,[45] which has

been shown to be associated with adverse effects in animal models of HF.[14] Direct hepatoxicity of LNA nucleotides has also been observed *in vivo*, where adverse effects have been related to the use of particular LNA-modified oligonucleotide sequences.[46] Nevertheless, LNAs show promise as they are well tolerated *in vivo* and are currently being evaluated in human clinical trials.

The ZEN modifier

Recently, Lennox *et al*.[47] introduced a different approach to microRNA inhibition by using the non-nucleotide modifier ZEN (N,N-diethyl-4-((4-nitronaphthalen-1-yl)diazenyl) aniline unit) bound at various locations in the phosphate backbone of the RNA structure of oligonucleotide sequences. Using this ZEN modifier on both 5'and 3'terminal ends of 2'OMe modified AMOs resulted in full resistance against enzymatic degradation in serum and cell extracts and using miR-21 as an example demonstrated that ZEN modification was able to reduce AMOs to a length as short as 15-mers.[47] *In vivo* testing of ZEN-AMOs is currently in progress but preliminary data indicate no obvious toxicity after systemic administration in mice.[47]

GalNac conjugation

After successful subcutaneous delivery of RNAi therapeutics by conjugation to GalNAc (N-Acetylgalactosamine) sugar,[48] a carbohydrate-based chemistry developed by Alnylam (www. alnylam.com) other commercial organizations have adopted this approach. In 2013, Regulus Therapeutics (www.regulusrx.com) reported the use of GalNAc conjugated nucleotides indicating that they showed a 20-fold enhanced potency on hepatocytes and decreased expression of miR-122 target mRNAs as compared to unconjugated oligonucleotides. The company has also described data evaluating the use of GalNAc-conjugated oligonucleotides for *in vitro* and *in vivo* potency, pharmacokinetic/pharmaco- dynamics, toxicology and safety pharmacology, and inhibition of hepatitis C virus (HCV) replication. Efficacy was tested in a mouse-human chimeric liver model of HCV and showed up to a 2-log reduction in viral load titer after just a single dose. Phase 1 clinical trials are ongoing and so far no serious adverse side effects have been observed (http://regulusrx.com).

PNA

In addition to the various sugar modifications, steric blockers can be made from a neutral backbone that is entirely different from DNA or RNA sugar-phosphate backbones. Peptide nucleic acid (PNA) oligonucleotides contain bases linked by

amide bonds.[49] Due to the neutral charge of the amide backbone, binding to complementary sequences is very stable and occurs with high hybridization rates.[50] PNAs complementary to miR-122 have been shown to inhibit of target microRNA function both *in vitro*[51] and *in vivo*.[52]

Morpholinos

A different type of (uncharged) DNA analogue is the phosphoro-diamidate morpholine oligomer also known as a morpholino. The sugar backbone of these oligonucleotides has the ribose (or desoxyribose) ring replaced by a morpholine ring, which is attached to the phosphate backbone through the nitrogen of the morpholine ring. In addition, it has one of the phosphate oxygen's replaced by a dimethylamino group. Although binding to complementary RNA does not have as high affinity as PNA binding, morpholinos have been successfully used to silence miR-375[53] and mIR-206[54] in zebrafish, revealing the roles these microRNAs play in pancreatic islet development and angiogenesis, respectively. Furthermore, since the backbone of morpholinos is neutral in charge, nonselective interactions with proteins, is less likely. Finally, morpholinos can be manufactured at low cost making them attractive for large *in vivo* studies.

Sponges, masks, and erasers

Recently, several methods to increase microRNA target specificity have been developed. One example is the use of microRNA sponges, where perfectly or imperfectly paired binding sites for the target microRNA sequences are inserted into an expression cassette in the 3' UTR of a reporter gene. Those binding sites competitively inhibit and occupy the native microRNA-programmed microRNA-induced silencing complex, thereby decreasing microRNA-induced silencing complex concentrations available for binding, and reversing the microRNA inhibitory effect on its target mRNA.[55] This method has been shown to be effective *in vivo* using lentiviral vectors that stably and specifically silence miR-223 and subsequently upregulate its target sequences.[56]

Another way, in which microRNA binding to its target mRNA can be blocked, is to use an oligonucleotide with perfect complementarity to the microRNA target sequence in the 3' UTR of the mRNA. In this case, the binding site is masked, which prevents microRNA combining with the target mRNA. A distinct advantage of this approach is the specific targeting of microRNA binding to one particular mRNA. The third indirect method of microRNA inhibition involves "erasers", which are tandem

repeats of a specific microRNA antisense sequence that induce almost complete elimination of endogenous microRNA.[57] This method is comparable to the microRNA sponges, however erasers use only two antisense copies with perfect complementarity to the microRNA, while sponges contain multiple antisense copies of a microRNA.[58]

Efficiency of AMOs in cardiovascular disease

Antisense microRNA inhibitors have been successfully used to knockdown microRNAs in small animals for nearly a decade. After the breakthrough study by Krützfeldt *et al*.,[37] several publications reported efficient microRNA knockdown by AMOs in mammalian cardiac tissue (**Figure 2**). Carè *et al*.[20] were the first to use an antagomir to silence a cardiac microRNA showing that miR-133 silencing was sufficient to induce significant cardiac hypertrophic growth in mice. Many other cardiovascular microRNAs have subsequently been targeted (**Figure 2**; **Table 1**). Delivery of a specific antagomir to miR-21 in a mouse model of pressure-overload-induced cardiac disease prevented cardiac fibrosis and attenuated cardiac dysfunction.[24] *In vivo* inhibition of miRNA-199b, a dysregulated microRNA involved in NFAT signaling, caused marked inhibition and even reversal of cardiac hypertrophy and fibrosis in mouse models of HF.[21] Antagomir-mediated silencing of miRNA-214, which plays a pivotal role in regulating cardiac mitochondrial substrate flux, resulted in restored fatty acid oxidation and sub- sequent improvement in cardiac function.[59] In mouse models of limb ischemia and MI antagomir-mediated inhibition of miR-92a enhanced blood vessel growth and functional recovery of dam- aged tissue.[60] Inhibition of miR-208a by systemic administration of a specific LNA, in rats, led to improvement of cardiac function and attenuated pathological remodeling, indicating the exciting potential for this class of drugs.[61] Furthermore, delivery of an LNA targeting miR-92a via a catheter in a pig model of MI resulted in reduced infarct size and improved cardiac function. Intravenous administration of the same LNA did not result in decreased infarct size compared to control animals, suggesting local administration might be preferred over systemic delivery for some types of AMOs.[45] In 2008, the first publication appeared testing LNA chemistry constructs in nonhuman primates. Systemic administration of three doses of 10 mg/kg of unconjugated LNA oligonucleotide effectively silenced miR-122 in African green monkeys, without any signs of LNA-associated toxicities or histopathological alterations in the tissues examined.[43] This LNA antagonist (miravirsen, SPC3649) proved to be an effective drug in treating hepatitis C viral infection in chimpanzees.[62] More recently, two other studies in nonhuman primates, showed that inhibition of miR-33a and miR-33b by either a 2'F/MOE- or 8-mer LNA-modified

AMOs resulted in derepression of miR-33 target genes such as the ATP- binding cassette transporter ABCA1, essential for the biogenesis and transport of high-density lipoprotein (HDL), and increased plasma HDL cholesterol levels.[41] These findings indicate the potential of seed-targeting AMOs to pharmacologically inhibit microRNAs and microRNA families in nonhuman primates. This opens up the exciting possibility that inhibiting the miR-33 family may reverse dyslipidaemia and atherosclerosis, which are risk factors in cardiovascular disease.

AMOs from bench to bedside: perspectives and challenges

To date, no clinical trials using AMOs have been initiated for the treatment of cardiovascular diseases. However, two companies, Regulus Therapeutics and Santaris Pharma, are developing therapeutics aimed at inhibiting miR-122 for the treatment of HCV infection in humans. Regulus Therapeuthics is developing a GalNAC-conjugated AMO-122 (RG-101) which entered a phase 1 study on healthy volunteers (http://www.regulusrx.com). Santaris Pharma is developing another antisense microRNA-122 drug, (miravirsen),[62, 63] for which phase 1 and phase 2 trials have been completed. Phase 1 studies confirmed preclinical findings in rodents and nonhuman primates,[62, 64] which showed good tolerability of the compound. The phase 2 trial in 36 patients with chronic HCV infection showed that miravirsen dose-dependently reduced HCV RNA levels with long-lasting (>18 weeks) antiviral activity. However, the 4-week monotherapy (at a weekly dose of 7 mg/kg) was not sufficient to achieve a sustained response,[65] with some patients displaying viral rebound by the end of the study. The patients were randomly assigned to receive five weekly subcutaneous injections of miravirsen at doses of 3, 5, or 7 mg per kg of body weight or placebo over a 29-day period. They were followed until 18 weeks after randomization.

Altogether, these studies indicate that pharmacological inhibition of microRNA expression and activity can be achieved in a clinical setting, representing a feasible therapeutic strategy for patients. Nevertheless, various challenges still remain in the clinical use of microRNA-targeting drugs. The main technical hurdles are delivery, specificity and duration of action. Efficient *in vivo* delivery of therapeutic oligonucleotides is crucial for developing successful microRNA-based treatment modalities. In order to enter the cell, the oligonucleotide must travel across the lipid bilayer of the cell membrane. Currently, two strategies for microRNA delivery into the cell have been tested: conjugation and formulation. Conjugation approaches include attachment of lipophilic ligands that bind specific cell surface receptors increasing the rate of internalization into the cell whilst also allowing cell subset specific targeting. For instance conjugation of oligonucleotides to cholesterol has

been demonstrated to greatly enhance cellular uptake.[66] Formulation strategies are mostly used when localized delivery is not possible and utilize supramolecular nano-carriers, such as liposomes or polymeric nanoparticles.[67]

At the current time, organ-specific targeting of oligonucleotides has only shown to be successful in the liver.[43] In order to become of greater utility, effective delivery methods to other organs, especially the heart, are absolutely required. While conventional drugs are usually designed to be specific for a single cellular target (*i.e.*, an enzyme or receptor), the fact that micro- RNAs have numerous downstream targets, many still to be identified, can lead to undesired effects. Understanding such effects is of major importance in developing microRNA-based therapies. Targeting a single microRNA might be a balance between beneficial and pathogenic effects. *In vivo* animal experiments have shown that administration of synthetic oligonucleotides results in long-lasting but reversible effects in non-human primates and mice.[43, 68] Most studies used multiple daily-dosing regimens to efficiently reduce the level of the microRNA of interest for an extended period of time (3 weeks in mice and 7 weeks in African green monkeys). However, the fact that multiple injections are necessary for sustained effects may mean there is a limited possibility for a physician to intervene in case of unexpected or unwanted side effects. In theory this problem could be overcome by administration of sense microRNAs that would compete and neutralize AMO binding compared with its cell-associated target.

The problems encountered with the tolerability of oligonucleotides have received little attention so far. Intravenous administration of oligonucleotides to humans has been reported to be associated with flu-like symptoms that increase in severity upon repeated dosing.[69, 70] This mode of administration has been largely abandoned and replaced by subcutaneous dosing even though injection site reactions have been reported for all classes of oligonucleotides currently in the clinic.[65, 69, 71] These injection site reactions appear to be related to an immunological memory response as upon increased dosing lesions appear not only at the site of administration but also at sites of previous injections.[72, 73] This may ultimately limit the use of current AMOs in settings that require repeat or chronic administration. Another unresolved issue is the accumulation of oligonucleotides in proximal tubule cells of the kidney.[74] Although this is generally not associated with adverse clinical events, a few case reports of serious kidney problems occurring after administration of oligonucleotides in patients with Duchenne's muscular dystrophy showed dose-related proteinuria, suggesting that the effects on the kidney in humans may differ as such effects were not seen in preclinical models.[73, 75] Thus, adequate evaluation of the physiological impact of long-term microRNA inhibition *in vivo* is key to the development of successful microRNA therapeutics.

A final consideration in the future development of drugs in this area is their potential high cost. Large sums of money have been spent in the research phase of microRNA-based oligonucleotide drugs and such costs may have to be recouped if and when they become approved for use in humans. The area of synthetic microRNA-based oligonucleotides is still in its infancy and while large-scale production of microRNA mimics and AMOs will lower the fixed costs, likely making them more attractive for clinical use, it remains unclear to what extend the costs can and will be decreased in the future.

Concluding remarks

Antisense inhibition of microRNAs by chemically modified oligonucleotides has proven to be a promising field of therapy for the treatment of cardiovascular diseases. It is a widely used tool in rodents to silence microRNA expression and thereby improve cardiac function. The high potency and metabolic stability of AMO technology emphasizes its potential to target microRNAs. Absence of toxicity in rodents, large animals and nonhuman primates suggests that AMO-based therapeutics could be safe as well as efficacious although it has yet to be confirmed that this translates into humans. The recent data from the phase II trial in HCV infected patients treated with miravirsen, an LNA against miR-122, is a milestone in the development of microRNA therapeutics. Therefore, it might be expected that the cardiovascular field will follow soon, marking the way toward microRNAs as a new class of drug targets for the treatment of people suffering with cardiovascular disease.

Acknowledgements

L.J.d.W. acknowledges support from the *Netherlands CardioVascular Research Initiative*: the Dutch Heart Foundation, Dutch Federation of University Medical Centers, the Netherlands Organization for Health Research and Development (ZonMW) and the Royal Netherlands Academy of Sciences. L.J.d.W. was further supported by grant 311549 from the European Research Council (ERC). P.A.d.C.M. was support- ed by a Leducq Career Development Award (no.11 CDA02), NWO-MEERVOUD 836.12.001 and the Dutch Heart Foundation grant NHS2010B261. None of the authors has conflicts of interest to declare.

Table 1 Overview of preclinical studies applying anti-microRNA oligonucleotides to inhibit specific microRNAs in relevant models of heart failure

Chemistry	miR	Dose/delivery	Model	Target	Outcome	Ref.
2'-Ome	21	80 mg/kg/bw; two injections; jugular vein catheter	Mouse, TAC	Spry1	Reduced cardiac ERK-MAP kinase activity, inhibited interstitial fibrosis, and attenuated cardiac dysfunction	24
	23a	25 mg/kg/bw; 1 week; osmotic minipumps	Mouse, isoproterenol infusion	MuRF1	Attenuated hypertrophy	76
	24	80 mg/kg/bw; three daily injection every 6 weeks (30 weeks); iv	Mouse, TAC	N/A	No effect on hypertrophy, prevented decreases in L-type Ca2+ channel–ryanodine receptor signaling efficiency and whole-cell Ca^{2+} transients, protected T-tubule–sarcoplasmic reticulum junctions from disruption	77
	24	5 or 80 mg/kg/bw; days 0 and 2; ro	Mouse, MI	PAK4, GATA2	Reduced endothelial apoptosis, enhanced vascularization, decreased infarct size, and improved cardiac function	78
	25	80 mg/kg/bw; 3 daily injection week 1 and week 4; ip	Mouse, TAC	Hand2	Spontaneous cardiac dysfunction, increased hypertrophy, and fibrosis	14
	25	300 mg, three daily injection/week for 3 weeks; iv	Mouse, TAC	Serca2A	Improved cardiac function, decreased hypertrophy, and fibrosis	79
	29b	80 mg/kg/bw; two injections; ip	Mouse, MI	COL1A1, COL1A2, COL3A1, ELN1, FBN1	Increased expression of collagens, no effect on cardiac function	23
	34a	8 mg/ kg/ bw; iv	Mouse, MI	PNUTS	Reduced cell death and fibrosis, improved cardiac function, increased capillary density in the border zone	80
	92a	8 mg/kg/bw; day 1, 3 and 5; iv	Mouse, MI	ITGA5	Enhanced blood vessel growth, functional recovery of damaged tissue, and decreased apoptosis	60
	132	80 mg/kg/bw; day 0 and 1; ro	Mouse, TAC	Fox03	Decreased hypertrophy and fibrosis, preserved cardiac function	81
	199a~214	20 mg/kg/bw; three daily injection; ip	Mouse, TAC	PPARd	Decreased hypertrophy and fibrosis, preserved cardiac function	59
	199b	80 mg/kg/bw; three daily injection, week 1 and 4; ip	Mouse, TAC	Dyrk1A	Reduced nuclear NFAT activity, inhibition and reversal of hypertrophy and fibrosis	21
	133	80 mg/kg/bw; three daily injection; ip	Mouse	RhoA, Cdc42 Nelf-A/ WHSC2	Marked and sustained hypertrophy	20
	146a	8 mg/kg/bw; four injections in 1 week; iv	Mouse, Stat3 KO	NRAS	Improved cardiac function, reduced fibrosis and enhanced capillary density	82
LNA	92a	0.03 mg/kg/bw; iv or catheter local delivery to the heart	Pig, ischemia reperfusion	N/A	Reduced infarct size, increased capillary density, and decreased inflammation	45
	34 family	25 mg/kg/bw; three daily injection; sc	Mouse, TAC and MI	Vinculin, Sema4b, Pofut1, and Bcl6	Improved cardiac function, reduced inflammation and fibrosis, attenuated hypertrophy	83
	208a	25 mg/kg/bw;injection every 2 weeks; iv	Mouse; Dahl salt-sensitive rats/high-salt diet	N/A	Increased survival, increased body weight, reduced fibrosis, and attenuated hypertrophy	61
	155	10 mg/kg/bw; three daily injection; iv	Mouse, angiotension II	Socs1	Improved cardiac function, decreased heart weight, and reduced inflammation	84
	21	25 mg/kg/bw; three daily injection; iv	Mouse, TAC, angiotension II	Pdcd4	No effect on cardiac remodeling or function	85
	21	10–80 mg/kg/bw; iv	Mouse, TAC	N/A	Attenuated hypertrophy and improved cardiac function	40
	26a	24 mg/kg/bw; one injection; iv	Mouse, MI	Smad1	Induced angiogenesis, improved cardiac function, reduced infarct size, and decrease apoptosis	86
	652	25 mg/kg/bw; three daily injection; sc	Mouse, TAC	Jagged1	Preserved capillary density, improved cardiac function, attenuated hypertrophy, and reduced fibrosis	87
F'MOE	21	10–80 mg/kg/bw; iv	Mouse, TAC	N/A	Attenuated hypertrophy and improved cardiac function	40

ip, intraperitoneal injection; iv, intravenous injection; MI, myocardial infarction; N/A, not applicable; ro, retroorbital injection; sc, subcutaneous injection; TAC, transverse aortic constriction.

References

1. Ambros, V. The functions of animal microRNAs. *Nature* **431**, 350-5 (2004).
2. Kim, V.N. MicroRNA biogenesis: coordinated cropping and dicing. *Nat Rev Mol Cell Biol* **6**, 376-85 (2005).
3. Bartel, D.P. MicroRNAs: target recognition and regulatory functions. *Cell* **136**, 215-33 (2009).
4. Ventura, A. & Jacks, T. MicroRNAs and cancer: short RNAs go a long way. *Cell* **136**, 586-91 (2009).
5. Nana-Sinkam, S.P. & Croce, C.M. Clinical applications for microRNAs in cancer. *Clin Pharmacol Ther* **93**, 98-104 (2013).
6. Salta, E. & De Strooper, B. Non-coding RNAs with essential roles in neurodegenerative disorders. *Lancet Neurol* **11**, 189-200 (2012).
7. Pogue, A.I., Hill, J.M. & Lukiw, W.J. MicroRNA (miRNA): Sequence and stability, viroid-like properties, and disease association in the CNS. *Brain Res* (2014).
8. Rottiers, V. & Naar, A.M. MicroRNAs in metabolism and metabolic disorders. *Nat Rev Mol Cell Biol* **13**, 239-50 (2012).
9. Latreille, M. et al. MicroRNA-7a regulates pancreatic beta cell function. *J Clin Invest* **124**, 2722-35 (2014).
10. Olson, E.N. MicroRNAs as Therapeutic Targets and Biomarkers of Cardiovascular Disease. *Sci Transl Med* **6**, 239ps3 (2014).
11. Da Costa Martins, P.A. & De Windt, L.J. MicroRNAs in control of cardiac hypertrophy. *Cardiovasc Res* **93**, 563-72 (2012).
12. Ikeda, S. et al. Altered microRNA expression in human heart disease. *Physiol Genomics* **31**, 367-73 (2007).
13. van Rooij, E., Marshall, W.S. & Olson, E.N. Toward microRNA-based therapeutics for heart disease: the sense in antisense. *Circ Res* **103**, 919-28 (2008).
14. Dirkx, E. et al. Nfat and miR-25 cooperate to reactivate the transcription factor Hand2 in heart failure. *Nat Cell Biol* **15**, 1282-93 (2013).
15. Levy, D., Garrison, R.J., Savage, D.D., Kannel, W.B. & Castelli, W.P. Prognostic implications of echocardiographically determined left ventricular mass in the Framingham Heart Study. *N Engl J Med* **322**, 1561-6 (1990).
16. Kannel, W.B., Doyle, J.T., McNamara, P.M., Quickenton, P. & Gordon, T. Precursors of sudden coronary death. Factors related to the incidence of sudden death. *Circulation* **51**, 606-13 (1975).
17. Thum, T., Catalucci, D. & Bauersachs, J. MicroRNAs: novel regulators in cardiac development and disease. *Cardiovasc Res* **79**, 562-70 (2008).
18. Ikeda, S. et al. MicroRNA-1 negatively regulates expression of the hypertrophy-associated calmodulin and Mef2a genes. *Mol Cell Biol* **29**, 2193-204 (2009).
19. Karakikes, I. et al. Therapeutic cardiac-targeted delivery of miR-1 reverses pressure overload-induced cardiac hypertrophy and attenuates pathological remodeling. *J Am Heart Assoc* **2**, e000078 (2013).
20. Care, A. et al. MicroRNA-133 controls cardiac hypertrophy. *Nat Med* **13**, 613-8 (2007).
21. da Costa Martins, P.A. et al. MicroRNA-199b targets the nuclear kinase Dyrk1a in an auto-amplification loop promoting calcineurin/NFAT signalling. *Nat Cell Biol* **12**, 1220-7 (2010).
22. Berk, B.C., Fujiwara, K. & Lehoux, S. ECM remodeling in hypertensive heart disease. *J Clin Invest* **117**, 568-75 (2007).
23. van Rooij, E. et al. Dysregulation of microRNAs after myocardial infarction reveals a role of miR-29 in cardiac fibrosis. *Proc Natl Acad Sci U S A* **105**, 13027-32 (2008).
24. Thum, T. et al. MicroRNA-21 contributes to myocardial disease by stimulating MAP kinase signalling in fibroblasts. *Nature* **456**, 980-4 (2008).
25. Syed, I.S., Sanborn, T.A. & Rosengart, T.K. Therapeutic angiogenesis: a biologic bypass. *Cardiology* **101**, 131-43 (2004).
26. Fish, J.E. et al. miR-126 regulates angiogenic signaling and vascular integrity. *Dev Cell* **15**, 272-84 (2008).

27. Di Gregoli, K. et al. MicroRNA-24 Regulates Macrophage Behavior and Retards Atherosclerosis. *Arterioscler Thromb Vasc Biol* (2014).
28. Schober, A. et al. MicroRNA-126-5p promotes endothelial proliferation and limits atherosclerosis by suppressing Dlk1. *Nat Med* **20**, 368-76 (2014).
29. Lemaitre, M., Bayard, B. & Lebleu, B. Specific antiviral activity of a poly(L-lysine)-conjugated oligodeoxyribonucleotide sequence complementary to vesicular stomatitis virus N protein mRNA initiation site. *Proc Natl Acad Sci U S A* **84**, 648-52 (1987).
30. Boutla, A., Delidakis, C. & Tabler, M. Developmental defects by antisense-mediated inactivation of micro-RNAs 2 and 13 in Drosophila and the identification of putative target genes. *Nucleic Acids Res* **31**, 4973-80 (2003).
31. Wu, H. et al. Determination of the role of the human RNase H1 in the pharmacology of DNA-like antisense drugs. *J Biol Chem* **279**, 17181-9 (2004).
32. Smith, C.C., Aurelian, L., Reddy, M.P., Miller, P.S. & Ts'o, P.O. Antiviral effect of an oligo(nucleoside methylphosphonate) complementary to the splice junction of herpes simplex virus type 1 immediate early pre-mRNAs 4 and 5. *Proc Natl Acad Sci U S A* **83**, 2787-91 (1986).
33. Davis, S. et al. Potent inhibition of microRNA in vivo without degradation. *Nucleic Acids Res* **37**, 70-7 (2009).
34. Davis, S., Lollo, B., Freier, S. & Esau, C. Improved targeting of miRNA with antisense oligonucleotides. *Nucleic Acids Res* **34**, 2294-304 (2006).
35. Hutvagner, G., Simard, M.J., Mello, C.C. & Zamore, P.D. Sequence-specific inhibition of small RNA function. *PLoS Biol* **2**, E98 (2004).
36. Wolfrum, C. et al. Mechanisms and optimization of in vivo delivery of lipophilic siRNAs. *Nat Biotechnol* **25**, 1149-57 (2007).
37. Krutzfeldt, J. et al. Silencing of microRNAs in vivo with 'antagomirs'. *Nature* **438**, 685-9 (2005).
38. Esau, C. et al. MicroRNA-143 regulates adipocyte differentiation. *J Biol Chem* **279**, 52361-5 (2004).
39. Esau, C. et al. miR-122 regulation of lipid metabolism revealed by in vivo antisense targeting. *Cell Metab* **3**, 87-98 (2006).
40. Thum, T. et al. Comparison of different miR-21 inhibitor chemistries in a cardiac disease model. *J Clin Invest* **121**, 461-2; author reply 462-3 (2011).
41. Rayner, K.J. et al. Inhibition of miR-33a/b in non-human primates raises plasma HDL and lowers VLDL triglycerides. *Nature* **478**, 404-7 (2011).
42. Vester, B. & Wengel, J. LNA (locked nucleic acid): high-affinity targeting of complementary RNA and DNA. *Biochemistry* **43**, 13233-41 (2004).
43. Elmen, J. et al. LNA-mediated microRNA silencing in non-human primates. *Nature* **452**, 896-9 (2008).
44. Weiler, J., Hunziker, J. & Hall, J. Anti-miRNA oligonucleotides (AMOs): ammunition to target miRNAs implicated in human disease? *Gene Ther* **13**, 496-502 (2006).
45. Hinkel, R. et al. Inhibition of microRNA-92a protects against ischemia/reperfusion injury in a large-animal model. *Circulation* **128**, 1066-75 (2013).
46. Swayze, E.E. et al. Antisense oligonucleotides containing locked nucleic acid improve potency but cause significant hepatotoxicity in animals. *Nucleic Acids Res* **35**, 687-700 (2007).
47. Lennox, K.A., Owczarzy, R., Thomas, D.M., Walder, J.A. & Behlke, M.A. Improved Performance of Anti-miRNA Oligonucleotides Using a Novel Non-Nucleotide Modifier. *Mol Ther Nucleic Acids* **2**, e117 (2013).
48. Akinc, A. et al. Targeted delivery of RNAi therapeutics with endogenous and exogenous ligand-based mechanisms. *Mol Ther* **18**, 1357-64 (2010).
49. Nielsen, P.E., Egholm, M., Berg, R.H. & Buchardt, O. Sequence-selective recognition of DNA by strand displacement with a thymine-substituted polyamide. *Science* **254**, 1497-500 (1991).
50. Smulevitch, S.V., Simmons, C.G., Norton, J.C., Wise, T.W. & Corey, D.R. Enhancement of strand invasion by oligonucleotides through manipulation of backbone charge. *Nat Biotechnol* **14**, 1700-4 (1996).

51. Fabani, M.M. & Gait, M.J. miR-122 targeting with LNA/2'-O-methyl oligonucleotide mixmers, peptide nucleic acids (PNA), and PNA-peptide conjugates. *RNA* **14**, 336-46 (2008).
52. Fabani, M.M. et al. Efficient inhibition of miR-155 function in vivo by peptide nucleic acids. *Nucleic Acids Res* **38**, 4466-75 (2010).
53. Kloosterman, W.P., Lagendijk, A.K., Ketting, R.F., Moulton, J.D. & Plasterk, R.H. Targeted inhibition of miRNA maturation with morpholinos reveals a role for miR-375 in pancreatic islet development. *PLoS Biol* **5**, e203 (2007).
54. Lin, C.Y. et al. miR-1 and miR-206 target different genes to have opposing roles during angiogenesis in zebrafish embryos. *Nat Commun* **4**, 2829 (2013).
55. Ebert, M.S., Neilson, J.R. & Sharp, P.A. MicroRNA sponges: competitive inhibitors of small RNAs in mammalian cells. *Nat Methods* **4**, 721-6 (2007).
56. Gentner, B. et al. Stable knockdown of microRNA in vivo by lentiviral vectors. *Nat Methods* **6**, 63-6 (2009).
57. Sayed, D. et al. MicroRNA-21 targets Sprouty2 and promotes cellular outgrowths. *Mol Biol Cell* **19**, 3272-82 (2008).
58. Fasanaro, P., Greco, S., Ivan, M., Capogrossi, M.C. & Martelli, F. microRNA: emerging therapeutic targets in acute ischemic diseases. *Pharmacol Ther* **125**, 92-104 (2010).
59. el Azzouzi, H. et al. The hypoxia-inducible microRNA cluster miR-199a approximately 214 targets myocardial PPARdelta and impairs mitochondrial fatty acid oxidation. *Cell Metab* **18**, 341-54 (2013).
60. Bonauer, A. et al. MicroRNA-92a controls angiogenesis and functional recovery of ischemic tissues in mice. *Science* **324**, 1710-3 (2009).
61. Montgomery, R.L. et al. Therapeutic inhibition of miR-208a improves cardiac function and survival during heart failure. *Circulation* **124**, 1537-47 (2011).
62. Lanford, R.E. et al. Therapeutic silencing of microRNA-122 in primates with chronic hepatitis C virus infection. *Science* **327**, 198-201 (2010).
63. Li, Y.P., Gottwein, J.M., Scheel, T.K., Jensen, T.B. & Bukh, J. MicroRNA-122 antagonism against hepatitis C virus genotypes 1-6 and reduced efficacy by host RNA insertion or mutations in the HCV 5' UTR. *Proc Natl Acad Sci U S A* **108**, 4991-6 (2011).
64. Hildebrandt-Eriksen, E.S. et al. A locked nucleic acid oligonucleotide targeting microRNA 122 is well-tolerated in cynomolgus monkeys. *Nucleic Acid Ther* **22**, 152-61 (2012).
65. Janssen, H.L. et al. Treatment of HCV infection by targeting microRNA. *N Engl J Med* **368**, 1685-94 (2013).
66. Soutschek, J. et al. Therapeutic silencing of an endogenous gene by systemic administration of modified siRNAs. *Nature* **432**, 173-8 (2004).
67. Juliano, R., Alam, M.R., Dixit, V. & Kang, H. Mechanisms and strategies for effective delivery of antisense and siRNA oligonucleotides. *Nucleic Acids Res* **36**, 4158-71 (2008).
68. Krutzfeldt, J. et al. Specificity, duplex degradation and subcellular localization of antagomirs. *Nucleic Acids Res* **35**, 2885-92 (2007).
69. Kastelein, J.J. et al. Potent reduction of apolipoprotein B and low-density lipoprotein cholesterol by short-term administration of an antisense inhibitor of apolipoprotein B. *Circulation* **114**, 1729-35 (2006).
70. van Dongen, M.G. et al. First proof of pharmacology in humans of a novel glucagon receptor antisense drug. *J Clin Pharmacol* (2014).
71. Raal, F.J. et al. Mipomersen, an apolipoprotein B synthesis inhibitor, for lowering of LDL cholesterol concentrations in patients with homozygous familial hypercholesterolaemia: a randomised, double-blind, placebo-controlled trial. *Lancet* **375**, 998-1006 (2010).
72. van Deutekom, J.C. et al. Local dystrophin restoration with antisense oligonucleotide PRO051. *N Engl J Med* **357**, 2677-86 (2007).
73. Goemans, N.M. et al. Systemic administration of PRO051 in Duchenne's muscular dystrophy. *N Engl J Med* **364**, 1513-22 (2011).

74. Henry, S.P. et al. Renal uptake and tolerability of a 2'-O-methoxyethyl modified antisense oligonucleotide (ISIS 113715) in monkey. *Toxicology* **301**, 13-20 (2012).
75. Voit, T. et al. Safety and efficacy of drisapersen for the treatment of Duchenne muscular dystrophy (DEMAND II): an exploratory, randomised, placebo-controlled phase 2 study. *Lancet Neurol* **13**, 987-96 (2014).
76. Lin, Z. et al. miR-23a functions downstream of NFATc3 to regulate cardiac hypertrophy. *Proc Natl Acad Sci U S A* **106**, 12103-8 (2009).
77. Li, R.C. et al. In vivo suppression of microRNA-24 prevents the transition toward decompensated hypertrophy in aortic-constricted mice. *Circ Res* **112**, 601-5 (2013).
78. Fiedler, J. et al. MicroRNA-24 regulates vascularity after myocardial infarction. *Circulation* **124**, 720-30 (2011).
79. Wahlquist, C. et al. Inhibition of miR-25 improves cardiac contractility in the failing heart. *Nature* **508**, 531-5 (2014).4. Thum, T. et al. MicroRNA-21 contributes to myocardial disease by stimulating MAP kinase signalling in fibroblasts. *Nature* **456**, 980-4 (2008).
80. Boon, R.A. et al. MicroRNA-34a regulates cardiac ageing and function. *Nature* **495**, 107-10 (2013).
81. Ucar, A. et al. The miRNA-212/132 family regulates both cardiac hypertrophy and cardiomyocyte autophagy. *Nat Commun* **3**, 1078 (2012).
82. Halkein, J. et al. MicroRNA-146a is a therapeutic target and biomarker for peripartum cardiomyopathy. *J Clin Invest* **123**, 2143-54 (2013).
83. Bernardo, B.C. et al. Therapeutic inhibition of the miR-34 family attenuates pathological cardiac remodeling and improves heart function. *Proc Natl Acad Sci U S A* **109**, 17615-20 (2012).
84. Heymans, S. et al. Macrophage microRNA-155 promotes cardiac hypertrophy and failure. *Circulation* **128**, 1420-32 (2013).
85. Patrick, D.M. et al. Stress-dependent cardiac remodeling occurs in the absence of microRNA-21 in mice. *J Clin Invest* **120**, 3912-6 (2010).
86. Icli, B. et al. MicroRNA-26a regulates pathological and physiological angiogenesis by targeting BMP/SMAD1 signaling. *Circ Res* **113**, 1231-41 (2013).
87. Bernardo, B.C. et al. Therapeutic silencing of miR-652 restores heart function and attenuates adverse remodeling in a setting of established pathological hypertrophy. *FASEB J* **28**, 5097-110 (2014).

CHAPTER 4

miR-148a regulates gp130-coupled signaling dynamics in heart failure

[1,2]Leonne E. Philippen, [1,3]Ellen Dirkx, [1]Rio Juni, [4]Amaya Fernandez-Celis, [1,5]Hamid el Azzouzi, [1]Andrea Raso, [1]Nicole Bitsch, [1]Serve Olieslagers, [5]Roel A. de Weger, [3]Mauro Giacca, [1,6]Paula A. da Costa Martins, [4]Natalia López-Andrés, [1]Leon J. De Windt

[1]Department of Cardiology, CARIM School for Cardiovascular Diseases, Maastricht University, 6229 ER Maastricht, The Netherlands; [2]Cardiovascular Research Institute, Baylor College of Medicine, Houston, Texas; Department of Molecular Physiology & Biophysics, Baylor College of Medicine, Houston, Texas USA; [3]Molecular Medicine, International Centre for Genetic Engineering and Biotechnology (ICGEB), AREA Science Park, Padriciano 99, 34149 Trieste, Italy; [4] Cardiovascular Translational Research, Navarrabiomed, Instituto de Investigación Sanitaria de Navarra (IdiSNA), Pamplona, Spain; [5]Department of Cardiology and Pathology, University Medical Center Utrecht, 3584 CX Utrecht, The Netherlands; [6]Department of Physiology and Cardiothoracic Surgery, Faculty of Medicine, University of Porto, Porto, Portugal.

In revision at EMBO Mol Med

Abstract

Heart failure, a major cause of morbidity, is preceded by ventricular remodeling, changes in left ventricular mass and volume of the myocardium in response to alterations in loading conditions. Concentric hypertrophy arises in pressure overload situations, involves wall thickening and often forms a substrate for left ventricular diastolic dysfunction. Eccentric hypertrophy develops in conditions of volume overload, results in wall thinning and chamber dilation and reduces ejection fraction. The molecular events that underlie these distinct forms of cardiac remodeling still remain poorly understood. Here, we demonstrate that expression of *miR-148a* changes dynamically in distinct subtypes of human and mouse forms of heart failure, where in human and mouse forms of concentric hypertrophy *miR-148a* expression is elevated, while forms of dilated cardiomyopathy are accompanied by profoundly decreased *miR-148a* myocardial expression. In line, antagomir mediated silencing of *miR-148a in vivo* resulted in spontaneous wall thinning, chamber dilation and an increased volume of the left ventricle associated with a reduced ejection fraction. Additionally, adeno-associated viral (AAV) delivery of *miR-148a* protected the mouse heart from pressure overload-induced systolic dysfunction by preventing the transition of concentric hypertrophic remodeling towards dilation. Mechanistically, *miR-148a* targets the cytokine co-receptor glycoprotein 130 (gp130) and connects the responsiveness of cardiomyocytes to extracellular cytokines to activation of Stat3 signaling by altering the abundance of gp130. These findings show the ability of *miR-148a* to prevent the transition of pressure-overload induced concentric hypertrophic remodeling towards eccentric hypertrophy and dilated cardiomyopathy and provide evidence for the existence of separate molecular programs that induce distinct forms of myocardial remodeling.

Introduction

Heart failure is a major cause of morbidity and death with little recent progress to reduce its high mortality. This disease is preceded by ventricular remodeling, changes in left ventricular mass and volume of the myocardium in response to alterations in loading conditions, with two distinct outcomes. Concentric hypertrophy results from cardiac growth and wall thickening which arises from pressure overload situations on the heart, as observed in patients with chronic hypertension, aortic valve stenosis or inherited forms of hypertrophic cardiomyopathy, and often yields a substrate for left ventricular diastolic dysfunction.[1,2] Contrary, eccentric hypertrophy often develops under conditions of volume overload of the myocardium, with mitral- and aortic regurgitation or familial dilated cardiomyopathy as clinical correlates, resulting in pronounced systolic dysfunction and a concomitant decrease in ejection fraction.[2] Pathological forms of concentric hypertrophy in certain hypertensive or aortic stenosis patients in time eventually gradually transform to eccentric remodeling of the heart and a worsening of prognosis.[3] Despite this spectrum of clinically relevant cardiac remodeling phenotypes, the molecular events that underlie these distinct forms of cardiac hypertrophy still remain poorly understood.[4] Accordingly, the stimulatory circulatory agonists, membrane-bound receptors and intracellular signaling cascades that connect biomechanical forces and the activation of myocardial stress pathways are central to understanding the initiation and progression to concentric *versus* eccentric hypertrophy.

Cardiotrophin-1 (CT-1), a member of the interleukin-6 cytokine superfamily, exerts its pleiotropic functions using a gp130 homodimer or gp130/leukemia inhibitory factor receptor-β (LIFRβ) heterodimer, induces eccentric hypertrophy in cultured primary cardiomyocytes *in vitro*[5-7] and exerts cardioprotective proliferative and survival effects in cultured embryonic, neonatal or adult cardiomyocytes.[8 9-11] *In vivo*, CT-1 treatment induces left ventricular dilation in rats.[12] In humans, increased CT-1 serum levels are observed in patients with unstable angina[13], acute myocardial infarction[14], hypertension, valvular diseases or heart failure[15], correlated with the degree of left ventricular systolic dysfunction[16,17] and left ventricular mass index in patients with dilated cardiomyopathy.[18 19]

Cytokines of the interleukin-6 superfamily couple to gp130 receptors and confer a level of cellular protection against cell death mechanisms in a variety of cardiac stress conditions, and genetic deletion strategies of gp130 or downstream signaling components render widespread cell death in the myocardium in response to biomechanical stress.[20-22] On the other hand, unrestrained activation of cytokine/gp130 signaling transmits prohypertrophic cues that facilitate the

transition to eccentric hypertrophy and systolic dysfunction[23], suggesting that the expression of gp130 is determinant in the balance between cellular survival pathways *versus* maladaptive hypertrophic remodeling in the myocardium.

Here, we demonstrate that cardiac expression of *miR-148a* alters dynamically in distinct subtypes of human and mouse forms of heart failure. In human and mouse forms of concentric hypertrophy *miR-148a* expression is elevated, while forms of dilated cardiomyopathy are accompanied by profoundly decreased *miR-148a* myocardial expression. In the heart, *miR-148a* targets gp130 and determines the extracellular cytokines responsiveness and cardiac signaling strength of canonical STAT3 hypertrophic signaling by altering the abundance of gp130. These findings provide evidence that myocardial *miR-148a* functions to prevent the transition of pressure-overload induced concentric hypertrophic remodeling towards eccentric hypertrophy and are proof of the existence of separable molecular cues that provoke distinct forms of hypertrophy in the early steps toward end-stage heart failure.

Results

miR-148a is dynamically expressed in heart failure subtypes

From microRNA profiling studies in human cardiac biopsies and mouse cardiac disease models, *miR-148a-3p* displayed opposite expression patterns depending on the type of heart disease studied. *miR-148a* is an intergenic microRNA, located on chromosome 6 or 7 in the murine and human genome, respectively, and distantly flanked by lncRNA genes (**Fig.1a**). The major mature *miR-148a* form in the heart is miR-148a-3p, which is fully conserved from the mouse to human genome, indicating an evolutionary pressure to resist variations in this microRNA gene (**Fig.1a**). Northern blotting revealed that *miR-148a* is broadly expressed in various tissues, with a relatively high expression in kidney, spleen and lung, to a lesser extent in liver and heart, and with traces of expression in brain, muscle and fat tissue (**Fig.1b**).

Most remarkable, *miR-148a* displayed an opposite direction of differential expression in human cardiac biopsies of end-stage heart failure, with a pronounced decrease of *miR-148a* in left ventricular biopsies of dilated cardiomyopathy compared to healthy controls (**Fig.1c**), compared to a pronounced four-fold increased expression of *miR-148a* in the left ventricular myocardium of patients with hypertrophic cardiomyopathy compared to the respective healthy controls (**Fig.1d**). Next, we compared cardiac miR-148a expression differences in mouse models of dilated or hypertrophic cardiac remodeling. Cysteine and glycine-rich protein 3 (*Csrp3*), also known as Muscle LIM Protein, is a Z disc protein involved in

cardiac mechanical stretch sensing and required for proper cardiac geometry, energy metabolism and function. Mice homozygous null for *Csrp3* develop early onset dilated cardiomyopathy and have been extensively used to study the pathophysiology of this subtype of heart failure. *Csrp3* null mice displayed a very strong reduction of *miR-148a* in left ventricular tissue (**Fig.1e**). In contrast, mice harboring a constitutively activated mutant of Calcineurin A (CnA) under control of the myosin heavy chain promoter (Myh6-CnA) develop severe hypertrophic concentric remodeling soon after birth. Hearts from young Myh6-CnA mice revealed an increase in *miR-148a* expression (**Fig.1f**). Taken together, cardiac *miR-148a* abundance is increased in human and mouse forms of concentric hypertrophic cardiac remodeling and decreased in human and mouse forms of eccentric remodeling or dilated cardiomyopathy.

miR-148a silencing provokes severe dilated cardiac remodeling

To begin to address the involvement of *miR-148a* in cardiac remodeling, we made use of an antagomir to specifically silence endogenous *miR-148a* expression *in vivo*, a situation that mimics cardiac *miR-148a* reduction as observed in hearts from human and mouse models of dilated cardiomyopathy (**Fig.1c,e**). To this end, we designed chemically modified antisense oligonucleotides to target either *Caenorhabditis elegans miR-39-5p* as control antagomir (antagomir-ctrl or antagomir-*Cel*-39) or *mmu-miR-148a-3p* (antagomir-148a). Antagomirs (80 mg/kg/day) were delivered by IP injection on three consecutive days to wild-type mice randomized to receive sham or transverse aortic constriction (TAC) surgery for six weeks (**Fig.2a**). Cardiac *miR-148a* expression was efficiently and specifically silenced (**Fig.2b**).

Remarkably, antagomir-148a treatment sufficed to provoke a form of dilated cardiomyopathy already in sham-operated mice as evidenced by increased cardiac geometry and mild fibrosis at six weeks after sham operation (**Fig.2c**). As expected, upon TAC surgery the heart weight to body weight ratio increased, however this was not further affected by the antagomir-148a treatment (**Fig.2d**). Analysis of cardiac function by Doppler/echocardiography revealed that antagomir-148a treated animals show a mildly reduced systolic contractile function (**Fig.2e, Table1**), provoked LV dilation accompanied by increased LV volumes (**Fig.2f,g**). As expected, TAC surgery in mice treated with a control antagomir provoked transient hypertrophic remodeling with relatively well-preserved cardiac function at three weeks (**Table1**). Six weeks of TAC surgery in mice treated with a control antagomir resulted in severe myocyte disarray, interstitial fibrosis, systolic and diastolic dysfunction, left ventricular dilation, increased heart weight as well as an induction of a “fetal” gene program (**Fig.2c-h, Table1**). Strikingly, cardiac histopathology,

cardiomyocyte hypertrophy, contractile function, the extent of left ventricular dilation and left ventricular volumes were exacerbated upon TAC surgery in the presence of *miR-148a* silencing (**Fig.2c-h, Table1**), without discernable differences between the level of activation of classical "fetal" gene programs in hearts from mice receiving TAC surgery and receiving a control antagomir versus hearts from mice receiving TAC surgery and receiving antagomir-148a (**Fig.2h**). Taken together, these data demonstrate that *miR-148a* silencing *in vivo* evokes mild cardiac dilation under baseline conditions in sham-operated mice and produced exacerbation of pressure overload-induced cardiac remodeling and dysfunction.

miR-148a overexpression suppresses pressure overload-induced cardiac dilation

Next, we mimicked the increased expression of *miR-148a* as observed in conditions of concentric cardiac remodeling in human hypertrophic cardiomyopathy (**Fig.1d,f**). To this end, we made use of the high cardiac tropism and prolonged expression of viral vectors based on adeno-associated virus (AAV) serotype 9 upon systemic delivery. AAV9 vectors expressing *mmu-miR-148a* or a control vector were administered intravenously via injection into the internal jugular vein of adult mice (**Fig.3a**). The hearts of AAV-148a injected animals displayed an induction of *miR-148a* of 4 fold over control on average (**Fig.3b**) and appeared morphologically normal with no signs of cardiomyocyte hypertrophy, changes in collagen content or capillary density (**Fig.3c and data not shown**), indicating that increased miR-148a alone is not an active driver of cardiac hypertrophy *in vivo* in the absence of further stimuli.

To analyze miR-148a cardiac function under forced stimulation, AAV9-148a and AAV9-MCS animals were randomized to receive sham or TAC surgery. Six weeks of TAC surgery in AAV9-MCS mice resulted in increased heart weight, severe myocyte disarray, interstitial fibrosis, increased cardiomyocyte size, systolic and diastolic dysfunction, left ventricular dilation, as well as an induction of the classical "fetal" gene program (**Fig.3c-g, Table2**). Strikingly, cardiac histopathology, cardiomyocyte hypertrophy, systolic function, the extent of left ventricular dilation and left ventricular volumes were clearly attenuated in AAV9-148a injected mice after TAC surgery (**Fig.3c-g, Table2**). AAV9-148a treated hearts only displayed an induction of the "fetal" gene Nppa at baseline compared to hearts from AAV9-MCS mice. A more pronounced induction of transcripts encoding *Nppa* or *Myh7* as part of the "fetal" gene program was observed in hearts from AAV9-148a injected mice receiving TAC surgery, but no differences were observed in *Nppb* or *Acta1* transcript abundance (**Fig.3h**). Taken together, these data demonstrate that elevation of cardiac *miR-148a* expression *in vivo* protects the myocardium from dilation and cardiac dysfunction following pressure overload.

miR-148a directly targets cardiac glycoprotein 130 (gp130)

To understand the mechanistic role of *miR-148a* in suppressing cardiac dilatation, we analyzed bioinformatics databases to search for *miR-148a* binding sites in cardiac expressed transcripts. MicroRNAs exert their action by regulating gene expression at the post-transcriptional level by imperfect base pairing with protein-coding transcripts. We identified an enrichment of three putative *miR-148a* seed regions in interleukin 6 signal transducer (*Il6st*), better known as glycoprotein 130 (gp130). The more proximal *miR-148a* binding site in the ~2.5 kb gp130 3'UTR demonstrated a perfect match for the *miR-148a* heptametrical seed sequence and showed complete evolutionary conservation (**Fig.4a**). To more directly establish the regulation of gp130 by *miR-148a* in the myocardium, we generated series of luciferase reporters harboring either the complete or truncated forms of the gp130 3'UTR, including a reporter with site-directed mutagenesis of key nucleotides in the *miR-148a* binding site (**Fig.4b**). Transient transfection of synthetic precursor *miR-148a* in cultured Cos7 cells decreased gp130 3'UTR reporter activity when either the intact ~2.5 kb 3'UTR or a distal truncation was coupled to luciferase compared to co-transfection with scrambled precursor molecules (**Fig.4c**). In contrast, a proximal truncation of the gp130 3'UTR, harboring two putative miR-148a binding sites, as well as a site-directed mutant of the complete gp130 3'UTR, remained unresponsive to synthetic precursor *miR-148a* molecules (**Fig.4c**). In line, endogenous gp130 protein expression in primary cardiomyocytes was derepressed by transfection of *miR-148a* antimir molecules, while pretreatment with *miR-148a* precursor molecules provoked significant downregulation of endogenous gp130 at the protein level (**Fig.4d**).

The gp130 co-receptor couples the responsiveness of the heart to cytokines from the interleukin-6 (IL-6) family, including IL-6, leukaemia inhibitory factor (LIF), oncostatin M or cardiotrophin-1, and intracellular MAPK, PI3K or JAK/STAT signaling by homodimerisation or heterodimerisation with LIF receptors at the cell surface. Cardiotrophin 1 (CT-1)-mediated gp130 activation and signaling is well known to induce eccentric hypertrophic remodeling and chamber dilatation. Despite clinical and experimental evidence that CT-1 levels are elevated in plasma and myocardium of patient with heart failure, direct evidence that CT-1 is sufficient to promote aspects of cardiac disease *in vivo* is conspicuously lacking in literature. To address whether *miR-148a* expression attenuates eccentric cardiac remodeling by attenuating gp130 responsiveness to CT-1, we compared cardiac phenotypes of mice that were either left untreated, infused with 20 μg/kg/day of CT-1[12] or infused with 60 mg/kg/day isoproteronol[24] for two weeks (**Fig. 4e**). The data demonstrate that isoproterenol exposure produced a classical cardiac hypertrophy response accompanied by increased cardiac mass and wall thickening, interstitial fibrosis, and

reduced ejection fraction (**Fig.4f-i**). Remarkably, sustained CT-1 exposure produced typical features of eccentric remodeling with mild cardiac enlargement, wall thinning and severe systolic dysfunction (**Fig.4f-i**). Having established that CT-1 is a direct stimulator of eccentric cardiac remodeling *in vivo*, we observed that primary cardiomyocytes responded to CT-1 with a mild hypertrophic response *in vitro*, which was clearly attenuated by transfection of synthetic precursor *miR-148a* molecules (**Fig.4j,k**). Taken together, these data provide evidence for miR-148a-based regulation of gp130 expression in the adult heart, influencing the responsiveness of the heart to the pro-hypertrophic agonist CT-1.

miR-148a dynamically influences gp130 downstream signaling

The CT-1/gp130 co-receptor axis has been reported to result in ERK1/2 or ERK5 MAPK, PI3K/Akt or JAK/STAT3 downstream signaling activation in the heart [11]. *miR-148a* expression was found increased in forms of concentric hypertrophic cardiac remodeling, while its expression was downregulated in forms of eccentric cardiac remodeling (**Fig.1**). To mimic this dynamic expression pattern *in vivo* and study the ramifications of differential *miR-148a* expression on gp130 expression levels and downstream signaling events in the intact heart, we subjected cohorts of mice to pressure overload by TAC, serially assessed cardiac geometry and function and sacrificed mice at 0 weeks (sham) or 2, 4, 6 or 8 weeks of TAC to measure cardiac *miR-148a* expression and evaluate the activation status of signaling cascades (**Fig.5a**). In line with our previous observations[25-27], concentric hypertrophic remodeling with sustained systolic function was evident in mice in the first four weeks following TAC surgery, which gradually transitioned to eccentric remodeling and loss of systolic contractile performance. First, *miR-148a* expression gradually increased up to ten fold in pressure-overloaded hearts following 2 or 4 weeks of TAC compared to hearts from sham-operated mice (**Fig.5b**). In this time period, pressure-overloaded hearts increased in heart mass but still displayed sustained systolic function and showed no signs of left ventricular dilation, consistent with concentric hypertrophic remodeling (**Fig.5c-e**). More prolonged periods of pressure overload induced a subsequent steep reduction of cardiac *miR-148a* expression, resulting in a significantly lower *miR-148a* expression at 8 weeks of pressure overload compared to sham-operated mice (**Fig.5b**). Interestingly, at 6 and 8 weeks following TAC, when *miR-148a* expression steeply reduced, left ventricular mass did not change further but systolic function was drastically reduced and hearts displayed substantial left ventricular dilation concordant with eccentric cardiac remodeling (**Fig.5c-e**). Conclusively, in sustained pressure overload, concentric cardiac remodeling in early phases correlated with high *miR-148a* expression, while eccentric cardiac remodeling in later phases correlated with low expression of *miR-148a*.

Using this model of transient elevation and reduction of *miR-148a* accompanied with a phenotypic switch from concentric to eccentric cardiac remodeling, we assessed expression and activation status of the CT-1/gp130 co-receptor axis. The data show that cardiac CT-1 levels gradually increases in time with the pressure overload stimulus (**Fig.5f**). Interestingly, the expression of the direct *miR-148a* target gene gp130 was reduced by ~50% at week 4 after TAC, a time point that coincides with the highest induction of cardiac *miR-148a* expression (**Fig.5g**). No changes in LIF receptor expression were evident during this time period (**Suppl.Fig.1a**), further lending support to the specificity of the interaction between *miR-148a* and gp130. A reduction in gp130 expression would be expected to result in ramifications in the activation status of downstream ERK1/2 or ER5 MAPK, PI3K/Akt or JAK/STAT3 signaling. Indeed, in this model of sustained pressure overloading, a reduction in both phosphorylated STAT3 (**Fig.5h**) and phosphorylated Akt **(Suppl.Fig.1b**), but not total STAT3 or Akt expression, was evident at early time points after TAC, which coincided with the highest induction of cardiac *miR-148a* expression and lowest expression of gp130 (**Fig.5b,g**). No changes in ERK5 or ERK1/2 activation were evident at the time points analyzed (**Suppl.Fig.1c,d**).

Next, we also verified gp130 expression levels and STAT3, Akt, ERK5 or ERK1/2 MAPK activation status in hearts from mice that received antagomir to specifically silence endogenous *miR-148a* expression *in vivo*, a situation that mimics *miR-148a* reduction as observed in hearts from human and mouse models of dilated cardiomyopathy. In sham-operated mice receiving antagomir-148a, which spontaneously produced features of eccentric cardiac remodeling, gp130 protein expression as well as increased activation of STAT3 and ERK1/2 was evident (**Fig.5i, Suppl.Fig.1e**). No clear differences in downstream signaling of antagomir-148a on the pressure-overloaded myocardium were evident. Finally, we compared gp130 expression levels and STAT3, Akt, ERK5 or ERK1/2 MAPK activation status in hearts from pressure-overloaded mice that AAV9-MCS or AAV9-148a to increase endogenous *miR-148a* expression *in vivo*, a situation that mimics the situation we observed in hearts from human and mouse models of concentric cardiac remodeling. Here, a clear reduction in gp130 expression and a reduction in the activation status of STAT3 were evident (**Fig.5j, Suppl.Fig.1f**). Combined, our data reveal that *miR-148a* expression regulates cardiac gp130 expression and alters the responsiveness of the heart to cardiotrophin-1 stimulation and downstream STAT3 signaling strength, where relatively high miR-148a expression produces forms of concentric hypertrophic remodeling and dampens CT-1 overstimulation with deleterious eccentric cardiac remodeling (**Fig.5k**).

Discussion

Here, we demonstrate that cardiac expression of *miR-148a* alters dynamically in distinct subtypes of human and mouse forms of heart failure, with high *miR-148a* expression in human and mouse forms of concentric hypertrophy and decreased *miR-148a* expression in forms of dilated cardiomyopathy. Mechanistically, *miR-148a* targets an evolutionary conserved heptametrical seed region in gp130, a pivotal co-receptor for cytokines of the interleukin 6 superfamily, and determines the coupling between extracellular cardiotrophin-1 and cardiac signaling strength of the canonical STAT3, Akt, Erk5 and Erk1/2 hypertrophic cascades by altering the abundance of gp130. Using complimentary gain- and loss-of-function studies for *miR-148a* in the mouse, we demonstrate that the abundance of *miR-148a*, and consequently gp130, connects sustained biomechanical forces to diverse forms myocardial remodeling, with an overall conclusion that miR-148a expression acts as a protective molecular driver that promotes wall thickening and concentric remodeling. *Vice versa*, lowering of cardiac miR-148a expression results in increased gp130 expression leading to enhanced gp130-coupled intracellular signaling, and incites wall thinning and chamber dilation with the associated increase in stress on the ventricular wall, representing the first irreversible steps towards overt heart failure in dilated cardiomyopathy. Our findings are proof of the existence of separable molecular programs primary to concentric hypertrophy *versus* eccentric hypertrophy, chamber narrowing *versus* chamber dilation and wall thickening *versus* wall thinning, all occurring within the venue of biomechanical driven pathways of cardiac growth and failure.

Cardiac remodeling in patients with heart disease encompass all quantifiable changes in left ventricular mass and volume, with a wide variety in the ratio of left ventricular wall thickness to chamber radius, often referred to as relative wall thickness (RWT), and diagnosed by echocardiographic, and cardiac magnetic resonance imaging (MRI) data.[3] A normal left ventricular chamber size refers to normal geometry; differences in RWT distinguish concentric from normal and from eccentric remodeling. Concentric hypertrophy tend to arise from pressure overload situations on the heart, as observed in patients with aortic valve stenosis or hypertensive heart diseases, often yielding a substrate for left ventricular diastolic dysfunction. In contrast, eccentric hypertrophy develops secondary to conditions of volume overload of the myocardium, clinically observed in mitral and aortic regurgitation, precipitating in a strong reduction of ejection fraction.[3] Despite the existence of a relatively detailed clinical diagnosis and physiological underpinnings of this spectrum of clinically relevant remodeling phenotypes, the molecular events that underlie distinct forms of cardiac hypertrophy still remain poorly charted.[28] Accordingly, the stimulatory circulatory agonists, membrane-bound receptors and

intracellular signaling cascades that connect biomechanical forces and the activation of myocardial stress pathways are central to understanding the initiation and progression to concentric hypertrophy as clinically observed in hypertrophic cardiomyopathies versus eccentric hypertrophy as it occurs in forms of dilated cardiomyopathy.

In the heart, cardiotrophin-1 signals through a gp130 homodimer or gp130/leukemia inhibitory factor receptor-β (LIFRβ) heterodimer in cultured cardiomyocytes and was reported to induce a peculiar form of hypertrophy with increased cardiomyocyte size that is characterized by an increase in cell length but no significant change in cell width due to the assembly of sarcomeric units in series rather than in parallel, as is more commonly observed following stimulation with the canonical pro-hypertrophic adrenergic agonists or endothelin-1.[6,7] The involvement of ERK5 and STAT3 in cardiotrophin-1-induced longitudinal elongation has been reported in adult cardiomyocytes[7], and it is further supported by the molecular observation that overexpression of activated ERK5 induces serial insertion of sarcomeres in neonatal cardiomyocytes *in vitro.*[29] Interestingly, STAT3 upregulates ERK5 in other cell types (Song H, Oncogene 2004). Thus, the possibility that STAT3 mediates the longitudinal elongation through the downstream activation of ERK5, which determines cardiomyocyte elongation, requires further investigations. These morphological differences find a basis in the activation of distinct signaling cascades and proteomic outcomes between cytokines from the interleukin-6 superfamily or endothelin-1.[30] Elongated cardiomyocytes, myocardial dilation and decreased ejection fraction were also evident following 6 weeks of cardiotrophin-1 treatment in rats.[7] In line, in the current study we developed and characterized a mouse model with continuous cardiotrophin-1 infusion at a clinically relevant concentration of 20 µg/kg/day, which displayed the hallmarks of eccentric hypertrophy after two weeks: wall thinning, severe chamber dilation and a stark reduction in ejection fraction, in line with LV chamber dilatation and decreases ejection fraction in rats following continuous infusion of cardiotrophin-1. The cardiotrophin-1 infusion rodent models may proof useful for future studies examining the biochemical, geometric or functional ramifications of distinct hypertrophic agonists on the myocardium.

Genetic studies on the involvement of gp130 in cardiac remodeling reveal a requirement of gp130-dependent signaling for myocyte survival pathways, on the one hand, as well as transmitting prohypertrophic signals, on the other. Indeed, myocyte-restricted deletion of gp130 yields massive apoptotic cell death and rapid onset of dilated cardiomyopathy following biomechanical stress.[20] Heart-restricted overexpression of a dominant negative form of gp130 suppressed many molecular and morphological features of pressure overload-induced concentric hypertrophic

remodeling.[21] The molecular decision between survival and hypertrophy is regulated by the interplay between gp130-mediated JAK/STAT activation and suppressor of cytokine signaling 1/3 (SOCS1/3), intrinsic JAK inhibitors and negative feedback regulators for gp130 signaling. Adenovirus-mediated gene transfer of SOCS3 to ventricular cardiomyocytes completely suppressed both hypertrophy and antiapoptotic phenotypes in cultured cardiomyocytes induced by leukemia inhibitory factor (LIF).[31] Adeno-associated viral transfer of SOCS1 dampened JAK/STAT activation and the transition of hypertrophy to failure in a pressure overload model *in vivo.*[32] Cardiac-specific SOCS3 knockout mice demonstrated enhanced activation of the signaling targets STAT3, Akt, ERK1/2 - and p38 MAPK and spontaneous cardiac eccentric remodeling, occurrence of arrhythmias and signs of heart failure, all of which were dependent on the presence of gp130, since SOCS3/gp130 double knockout mice displayed suppression of the cardiomyopathic phenotype.[33] Further downstream of gp130, a variety of signaling branches are differentially activated by IL-6 cytokines, including the ERK1/2, p38 and ERK5 MAPK terminal branches, JAK/STAT3, PI3K/Akt, Gab1/SHP2 and RhoA.[11,34,35] In line, Mek5 transgenic mice displayed a severe form of eccentric remodeling with wall thinning, chamber dilation and severe fibrosis[29], a phenotype that was largely recapitulated by silencing endogenous *miR-148a* using an antagomir strategy in the current study. In contrast, STAT3-deficient mice spontaneously develop signs of injury, inflammation and cardiac dysfunction with advancing age and in response to cardiac stress. Accordingly, the prevailing message supports a model where IL-6 cytokine/gp130 confers a level of protective signaling in a variety of cardiac stress conditions, and that complete (genetic) deletion of gp130 signaling components causes widespread cell death. On the other hand, unrestrained activation of cytokine/gp130 signaling also confers prohypertrophic cues that facilitate the transition to eccentric hypertrophy and systolic dysfunction in situations of biomechanical stress. This model of cytokine/gp130 signaling is in line with a regulatory function of cardiac *miR-148a,* where higher *miR-148a* expression, and concomitantly reduced gp130 expression, sustains the protective cell survival effects while dampens over-activation of downstream signaling cascades, yielding concentric forms of hypertrophy. With sustained periods of biomechanical stress, decreased *miR-148a* expression, and concomitant derepression of gp130, promotes over-activation of a variety of hypertrophic intracellular signals, yielding eccentric hypertrophic remodeling, dilated cardiomyopathy and systolic dysfunction. As such, the biphasic regulation of *miR-148a* provides a mechanistic explanation for the clinically observed transition from early phase “compensatory” forms of hypertrophy to later phase decompensation and overt heart failure in the setting of sustained biomechanical stress.

Materials and Methods

Human heart samples. Approval for studies on human tissue samples was obtained from the Medical Ethics Committee of the University Medical Center Utrecht, The Netherlands. All patients or their relatives gave written informed consent before operation. In this study, we included tissue from the left ventricular free wall of patients with end-stage heart failure secondary to ischemic heart disease. Control tissue was taken from the left ventricular free wall of refused donor hearts. Failing hearts were also obtained from patients undergoing heart transplantation because of terminal heart failure. Non-failing donor hearts that could not be transplanted for technical reasons were used for comparison, where neither donor patient histories nor echocardiography revealed signs of heart disease.

Mouse models. Mice used in this study were male and female B6CBAF1 wild-type mice (Charles River Laboratories) of 2–6 months of age. Other mice used in this study were male calcineurin transgenic mice in a B6CBAF1 background expressing an activated mutant of calcineurin in the postnatal heart under control of the 5.5 kb murine *Myh6* promoter (Myh6-CnA[36]). Sample size was determined by a power calculation based on an echocardiographic effect size. Randomization of subjects to experimental groups was based on a single sequence of random assignments. Animal caretakers and investigators were blinded to group allocation during the experiment and/or when assessing the outcome. All protocols were performed according to institutional guidelines and approved by local Animal Care and Use Committees. All mice were housed were housed on a 12hr:12hr light:dark cycle in a temperature-controlled environment with *ad libitum* access to water and chow at Innoser Netherlands BV, a commercial mouse breeding company with a quarterly animal health monitoring system that complies with FELASA guidelines and recommendations.

Aortic banding, CT-1 infusion and transthoracic echocardiography. Transverse aortic constriction (TAC) or sham surgery was performed in 2-month-old wildtype B6CBAF1 female and male mice by subjecting the aorta to a defined 27-gauge constriction between the first and second truncus of the aortic arch, as described previously.[25,37] For Doppler-echocardiography, mice were shaved, lightly anaesthetized with isoflurane (mean 1% in oxygen) and allowed to breathe spontaneously through a nasal cone. Non-invasive, echocardiography was performed as describes previously in detail.[26] Doppler was used to calculate the pressure gradient between the proximal and distal sites of the transverse aortic constriction and only mice with a pressure gradient >50 mm Hg were included. Chronic cardiotrophin 1 (20 μg/kg/day dissolved in phosphate-buffered saline),

isoproterenol (60 mg/kg/day dissolved in phosphate-buffered saline) or saline administration was performed using Alzet miniosmotic pumps (no. 2002; Alza) surgically inserted dorsally and s.c. in 2-month-old wild-type B6CBAF1 female and male mice under isoflurane anesthesia and left for an additional 2 weeks. All protocols were performed according to institutional guidelines and approved by local Animal Care and Use Committees.

Antagomir studies. Chemically modified antisense oligonucleotides designed to target *mmu-miR-148a-3p* (5′-ACAAAGUUCUGUAGUGCAC-3′/3CholTEG-3′ or *C.elegans miR-39-5p* (5′-AAGGCAAGCUGACCCUGAAGUU-3′/3CholTEG-3′) with a 3′ cholesterol conjugation and 2 phosphorothioate bonds at the very first 5′ end and 4 phosphorothioate bonds between the last 3′ bases [38] were synthesized at Integrated DNA Technologies (IDT). All antagomirs were HPLC purified and desalted before use. Female and male wild-type B6CBAF1 mice (8–10 weeks of age) were subjected to sham or TAC surgery. Following 3 days, mice were injected (intraperitoneally) with antagomir-148a (80 mg kg^{-1} body weight) or control antagomir (80 mg kg^{-1} body weight) for 3 consecutive days. Echo analysis was performed at 3 weeks and 6 weeks after surgery.

AAV Vectors. All of the AAV vectors used in this study were generated by the International Centre for Genetic Engineering and Biotechnology (ICGEB) AAV Vector Unit (AVU) (www.icgeb.org/avu-core-facility.html) using a dual/triple plasmid cotransfection procedure followed by PEG precipitation and purification through CsCl2 gradient centrifugations as described previously.[39] Adult mice were intravenously injected with AAV9-MCS and AAV9-miR-148a via the jugular vein at a dose of $1x10^{12}$ viral genome particles per animal.

Primary cardiomyocytes cultures and immunocytochemistry. Cardiomyocyte cultures were isolated by enzymatic dissociation of 1–2-day-old neonatal rat hearts and processed for immunofluorescence microscopy as described previously.[40] Neonatal cardiomyocytes were transfected with precursors (Ambion) and inhibitors (Exiqon) of microRNAs (10 nM) using Oligofectamine (Invitrogen). For visualization of cardiomyocyte size and sarcomeric organization, the cells were stained for α2-actinin with mouse monoclonal anti-sarcomeric α-actinin antibody (Sigma-Aldrich, A7811 clone EA-53, 1:500) followed by rat anti-mouse phenylephrine–Texas red-conjugated monoclonal antibody (Life Technologies, RM2817 clone M1/70.15, 1:800). Nuclear staining was performed with VECTASHIELD Mounting Medium (Vector Laboratories) containing 4′,6-diamidino-2-phenylindole (DAPI). Myocyte

hypertrophy was induced by stimulation for 24 h with phenylephrine (10 µM) as described previously[40] or with Cardiotrophin-1 (CT-1, 2nM).

pMIR-reporter assays. Cos7 cells were purchased at the American Type Culture Collection (ATCC; CRL-1651) and cultured in DMEM supplemented with 10% FBS, 100 units/ml penicillin/streptomycin and 2 mmol/liter L-glutamine (Thermo Fischer). Cos7 cells were screened for mycoplasma with the MycoAlert PLUS Mycoplasma Detection kiet (Lonza) upon receipt from ATCC and subsequently checked on a yearly basis. Cos7 cells were transfected with pMIR reporter plasmids harboring the entire 3' UTR of mouse gp130, or with pMIR reporter plasmids harboring the first part of the 3' UTR of mouse gp130, or with pMIR reporter plasmids harboring the latter section of the gp130 3' UTR using X-tremeGENE 9 (Roche) transfection reagent, followed by transfection with *miR-148a* or scrambled miR precursor molecules using Oligofectamine reagent (Thermo Fisher). Luciferase activity was measured 24 h after transfection with a dual luciferase assay kit (Promega) using Renilla luciferase as internal control to correct for transfection efficiency.

Northern blot analysis. Northern blotting was performed as described previously[26] using 3'-digoxigenin-labelled locked nucleic acid oligonucleotides for *miR-148a* and U6 small nuclear RNA (*Rnu6-2*). Detection was achieved with Fab fragments from polyclonal anti-digoxigenin antibodies, conjugated to alkaline phosphatase (Roche).

Western blot analysis. SDS PAGE electrophoresis and blotting were performed as described previously.[7] Primary antibodies that were used included anti-gp130 (Cell Signaling Technology; rabbit pAb cat. no. 3732), anti-LIFR (Santa Cruz Biotechnology; mouse mAb cat sc-515337), anti-CT-1 (Santa Cruz Biotechnology; mouse mAb cline AN-B3 cat. no. sc-9991), anti-GAPDH (Millipore; mouse mAb clone 6C5, cat. no. MAB374), anti-STAT3 (Cell Signaling Technology; mouse mAb clone 124H6, cat. no. 9139), anti-phospho-STAT3 (p-Tyr705) (Cell Signaling Technology; mouse mAb clone M9C6 cat. no. 4113), anti-Akt (Cell Signaling Technology; mouse mAb clone 2H10 cat. no. 2967), anti-phospho-Akt (pSer473) (Cell Signaling Technology; rabbit mAb clone D7F10 cat. no. 9018), anti-p44/42 MAPK (ERK1/2) (Cell Signaling Technology; rabbit mAb clone 137F5 cat. no. 4695), anti-phopsho-p44/42 MAPK (p-Thr202-204-Erk1/2) (Cell Signaling Technology; rabbit mAb clone D13.14.4E cat. no. 4370), anti-ERK5 (Cell Signaling Technology' rabbit mAb clone D3I5V cat. no. 12950), anti-phospho-ERK5 (p-Thr218/Tyr220) (Cell Signaling Technology; rabbit pAb cat. no. 3371) followed by corresponding horseradish peroxidase (HRP)-conjugated

secondary antibodies and enhanced chemiluminescence ECL detection. Western Blots were performed with Stain Free gels for loading control. Signals were detected using the ECL system (Amersham Pharmacia Biotech; Piscataway, NJ, USA). Results are expressed as an n-fold increase over the values of the control group in densitometric arbitrary units.

Quantitative real-time PCR. Total RNA (1 µg) was applied to either miR-based or mRNA-based reverse transcription. Real-time PCR was performed on a BioRad iCycler (Biorad) using SYBR Green. Transcript quantities were compared using the relative Ct method, where the amount of target normalized to the amount of endogenous control (L7) and relative to the control sample is given by $2^{-\Delta\Delta Ct}$. For microRNA real-time PCR, miRNAs were isolated with TRIzol reagent (Invitrogen) and cDNA was generated with the miScript Reverse Transcription Kit (Qiagen). For real-time PCR detection of miRNAs, miScript Primer Assays and the miScript SYBR Green PCR Kit (Qiagen) were used.

microRNA target prediction. Putative microRNA-148a target genes were identified using the microRNA databases and target prediction tools miRBase (http://microrna.sanger.ac.uk/), PicTar (http://pictar.mdc-berlin.de/) and TargetScan (http://targetscan.org/index.html).

Histological analysis and (immunofluorescence) microscopy. Hearts were arrested in diastole, perfusion fixed with 4% paraformaldehyde/PBS solution, embedded in paraffin and sectioned at 4 µm. Paraffin sections were stained with haematoxylinand eosine for routine histological analysis; Sirius red for the detection of fibrillar collagen; and FITC-labelled wheat-germ-agglutinin (Sigma-Aldrich, 1:100) to visualize and quantify myocyte cross-sectional area. Slides were visualized using a Zeiss Axioskop 2Plus with an AxioCamHRc. Cell surface areas were determined using ImageJ imaging software (http://rsb.info.nih.gov/ij/).

Statistical analysis. The results are presented as mean ± standard error of the mean. Statistical analyses were performed using Prism software (GraphPad Software Inc.), and consisted of ANOVA followed by Bonferroni's Multiple Comparison Test when group differences were detected at the 5% significance level, or Student's *t*-test when comparing two experimental groups. For Western blots analysis, normality of distributions was verified by means of the Kolmogorov–Smirnov test. Data were analyzed using a one-way analysis of variance, followed by a Newman-Keuls to assess specific differences among groups. Differences were considered significant when $P<0.05$.

ACKNOWLEDGEMENTS

We gratefully acknowledge members of the De Windt laboratory for technical support and helpful discussions. E.D. is supported by a VENI award 916-150-16 from the Netherlands Organization for Health Research and Development (ZonMW), P.D.C.M. is supported by a MEERVOUD grant from The Netherlands Organisation for Scientific Research (NWO) and is an Established Investigator of the Dutch Heart Foundation. N.L.A. is supported by Miguel Servet contract CP13/00221 from the "Instituto de Salud Carlos III-FEDER". L.D.W. acknowledges support from the *Netherlands CardioVascular Research Initiative*: the Dutch Heart Foundation, Dutch Federation of University Medical Centers, ZonMW and the Royal Netherlands Academy of Sciences. L.D.W. was further supported by grant 311549 from the European Research Council (ERC) and a VICI award 918-156-47 from NWO.

AUTHOR CONTRIBUTIONS

L.E.P., E.D., R.J., A.F.C., H.E.A., A.R., N.B. and S.O. performed experiments. L.E.P., E.D., P.D.C.M., N.L.A. and L.D.W. analyzed data. L.E.P., E.D., P.D.C.M. and L.D.W. designed the study. R.D.W, M.G. and N.L.A. provided reagents, models or data. L.E.P., E.D., P.D.C.M., N.L.A. and L.D.W. wrote the manuscript.

CONFLICT OF INTERESTS

P.D.C.M. and L.D.W. are co-founders and stockholders of Mirabilis Therapeutics BV. The data in the manuscript were not filed for patent protection.

THE PAPER EXPLAINED

Problem

The heart responds to stress situations by altering its mass, volume and geometry with two outcomes. In patients with chronic hypertension, aortic valve stenosis or inherited forms of hypertrophic cardiomyopathy, the heart walls typically thickens and displays abnormalities in relaxation in a process called concentric hypertrophic remodeling. In contrast, in patients with valvular disease or inherited forms of dilated cardiomyopathy, the heart walls typically become thinner, the chamber volume increases and systolic contraction force reduces in a process called eccentric hypertrophic remodeling. Although these subsets of myocardial remodeling have different clinical outcomes, virtually no information is available on the molecular events that distinguish concentric versus eccentric cardiac remodeling.

Results

Here, we demonstrate that the expression of a non-coding RNA gene, microRNA-148a (*miR-148a*), alters in opposite fashion in these two distinct subtypes of human and mouse forms of cardiac remodeling. In concentric hypertrophy *miR-148a* expression is elevated, while in forms of dilated cardiomyopathy myocardial *miR-148a* expression is strongly reduced. MicroRNAs target protein-coding messenger RNAs and control the translation of their protein. Mechanistically, we found that *miR-148a* is able to reduce the expression of the cytokine co-receptor glycoprotein 130 (gp130). When miR-148a expression is relatively high, gp130 expression is reduced, rendering cardiac muscle cells less responsive to cytokine stimulation by cardiotrophin-1, which promotes eccentric cardiac remodeling. Conversely, reduced miR-148a expression allows increased expression of gp130, increased sensitivity to cardiotrophin-1 stimulation, increased intracellular Stat3 signaling and increased eccentric remodeling.

Impact

These results demonstrate that *miR-148a* can reduce the transition of concentric hypertrophic remodeling towards eccentric hypertrophy and molecular programs exist that distinguish between these two opposite forms of cardiac remodeling. Additionally, new therapeutic approaches aimed to maintain myocardial *miR-148a* expression elevated in cardiac stress may protect the heart from eccentric remodeling and reduced systolic function.

REFERENCES

1 Opie, L. H., Commerford, P. J., Gersh, B. J. & Pfeffer, M. A. Controversies in ventricular remodelling. *Lancet* **367**, 356-367 (2006).

2 Dorn, G. W., 2nd, Robbins, J. & Sugden, P. H. Phenotyping hypertrophy: eschew obfuscation. *Circulation research* **92**, 1171-1175 (2003).

3 Gaasch, W. H. & Zile, M. R. Left ventricular structural remodeling in health and disease: with special emphasis on volume, mass, and geometry. *Journal of the American College of Cardiology* **58**, 1733-1740 (2011).

4 Heineke, J. & Molkentin, J. D. Regulation of cardiac hypertrophy by intracellular signalling pathways. *Nature reviews. Molecular cell biology* **7**, 589-600 (2006).

5 Pennica, D. *et al.* Expression cloning of cardiotrophin 1, a cytokine that induces cardiac myocyte hypertrophy. *Proceedings of the National Academy of Sciences of the United States of America* **92**, 1142-1146 (1995).

6 Wollert, K. C. *et al.* Cardiotrophin-1 activates a distinct form of cardiac muscle cell hypertrophy. Assembly of sarcomeric units in series VIA gp130/leukemia inhibitory factor receptor-dependent pathways. *The Journal of biological chemistry* **271**, 9535-9545 (1996).

7 Lopez, N., Diez, J. & Fortuno, M. A. Differential hypertrophic effects of cardiotrophin-1 on adult cardiomyocytes from normotensive and spontaneously hypertensive rats. *Journal of molecular and cellular cardiology* **41**, 902-913 (2006).

8 Sheng, Z., Pennica, D., Wood, W. I. & Chien, K. R. Cardiotrophin-1 displays early expression in the murine heart tube and promotes cardiac myocyte survival. *Development* **122**, 419-428 (1996).

9 Brar, B. K. *et al.* Cardiotrophin-1 can protect cardiac myocytes from injury when added both prior to simulated ischaemia and at reoxygenation. *Cardiovascular research* **51**, 265-274 (2001).

10 Liao, Z. *et al.* Cardiotrophin-1 (CT-1) can protect the adult heart from injury when added both prior to ischaemia and at reperfusion. *Cardiovascular research* **53**, 902-910 (2002).

11 Lopez, N., Diez, J. & Fortuno, M. A. Characterization of the protective effects of cardiotrophin-1 against non-ischemic death stimuli in adult cardiomyocytes. *Cytokine* **30**, 282-292 (2005).

12 Lopez-Andres, N. *et al.* Cardiotrophin 1 is involved in cardiac, vascular, and renal fibrosis and dysfunction. *Hypertension* **60**, 563-573 (2012).

13 Talwar, S., Squire, I. B., Downie, P. F., Davies, J. E. & Ng, L. L. Plasma N terminal pro-brain natriuretic peptide and cardiotrophin 1 are raised in unstable angina. *Heart* **84**, 421-424 (2000).

14 Talwar, S. *et al.* Plasma cardiotrophin-1 following acute myocardial infarction: relationship with left ventricular systolic dysfunction. *Clinical science* **102**, 9-14 (2002).

15 Talwar, S. *et al.* Elevated circulating cardiotrophin-1 in heart failure: relationship with parameters of left ventricular systolic dysfunction. *Clinical science* **99**, 83-88 (2000).

16 Pemberton, C. J., Raudsepp, S. D., Yandle, T. G., Cameron, V. A. & Richards, A. M. Plasma cardiotrophin-1 is elevated in human hypertension and stimulated by ventricular stretch. *Cardiovascular research* **68**, 109-117 (2005).

17 Lopez, B. *et al.* Is plasma cardiotrophin-1 a marker of hypertensive heart disease? *Journal of hypertension* **23**, 625-632 (2005).

18 Zolk, O., Ng, L. L., O'Brien, R. J., Weyand, M. & Eschenhagen, T. Augmented expression of cardiotrophin-1 in failing human hearts is accompanied by diminished glycoprotein 130 receptor protein abundance. *Circulation* **106**, 1442-1446 (2002).

19 Tsutamoto, T. *et al.* Relationship between plasma level of cardiotrophin-1 and left ventricular mass index in patients with dilated cardiomyopathy. *Journal of the American College of Cardiology* **38**, 1485-1490 (2001).

20 Hirota, H. *et al.* Loss of a gp130 cardiac muscle cell survival pathway is a critical event in the onset of heart failure during biomechanical stress. *Cell* **97**, 189-198 (1999).

21 Uozumi, H. *et al.* gp130 plays a critical role in pressure overload-induced cardiac hypertrophy. *The Journal of biological chemistry* **276**, 23115-23119 (2001).

22 Yoshida, K. *et al.* Targeted disruption of gp130, a common signal transducer for the interleukin 6 family of cytokines, leads to myocardial and hematological disorders. *Proceedings of the National Academy of Sciences of the United States of America* **93**, 407-411 (1996).
23 Kunisada, K. *et al.* Activation of gp130 transduces hypertrophic signals via STAT3 in cardiac myocytes. *Circulation* **98**, 346-352 (1998).
24 De Windt, L. J. *et al.* Targeted inhibition of calcineurin attenuates cardiac hypertrophy in vivo. *Proceedings of the National Academy of Sciences of the United States of America* **98**, 3322-3327 (2001).
25 Bourajjaj, M. *et al.* NFATc2 is a necessary mediator of calcineurin-dependent cardiac hypertrophy and heart failure. *The Journal of biological chemistry* **283**, 22295-22303 (2008).
26 da Costa Martins, P. A. *et al.* MicroRNA-199b targets the nuclear kinase Dyrk1a in an auto-amplification loop promoting calcineurin/NFAT signalling. *Nature cell biology* **12**, 1220-1227 (2010).
27 Dirkx, E. *et al.* Nfat and miR-25 cooperate to reactivate the transcription factor Hand2 in heart failure. *Nature cell biology* **15**, 1282-1293 (2013).
28 Torrado, M., Iglesias, R., Nespereira, B. & Mikhailov, A. T. Identification of candidate genes potentially relevant to chamber-specific remodeling in postnatal ventricular myocardium. *J Biomed Biotechnol* **2010**, 603159 (2010).
29 Nicol, R. L. *et al.* Activated MEK5 induces serial assembly of sarcomeres and eccentric cardiac hypertrophy. *The EMBO journal* **20**, 2757-2767 (2001).
30 Kuwahara, K. *et al.* Endothelin-1 and cardiotrophin-1 induce brain natriuretic peptide gene expression by distinct transcriptional mechanisms. *J Cardiovasc Pharmacol* **31 Suppl 1**, S354-356 (1998).
31 Yasukawa, H. *et al.* Suppressor of cytokine signaling-3 is a biomechanical stress-inducible gene that suppresses gp130-mediated cardiac myocyte hypertrophy and survival pathways. *The Journal of clinical investigation* **108**, 1459-1467 (2001).
32 Cittadini, A. *et al.* SOCS1 gene transfer accelerates the transition to heart failure through the inhibition of the gp130/JAK/STAT pathway. *Cardiovascular research* **96**, 381-390 (2012).
33 Yajima, T. *et al.* Absence of SOCS3 in the cardiomyocyte increases mortality in a gp130-dependent manner accompanied by contractile dysfunction and ventricular arrhythmias. *Circulation* **124**, 2690-2701 (2011).
34 Takahashi, N. *et al.* Hypertrophic responses to cardiotrophin-1 are not mediated by STAT3, but via a MEK5-ERK5 pathway in cultured cardiomyocytes. *Journal of molecular and cellular cardiology* **38**, 185-192 (2005).
35 Fahmi, A. *et al.* p42/p44-MAPK and PI3K are sufficient for IL-6 family cytokines/gp130 to signal to hypertrophy and survival in cardiomyocytes in the absence of JAK/STAT activation. *Cell Signal* **25**, 898-909 (2013).
36 Molkentin, J. D. *et al.* A calcineurin-dependent transcriptional pathway for cardiac hypertrophy. *Cell* **93**, 215-228 (1998).
37 Rockman, H. A. *et al.* Segregation of atrial-specific and inducible expression of an atrial natriuretic factor transgene in an in vivo murine model of cardiac hypertrophy. *Proceedings of the National Academy of Sciences of the United States of America* **88**, 8277-8281 (1991).
38 Krutzfeldt, J. *et al.* Silencing of microRNAs in vivo with 'antagomirs'. *Nature* **438**, 685-689 (2005).
39 Arsic, N. *et al.* Induction of functional neovascularization by combined VEGF and angiopoietin-1 gene transfer using AAV vectors. *Molecular therapy : the journal of the American Society of Gene Therapy* **7**, 450-459 (2003).
40 De Windt, L. J., Lim, H. W., Haq, S., Force, T. & Molkentin, J. D. Calcineurin promotes protein kinase C and c-Jun NH2-terminal kinase activation in the heart. Cross-talk between cardiac hypertrophic signaling pathways. *The Journal of biological chemistry* **275**, 13571-13579 (2000).

FIGURE LEGENDS

Figure 1 | **MicroRNA-148a is downregulated in heart failure. (a)** Schematic representation of the genomic localization and precursor sequence of *mmu-miR-148a* located on the opposite strand on chromosome 6 in the mouse genome. The mature *miR-148a-3p* strand is conserved among several species. **(b)** Northern blot analysis of *miR-148a-3p* expression in diverse mouse organs. **(c)** RT-PCR analysis of *miR-148a-3p* expression in non-failing and dilated cardiomyopathy human left ventricular myocardium. **(d)** RT-PCR analysis of *miR-148a-3p* expression in non-failing and hypertrophic cardiomyopathy human left ventricular myocardium. **(e)** RT-PCR analysis of *miR-148a-3p* expression in hearts from wild-type and *Csrp3* knockout mice, the gene encoding muscle LIM protein (MLP). **(f)** RT-PCR analysis of *miR-148a-3p* expression in hearts from 3 week-old non-transgenic littermates and Myh6-CnA transgenic mice.
Data information: Data are means ± SEM. Student's paired 2-tailed *t*-test was used to compare groups. *n*, number of hearts; RT-PCR, real-time-polymerase chain reaction; NF, non failing; DCM, dilated cardiomyopathy; HCM, hypertrophic cardiomyopathy; *Csrp3*, cysteine and glycine-rich protein 3; Myh6, alpha myosin heavy chain; CnA, calcineurin. **P < 0.05* vs corresponding control group.

Figure 2 | miR-148a silencing promotes spontaneous eccentric hypertrophic remodeling and dilated cardiomyopathy *in vivo*. (a) Design of the study. Two-month-old wild-type mice were injected with a control antagomir targeting *C. elegans miR-39* (antagomir-*Cel-39*) or and antagomir against *mmu-miR-148a-3p* and subjected to sham or TAC surgery. Cardiac geometry and function was determined by serial Doppler echocardiography at 3 weeks and 6 weeks after surgery. **(b)** RT-PCR analysis of *miR-148a* and unrelated *let-7b* expression in hearts from mice receiving control antagomir (antagomir-*Cel*-39) or antagomir against *miR-148a*. **(c)** Representative images of whole hearts (top panels), H&E-stained sections of four-chamber view (second panel), high-magnification H&E-stained sections (third panel), Sirius-red-stained sections (fourth panel) and WGA-stained (fifth panel) histological sections. **(d)** HW/BW ratio. **(e)** Quantification of EF by echocardiography in antagomir control and antagomir-148a treated mice after sham or TAC surgery. Measurements of **(f)** LVIDs, and **(g)** LV volumes in control and antagomir-148a treated mice after sham or TAC surgery. **(h)** RT-PCR analysis of transcript abundance of the hypertrophic stress marker genes *Nppa*, *Nppb*, *Acta1* and *Myh7* in hearts from control antagomir or antagomir-148a treated mice after sham or TAC surgery.
Data information: Data are means ± SEM. One-way ANOVA with Bonferroni's multiple comparison test was used to compare groups. *n*, number of hearts; C. elegans, Caenorhabditis *elegans ;* TAC, transverse aortic constriction; RT-PCR, real-

time-polymerase chain reaction; H&E, hematoxylin & eosin; WGA, wheat germ agglutinin; HW/BW, heart weight to body weight ratio; EF, ejection fraction; LVIDs, left ventricular mass internal diameter in systole; LV, left ventricular; *Nppa,* natriuretic peptide type A; *Nppb*, natriuretic peptide type A ; *Acta1*, alpha skeletal actin ; *Myh7*, beta myosin heavy chain. **P < 0.05* vs corresponding control group; #*P < 0.05* vs experimental group.

Figure 3 | Cardiac AAV9-miR-148a overexpression protects the heart against eccentric hypertrophy, chamber dilation and systolic dysfunction. (a) Design of the study. Two-month-old mice were injected with control AAV9 (AAV9-CMV) or an AAV9 designed to overexpress *mmu-miR-148a-3p* (AAV9-148a) and subjected to sham or TAC surgery. Cardiac geometry and function was determined by serial Doppler echocardiography at 4 and 7 weeks after surgery. **(b)** RT- PCR analysis of miR-148a expression in hearts from mice receiving AAV9-CMV or AAV9-148a virus. **(c)** Representative images of whole hearts (top panels), H&E-stained sections of four-chamber view (second panel), high-magnification H&E-stained sections (third panel), Sirius-red-stained sections (fourth panel) and WGA-stained (fifth panel) histological sections. **(d)** HW/BW ratio. (**e**) Quantification of LVPWs, **(f)** EF and **(g)** LV volume by echocardiography in AAV9-CMV and AAV9-148a treated mice after sham or TAC surgery. **(h)** RT- PCR analysis of transcript abundance of hypertrophic stress marker genes *Nppa*, *Nppb*, *Acta1* and *Myh7* in hearts from AAV9-CMV and AAV9-148a treated mice after sham or TAC surgery.
Data information: Data are means ± SEM. One-way ANOVA with Bonferroni**'**s multiple comparison test was used to compare groups. *n*, number of hearts; AAV9, adeno-associated virus serotype 9*;* TAC, transverse aortic constriction; RT-PCR, real-time-polymerase chain reaction; H&E, hematoxylin & eosin; WGA, wheat germ agglutinin; HW/BW, heart weight to body weight ratio; EF, ejection fraction; LVIDs, left ventricular mass internal diameter in systole; LV, left ventricular; *Nppa,* natriuretic peptide type A; *Nppb*, natriuretic peptide type A ; *Acta1*, alpha skeletal actin ; *Myh7*, beta myosin heavy chain.. **P < 0.05* vs corresponding control group; #*P < 0.05* vs experimental group.

Figure 4 | miR-148a targets glycoprotein 130 (gp130), co-receptor for IL-6 superfamily cytokines. (a) Location and evolutionary conservation of the *mmu-miR-148a* seed region on gp130. **(b)** Schematic representation of luciferase reporters. **(c)** Activity assay of luciferase reporter constructs in neonatal rat cardiomyocytes. **(d)** Western blot for endogenous gp130 in neonatal rat cardiomyocytes when transfected with scrambled control antimir (scr.anti-miR), antimir-148a (anti-miR-148a), or precursor for miR-148a (pre-miR-148a) and quantification of GAPDH-corrected gp130 western blot signals. **(e)** Study design of mice receiving continuous

infusion of CT-1 (20 µg/kg/day) or isoproterenol (60 mg/kg/day). **(f)** Representative image of whole hearts (top panels), H&E-stained sections of the left ventricular free walls (second panels), high magnification H&E-stained sections (third panels), or Sirius Red stained (lower panels) histological sections of hearts from saline, CT-1 infused and isoproterenol-infused mice. Measurements of **(g)** LV mass, **(h)** EF **(i)** IVSs in saline, CT-1-treated or isoproterenol-treated mice. **(j)** Confocal microscopy images of neonatal rat cardiomyocytes treated with scrambled or precursor-148a miR-148a with or without CT-1 stimulation. **(k)** Cell surface measurements from conditions in (**j**).

Data information: Data are means ± SEM. One-way ANOVA with Bonferroni**'**s multiple comparison test was used to compare groups. *n*, number of transfection experiments **(c)**, number of transfected wells **(d)**, number of mice **(g-i)** or number of cells quantified in each condition **(j)**; AAV9, adeno-associated virus serotype 9*;* TAC, transverse aortic constriction; RT-PCR, real-time-polymerase chain reaction; GAPDH, glyceraldehyde 3-phosphate dehydrogenase; CT-1, cardiotrophin 1; H&E, hematoxylin & eosin; WGA, wheat germ agglutinin; LV, left ventricular; EF, ejection fraction; IVSs, intraventricular septal thickness in systole; LVIDs, left ventricular mass internal diameter in systole. **P < 0.05* vs corresponding control group; #*P < 0.05* vs experimental group.

Figure 5 | miR-148a differentially regulates gp130 and STAT3 downstream signaling in concentric and eccentric cardiac remodeling. **(a)** Design of the study: two month-old mice were subjected to sham or TAC surgery for 2, 4, 6 or 8 weeks. Mice were subjected to echocardiographic evaluation and hearts harvested at indicated time points. **(b)** RT-PCR analysis of *miR-148a-3p* expression at indicated time points. **(c-e)** Echocardiographically determined LV mass, EF or LVIDs, respectively. **(f)** Western blot analysis of myocardial CT-1 expression and quantification at indicated time points. **(g)** Western blot analysis of myocardial gp130 expression and quantification at indicated time points. **(h)** Western blot analysis of myocardial phosphorylated and unphosphorylated forms of STAT3 and quantification at indicated time points. **(i)** Western blot analysis of myocardial gp130 or phosphorylated and unphosphorylated forms of STAT3 and quantification in hearts from mice subjected to sham or TAC surgery and receiving antagomir-148a or a control antagomir (antagomir-*Cel*-39). **(j)** Western blot analysis of myocardial gp130 or phosphorylated and unphosphorylated forms of STAT3 and quantification in hearts from mice receiving AAV9-148a or AAV9-MCS. **(k)** Model depicting the influence of miR-148a on CT-1 - gp130 – STAT3 signaling in cardiac stress situations, resulting in differential activation of STAT3 signaling and eccentric remodeling.

Data information: Data are means ± SEM. One-way ANOVA with Newman-Keuls multiple comparison test was used to compare groups. *n*, number of mice **(b-f)**,

number of independent WB experiments **(g-i)**; AAV9, adeno-associated virus serotype 9*;* TAC, transverse aortic constriction; RT-PCR, real-time-polymerase chain reaction; CT-1, cardiotrophin 1; LV, left ventricular; EF, ejection fraction; LVIDs, left ventricular mass internal diameter in systole. **P < 0.05* vs corresponding control group; #*P < 0.05* vs experimental group.

Supplemental Figure 1 | miR-148a differentially regulates ERK5, ERK1/2, Akt downstream signaling in concentric and eccentric cardiac remodeling. **(a)** Western blot analysis of myocardial LIFR expression and quantification at indicated time points. **(b)** Western blot analysis of phosphorylated and unphosphorylated forms of Akt and quantification at indicated time points. **(c)** Western blot analysis of phosphorylated and unphosphorylated forms of Erk5 and quantification at indicated time points. **(d)** Western blot analysis of phosphorylated and unphosphorylated forms of Erk1/2 and quantification at indicated time points. **(e)** Western blot analysis of phosphorylated and unphosphorylated forms of Akt, Erk5, Erk1/2 and quantification in hearts from mice subjected to sham or TAC surgery and receiving antagomir-148a or a control antagomir (antagomir-*Cel*-39). **(f)** Western blot analysis of myocardial gp130 or phosphorylated and unphosphorylated forms of Akt, Erk5 or Erk1/2 and quantification in hearts from mice receiving AAV9-148a or AAV9-MCS.
Data information: Data are means ± SEM. One-way ANOVA with Newman-Keuls multiple comparison test was used to compare groups. *n*, number of independent WB experiments; LIFR, leukemia inhibitory factor receptor; AAV9, adeno-associated virus serotype 9*;* TAC, transverse aortic constriction; CT-1, cardiotrophin 1. **P < 0.05* vs corresponding control group; #*P < 0.05* vs experimental group.

Table 1. Morphometric and echocardiographic characteristics of sham and TAC mice treated for 6 weeks with control antagomir or antagomir-148a.

	Sham		TAC	
	Ctrl antagomir	**Antagomir-148a**	**Ctrl antagomir**	**Antagomir-148a**
n	7	8	8	8
BW (g)	22.5±1.6	25.6±1.6	25.6±1.2	24.0±1.6
LV mass (mg)	84±3	102±10	123±12*	149±18*
LV mass/BW (mg/g)	3.8±0.3	4.0±0.2	4.8±0.4	6.1±0.5*#
IVSd (mm)	0.87±0.03	0.94±0.08	0.86±0.05	1.00±0.04
IVSs (mm)	1.39±0.04	1.31±0.11	1.13±0.04*	1.32±0.07
LVIDd (mm)	3.44±0.07	4.07±0.18*	4.39±0.16*	4.55±0.32*
LVIDs (mm)	2.07±0.11	2.93±0.25*	3.38±0.21*	3.62±0.35*
LVPWd (mm)	0.89±0.04	0.74±0.08*	0.88±0.12	0.91±0.07
LVPWs (mm)	1.28±0.06	0.91±0.09	1.13±0.13	1.08±0.09
EF (%)	78±3	62±5*	55±4*	51±4*
FS (%)	40±3	29±3*	24±2*	22±2*
E/A (mm/s)	1.33±0.09	1.32±0.13	1.52±0.18	1.27±0.04

Data are expressed as means ± SEM. BW, body weight; Ctrl, control; LV, left ventricular; IVSd, interventricular septal thickness at end-diastole; IVSs, interventricular septal thickness at end-systole; LVIDd, left ventricular internal dimension at end-diastole; LVIDs, left ventricular internal dimension at end-systole; LVPwd, left ventricular posterior wall thickness at end-diastole; LVPws, left ventricular posterior wall thickness at end-systole; EF, ejection fraction; FS, fractional shortening; E/A, Doppler E/A ratio; TAC, transverse aortic constriction. *, indicates $P<0.05$ vs sham group subjected to treatment with a control antagomir; #, indicates $P<0.05$ vs experimental group.

Table 2. Morphometric and echocardiographic characteristics of sham and TAC mice treated for 6 weeks with AAV-MCS or AAV9-miR-148a.

	Sham		TAC	
	AAV9-MCS	**AAV9-miR148a**	**AAV9-MCS**	**AAV9-miR148a**
n	11	10	10	14
BW (g)	19.1±0.5	23.8±1.0	22.6±1.2	25.1±0.9
LV mass (mg)	82±3	99±8	102±7*	116±5*
LV mass/BW (mg/g)	3.9±0.1	4.1±0.2	4.6±0.4*	4.6±0.2*
IVSd (mm)	0.84±0.02	0.93±0.02*	0.85±0.02	0.91±0.02*#
IVSs (mm)	1.21±0.05	1.39±0.03*	1.17±0.05	1.26±0.03
LVIDd (mm)	3.57±0.07	3.58±0.08	4.06±0.14*	4.09±0.08*
LVIDs (mm)	2.27±0.10	2.22±0.09	3.23±0.19*	3.08±0.11*
LVPWd (mm)	0.82±0.02	0.95±0.10	0.79±0.03	0.92±0.02#
LVPWs (mm)	1.23±0.03	1.38±0.09	1.00±0.04*	1.22±0.03#
EF (%)	74±2	76±2	46±5*	57±3*#
FS (%)	37±2	38±2	19±2*	26±2*#
E/A (mm/s)	1.24±0.04	1.25±0.05	1.35±0.03	1.19±0.02

Data are expressed as means ± SEM. AAV, adeno-associated virus; BW, body weight; LV, left ventricular; IVSd, interventricular septal thickness at end-diastole; IVSs, interventricular septal thickness at end-systole; LVIDd, left ventricular internal dimension at end-diastole; LVIDs, left ventricular internal dimension at end-systole; LVPwd, left ventricular posterior wall thickness at end-diastole; LVPws, left ventricular posterior wall thickness at end-systole; EF, ejection fraction; FS, fractional shortening; E/A, Doppler E/A ratio; TAC, transverse aortic constriction. *, indicates $P<0.05$ vs AAV-MCS sham group; #, indicates $P<0.05$ vs experimental group.

Figure 1

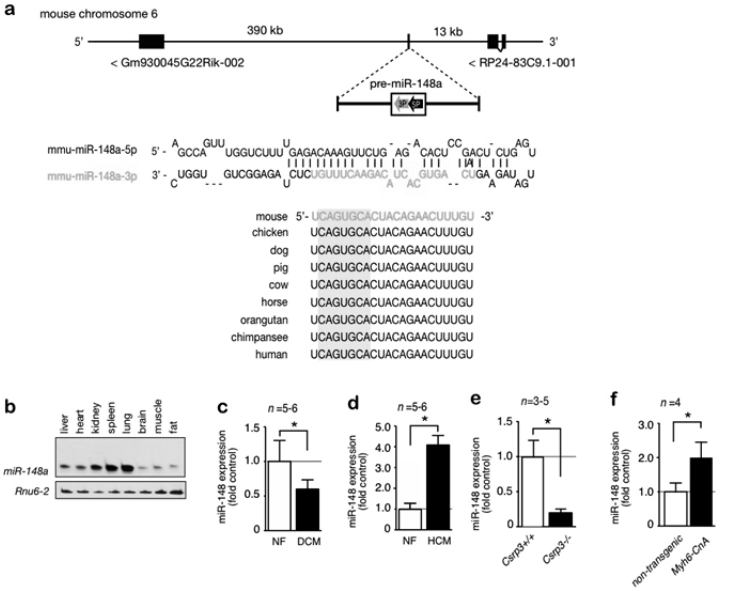
a
mouse chromosome 6
390 kb
13 kb
5'
3'
< Gm930045G22Rik-002
< RP24-83C9.1-001
pre-miR-148a
mmu-miR-148a-5p
mmu-miR-148a-3p
mouse 5'- UCAGUGCACUACAGAACUUUGU -3'
chicken UCAGUGCACUACAGAACUUUGU
dog UCAGUGCACUACAGAACUUUGU
pig UCAGUGCACUACAGAACUUUGU
cow UCAGUGCACUACAGAACUUUGU
horse UCAGUGCACUACAGAACUUUGU
orangutan UCAGUGCACUACAGAACUUUGU
chimpansee UCAGUGCACUACAGAACUUUGU
human UCAGUGCACUACAGAACUUUGU
b
liver
heart
kidney
spleen
lung
brain
muscle
fat
miR-148a
Rnu6-2
c
n =5-6
miR-148 expression (fold control)
NF
DCM
d
n =5-6
miR-148 expression (fold control)
NF
HCM
e
n=3-5
miR-148 expression (fold control)
Casp3+/+
Casp3-/-
f
n =4
miR-148 expression (fold control)
non-transgenic
Myh6-CnA

Figure 2

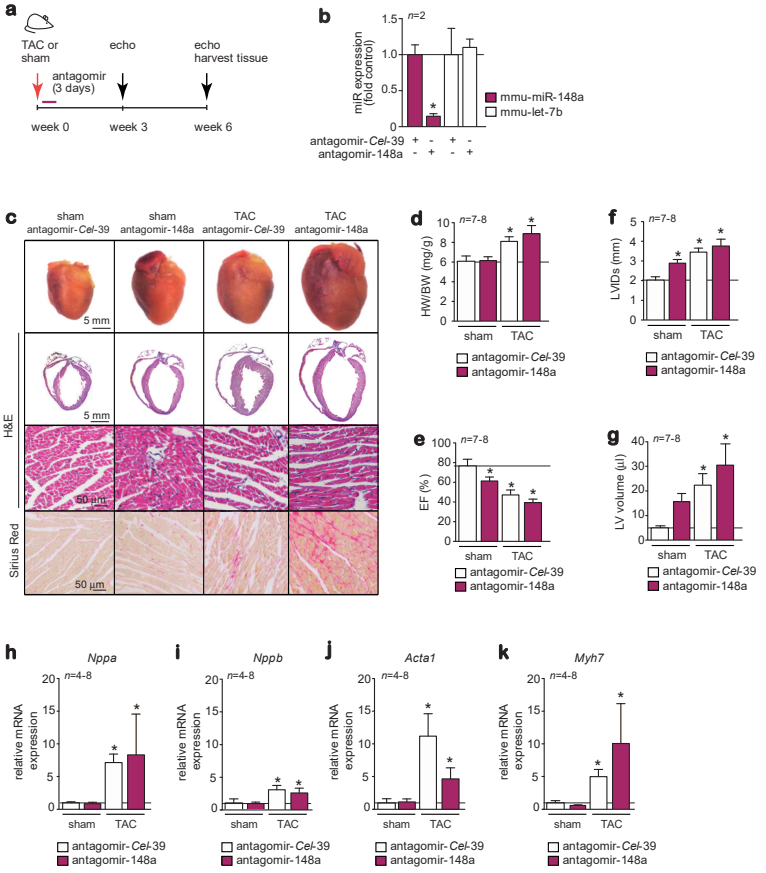
a
TAC or sham
echo
echo harvest tissue
antagomir (3 days)
week 0
week 3
week 6
b
n=2
miR expression (fold control)
mmu-miR-148a
mmu-let-7b
antagomir-Cel-39
antagomir-148a
c
sham antagomir-Cel-39
sham antagomir-148a
TAC antagomir-Cel-39
TAC antagomir-148a
H&E
Sirius Red
5 mm
50 µm
d
n=7-8
HW/BW (mg/g)
sham
TAC
antagomir-Cel-39
antagomir-148a
e
n=7-8
EF (%)
f
n=7-8
LVIDs (mm)
g
n=7-8
LV volume (µl)
h
Nppa
n=4-8
relative mRNA expression
i
Nppb
j
Acta1
k
Myh7

Figure 3

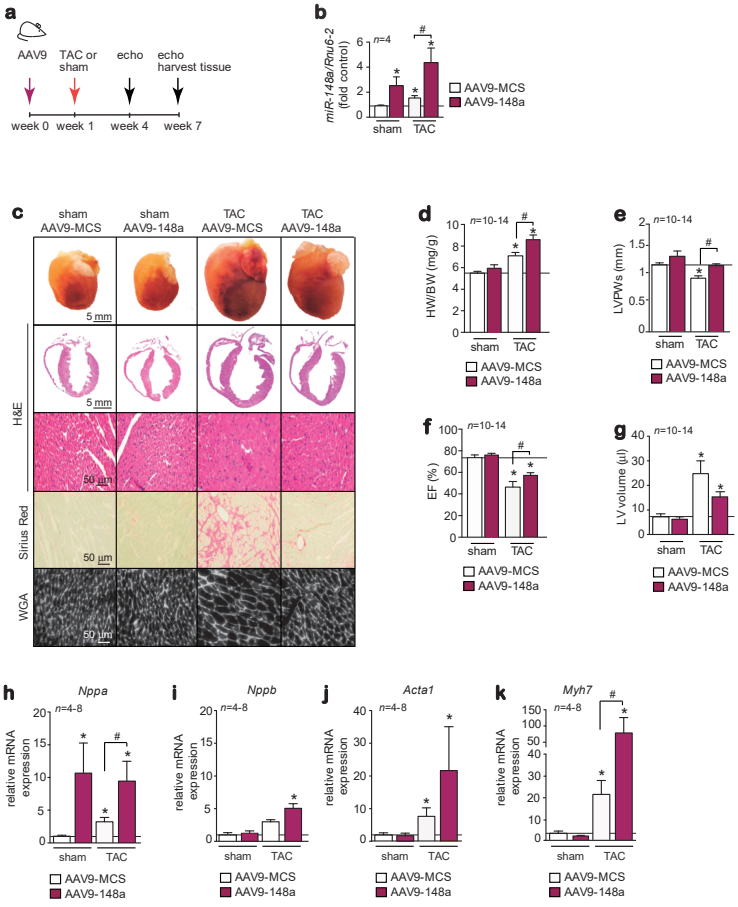
a
AAV9
TAC or sham
echo
echo harvest tissue
week 0
week 1
week 4
week 7
b
miR-148a/Rnu6-2 (fold control)
n=4
sham
TAC
AAV9-MCS
AAV9-148a
c
sham AAV9-MCS
sham AAV9-148a
TAC AAV9-MCS
TAC AAV9-148a
H&E
Sirius Red
WGA
5 mm
50 µm
d
HW/BW (mg/g)
n=10-14
e
LVPWs (mm)
f
EF (%)
g
LV volume (µl)
h
Nppa
i
Nppb
j
Acta1
k
Myh7
relative mRNA expression
n=4-8

Figure 4

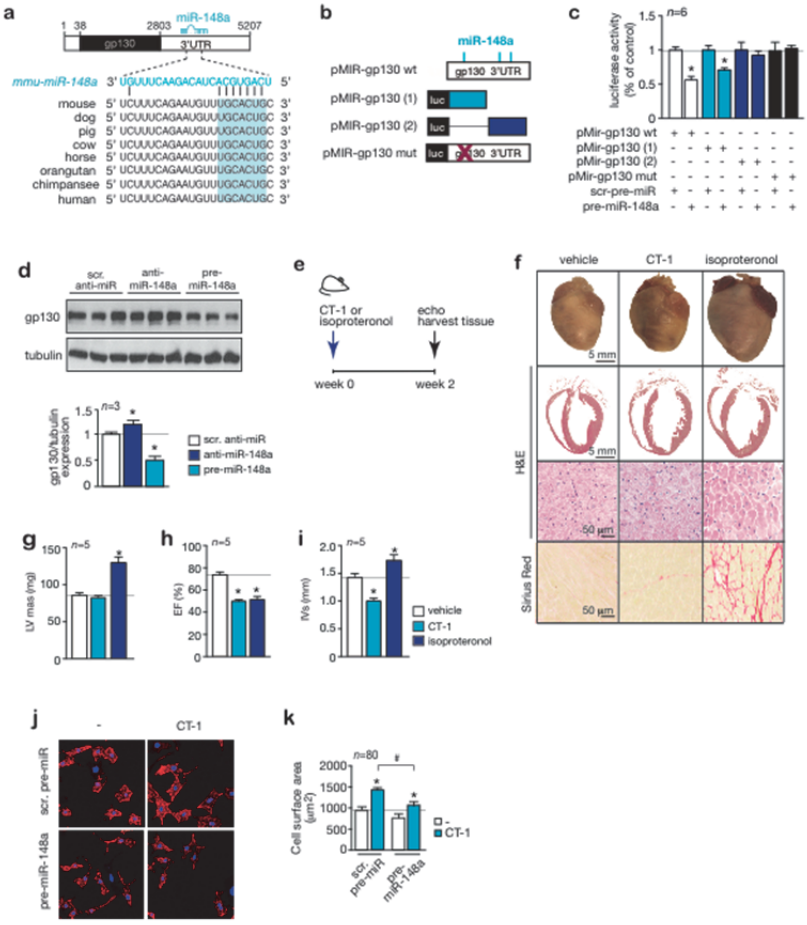
a
1 38 2803 5207
miR-148a
gp130
3'UTR
mmu-miR-148a 3' UGUUUCAAGACAUCACGUGACU 5'
mouse 5' UCUUUCAGAAUGUUUGCACUGC 3'
dog 5' UCUUUCAGAAUGUUUGCACUGC 3'
pig 5' UCUUUCAGAAUGUUUGCACUGC 3'
cow 5' UCUUUCAGAAUGUUUGCACUGC 3'
horse 5' UCUUUCAGAAUGUUUGCACUGC 3'
orangutan 5' UCUUUCAGAAUGUUUGCACUGC 3'
chimpansee 5' UCUUUCAGAAUGUUUGCACUGC 3'
human 5' UCUUUCAGAAUGUUUGCACUGC 3'
b
miR-148a
pMIR-gp130 wt
pMIR-gp130 (1)
pMIR-gp130 (2)
pMIR-gp130 mut
luc
gp130 3'UTR
c
n=6
luciferase activity (% of control)
pMir-gp130 wt
pMir-gp130 (1)
pMir-gp130 (2)
pMir-gp130 mut
scr-pre-miR
pre-miR-148a
d
scr. anti-miR
anti-miR-148a
pre-miR-148a
gp130
tubulin
gp130/tubulin expression
n=3
scr. anti-miR
anti-miR-148a
pre-miR-148a
e
CT-1 or isoproteronol
echo harvest tissue
week 0
week 2
f
vehicle
CT-1
isoproteronol
5 mm
H&E
Sirius Red
50 µm
g
n=5
LV mas (mg)
h
n=5
EF (%)
i
n=5
fVs (mm)
vehicle
CT-1
isoproteronol
j
-
CT-1
scr. pre-miR
pre-miR-148a
k
n=80
Cell surface area (µm2)
-
CT-1
scr. pre-miR
pre-miR-148a

Figure 5

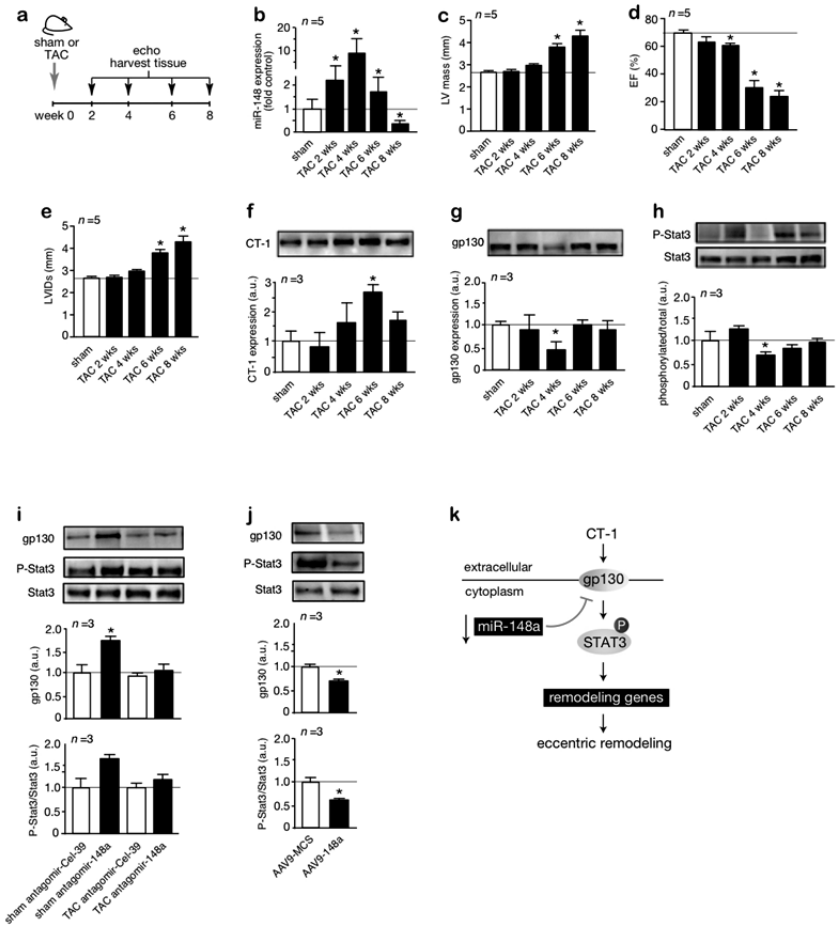
a
sham or TAC
echo
harvest tissue
week 0 2 4 6 8
b
n =5
miR-148 expression (fold control)
sham
TAC 2 wks
TAC 4 wks
TAC 6 wks
TAC 8 wks
c
n =5
LV mass (mm)
d
n =5
EF (%)
e
n =5
LVIDs (mm)
f
CT-1
n =3
CT-1 expression (a.u.)
g
gp130
n =3
gp130 expression (a.u.)
h
P-Stat3
Stat3
n =3
phosphorylated/total (a.u.)
i
gp130
P-Stat3
Stat3
n =3
gp130 (a.u.)
P-Stat3/Stat3 (a.u.)
sham antagomir-Col-39
sham antagomir-148a
TAC antagomir-Col-39
TAC antagomir-148a
j
gp130
P-Stat3
Stat3
n =3
gp130 (a.u.)
P-Stat3/Stat3 (a.u.)
AAV9-MCS
AAV9-148a
k
CT-1
extracellular
cytoplasm
gp130
miR-148a
P
STAT3
remodeling genes
eccentric remodeling

Supplemental Figure 1

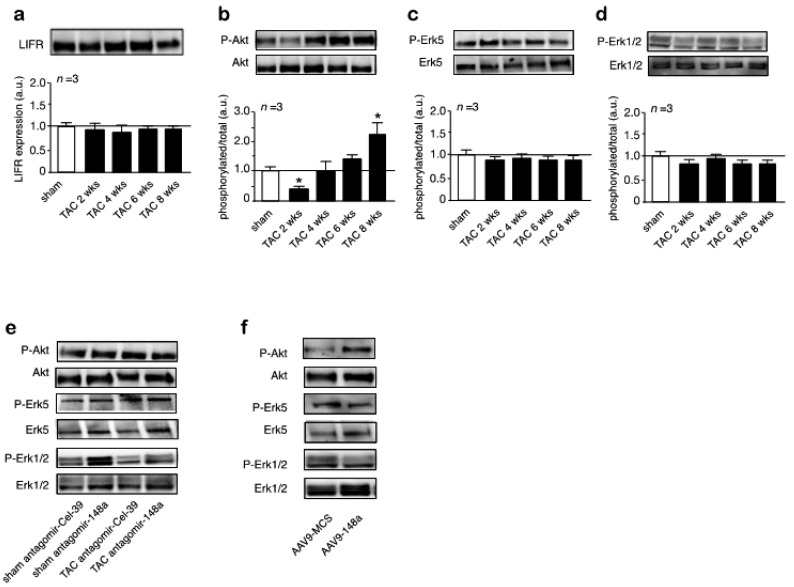

CHAPTER 5

A phenotypic, high-content screen to identify EccentriMIRS: microRNAs involved in eccentric cardiomyocyte hypertrophy

---

Leonne E. Philippen, Ellen Dirkx, Nicole Bitsch, Miguel Mano, Mauro Giacca, Leon J. de Windt

Department of Cardiology, Cardiovascular Research Institute Maastricht (CARIM), Maastricht University, the Netherlands

Manuscript in preparation

Abstract

MicroRNAs are single-stranded, non-coding RNA molecules of about 22 nucleotides in length. Increasing evidence associates microRNAs to cardiac remodeling and heart failure. Distinct forms of cardiac remodeling (concentric or eccentric) can occur, yet current pharmacotherapy only follows a “one-size-fits-all” approach, regardless of underlying type of remodeling. One signaling cascade that is closely associated with the development of eccentric hypertrophy and dilation of the ventricular chambers involves cardiotrophin-1 (CT-1) activation and downstream signaling. Previously, we showed that CT-1 infusion provokes eccentric hypertrophy and dilatation without an initial concentric hypertrophy response. Here, we establish a high content phenotypic screening assay in neonatal rat cardiomyocytes (NRCM) stimulated by CT-1, and identify microRNAs that influence eccentric cardiomyocyte hypertrophy.

Introduction

Pathological left ventricular hypertrophy, often caused by chronic hypertension or formed in the remote zone after a myocardial infarct, represents the main risk factor for the development of heart failure and lethal arrhythmias.[1] Although the underlying molecular mechanisms are still poorly understood, there now is compelling evidence that microRNA genes, employed in response to disease stimuli, are intimately involved in left ventricular hypertrophic enlargement and subsequently heart failure.[2] MicroRNAs are small non-coding RNA stress-responsive genes that act by suppressing a variety of protein coding genes at the post-transcriptional level. Various stress activated signaling cascades have the ability to increase the expression of series of microRNAs, which in turn suppress anti-hypertrophic modulators, allowing pathological cardiac hypertrophy to ensue.[3]

Cardiac hypertrophy has distinct morphological phenotypes at the organ level.[4-7] On the one hand, a form of cardiac remodeling that consists of thickening of the ventricular walls is also defined as concentric hypertrophy. This form of hypertrophy is often observed secondary to aortic stenosis, hypertension and associated with metabolic disorders in heart failure with preserved ejection fraction (HFpEF).[8] At the microscopic level, cardiomyocytes isolated from concentric hypertrophic hearts display an increase in size more in width than in length. In contrast, eccentric cardiac remodeling consists of thinning and dilation of the ventricular walls and an increase of the left ventricular cavity size. Clinically, eccentric hypertrophy is often observed with post-infarct healing and inherited forms of dilated cardiomyopathy.[9] At the microscopic level, cardiomyocytes isolated from eccentric remodeled hearts display a disproportional increase in length rather than width.
Despite these phenotypically distinct causes of heart failure, current pharmacotherapy follows a “one-size-fits-all” approach, regardless of the underlying type of remodeling that eventually evoked heart failure. It still remains unclear how the heart is able to react by concentric hypertrophy in response to e.g. chronic beta-adrenergic stimulation in early stages with near normal ejection fraction and in time gradually demonstrates eccentric remodeling with severe dilation and dramatically lowered ejection fraction.[10] Understanding the precise molecular underpinnings that drive concentric versus eccentric cardiac remodeling is crucial in striving towards a therapeutic approach for sub-type specific forms of heart failure.

To dissect these different types of remodeling, stimuli that specifically provoke one specific type of hypertrophy are the first step towards understanding phenotypically different forms of cardiac disease. In primary cultured cardiomyocytes, stimulation with the IL-6 cytokine family member cardiotrophin-1 (CT-1) causes a phenotype of cardiomyocyte hypertrophy with more pronounced increases in cell length and where sarcomeres are added in series (eccentric hypertrophy), rather than in parallel (concentric hypertrophy), as is often observed with α-adrenergic stimulation.[11 12]

To gain more insight in the signaling cascades and molecular mechanisms involved in eccentric remodeling and dilatation, we performed a high-content microscopy, high-throughput functional screening for microRNAs that influenced neonatal cardiomyocyte eccentric remodeling using a whole-genome miRNA library. We identified 26 microRNAs that decreased CT-1 induced cardiomyocyte hypertrophy compared to scrambled anti-miR treatment (control) with a z score < -2.0. We selected the LNA miRs based on the extent to which they had inhibited hypertrophy and the degree of conservation between mouse and human. Our top 4 microRNA candidates miR-125b-5p, miR-542-3p, miR-151-5p and miR-532-3p are specific inducers of eccentric hypertrophy.

Methods

Primary cardiomyocyte cultures

Primary cardiomyocytes were isolated from 1-2 days old Sprague Dawley rats after decapitation, and cardiomyocytes were isolated by enzymatic dissociation as described previously[13]. Briefly, hearts were collected, atria were removed and ventricles cut into small pieces in salt buffer on ice. The ventricular tissue was subjected to multiple rounds of enzymatic digestion using pancreatin (Sigma) and collagenase (Gibco) as digestive enzymes at 37 degrees. Every 20 min supernatant was collected in FBS, and 9 mL fresh enzyme solution was added to the residual tissue. Cells were pelleted and resuspended in DMEM medium (Gibco) supplemented with 15% fetal bovine serum, gentamycin (0.1%), and L-glutamine (1 mmol/liter). To separate the non-cardiomyocyte fraction from the cardiomyocytes, cells were pre-plated on uncoated T75 flasks for 1 h at 37 degrees. This allows fibroblasts to adhere to the culture flasks, while cardiomyocytes remain in suspension. Afterwards, the supernatant containing the cardiomyocytes was collected and cells were counted manually. The cardiomyocytes were plated on gelatinized 96-well plates (Ibidi) in a density of 2.5×10^4 cells per well. The following morning, neonatal rat cardiomyocytes (NRCM) were cultured in serum-free DMEM media containing M199 media (20%), gentamycin (0.1%) and 1 mmol/liter L-glutamine, and NRCM were transfected with a library of miR inhibitors.

MicroRNA transfection

Neonatal rat cardiomyocytes (NRCM) were transfected with the mouse miRCURY LNA microRNA inhibitor library (Exiqon,) corresponding to all mouse mature microRNAs (711 mouse microRNAs listed in miRBase v. 19.0). MiR inhibitors were transferred manually from stock library plates onto collagen-coated black clear-bottom 96-well plates (Ibidi). MiR inhibitors were transfected into NRCM using Oligofectamine (Invitrogen) according to the manufacturer's transfection protocol,

at a final concentration of 50 nM. Briefly, Oligofectamine was diluted in serum free medium and added to the miR inhibitors on the 96-well plates. Half an hour later, the NRCM previously seeded on black 96-well plates were transfected manually with the oligofectamine/ miR inhibitor mixtures. After 24h, culture medium was replaced by fresh medium and left unstimulated (serum free) or stimulated with a final concentration of 2nM cardiotrophin-1 (Peprotech) to induce eccentric cardiomyocyte hypertrophy. NRCM were fixed at 72 h after plating and processed for immunofluorescence (see Fig 1a).

Immunofluorescence

NRCM were fixed with 4% paraformaldehyde for 5 min, permeabilized with 0.1% NP40 in phosphate buffered saline (PBS) at room temperature. NRCM were then stained overnight at room temperature with the following primary antibodies diluted in 1% BSA solution: rabbit antibody against sarcomeric α-actinin (Abcam), mouse antibody against prolyl-4-hydroxylase beta (P4HB, Acris), and nuclear staining was performed with 4',6-diamidino-2-phenylindole (DAPI, Molecular Probes). The sarcomeric α-actinin was used to visualize sarcomeric organization and determine cardiomyocyte size. The P4HB antibody was used to visualize the fibroblasts. NRCM were incubated for 2 h with the respective secondary antibodies conjugated to Alexa Fluor-488 (green fluorescent, Life Technologies), and Alexa Fluor-647 (red fluorescent, Life Technologies). All antibody incubation steps were performed at room temperature and intermitted by three washing steps with PBS/ 0.1% NP40. Finally, NRCM were covered with 50% glycerol and stored at 4 °C until microscopic analysis.

Images and analysis

Image acquisition and analysis were performed at the ICGEB High-Throughput Screening Facility (http://www.icgeb.org/high-throughput-screening.html) using an ImageXpress Micro automated high-content screening fluorescence microscope. Per well 16 images were taken for each wavelength, resulting in circa 2500 cells analysed per well. For the image analysis MetaXpress software (Molecular Devices) was used. NRCM were only included in the analysis if they stained positive for both sarcomeric α-actinin, and Dapi for nuclei. Cardiac fibroblasts express prolyl 4-hydroxylase beta (P4HB) but do not express α-actinin, therefore those were excluded from analysis.

Statistical analysis

All the data are expressed as mean ± standard error (SEM). Statistical analyses were performed using Prism software (GraphPad Software), and consisted Student's *t*-test when comparing two experimental groups. For all data, differences were considered significant with a p value < than 0.05.

MiR target prediction

Putative miR targets were identified using miR target prediction tool software miRWalk (http://zmf.umm.uni-heidelberg.de/apps/zmf/mirwalk2/mirretsys.php version miRWalk 2.0). Targets were only included if predicted by 3 or all 4 databases: miRWalk, miRanda, RNA22 and Targetscan. The top predicted target genes of all miRs were subjected to bioinformatics analysis using GeneCodis software (http://genecodis.cnb.csic.es/analysis). Over 6000 genes were included in the analysis.

Results

High throughput screen experimental setup using a miR LNA inhibitor library

Since CT-1 administration causes cardiac eccentric hypertrophy without an initial concentric hypertrophic remodeling process (Chapter 4), this creates the opportunity to identify microRNAs specifically involved in eccentric remodeling and, possibly, forms of dilated cardiomyopathy. To this end, we performed a phenotypic, fluorescence-microscopy-based high throughput screening using a library of 711 microRNA LNA inhibitors. Assays that are based on cells require optimal cell plating density in order to achieve maximal resolution in the readout process. Cell seeding conditions were optimized in preliminary studies in our lab with culture duration of up to 72h (data not shown). As the seeding number increased, the cell area quantification accuracy decreased due to cells overgrowing each other in the limited plate area, making it difficult for the software to identify the accurate cell borders of each cell and quantify cell size accordingly. The optimum cell seeding conditions for this assay appeared to be a density of 2.5×10^4 cells per well.

Neonatal rat cardiomyocytes were plated on 96 well plates at 2.5×10^4 cells per well. The next morning, cardiomyocytes were manually transfected with the antimir LNA library containing 711 mouse microRNA inhibitors. Another 24h later, CT-1 was added to the cells to induce eccentric hypertrophy in vitro. After 72h, cells were fixed and stained with specific antibodies for fluorescence-based microscopy in an automated setup (Fig. 1a). In order to distinguish mycocytes from non-myocytes, cardiomyocytes were stained for sarcomeric α-actinin, fibroblasts for prolyl 4-hydroxylase beta (P4HB) and nuclei for Dapi (Fig. 1b). Cardiac fibroblasts do not express α-actinin, therefore we used this as a selection criterion for cells to be included in the analysis. Cells were only counted if they displayed both Dapi and α-actinin staining. Although non-myocytes were still detected due to their nuclear

staining, they were excluded for cell size quantification (Fig. 1c). Upon stimulation with CT-1, cardiomyocytes typically exhibited a 1.5-fold increase of their cell area relative to non-stimulated control cells (Fig. 1c).

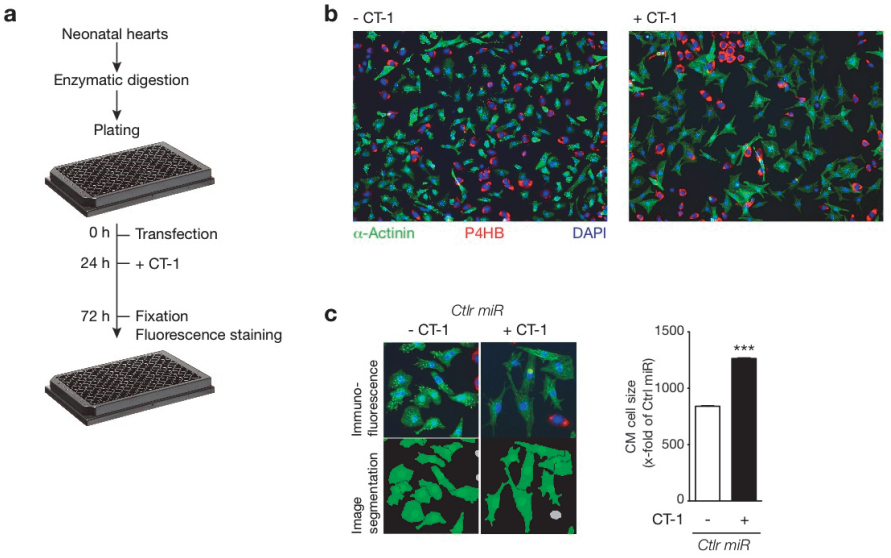

Figure 1. High throughput screen to identify microRNAs specifically involved in eccentric cardiomyocyte hypertrophy. (a) High-content screen workflow. (b) Representative microscopy images of cardiomyocytes (α-actinin) and fibroblasts (P4HB) in culture, treated with scrambled anti-miR. (c) Microscopy images and image reconstruction of NRCM treated with scrambled anti-miR (left) and quantification of NCRM cell size under indicated conditions using an automated system (right). P4HB, prolyl 4-hydroxylase beta.

Phenotypic high throughput screening identified microRNAs as regulators of eccentric remodeling (EccentriMIRs)

Since the majority of the LNA miR inhibitors only showed a significant effect on cell size after stimulation with CT-1, and our objective was to identify miRs involved in pathological eccentric remodeling, we focused on the hits acquired from this screen in CT-1-stimulated cardiomyocytes. Fig. 2 shows screen results as the z score of the cell size upon transfection of a specific LNA miR inhibitor compared to the mean of control scrambled-miR transfected cells included on each plate. In the z score

method, the mean score of all of the compounds on a plate are subtracted from the raw value of the compound of interest, and this difference is divided by the standard deviation of all of the values.[14] In our screen we also included a full plate of anti-miR scrambled LNA as an additional control. The screen identified 26 microRNAs that decreased CT-1 induced cardiomyocyte hypertrophy compared to scrambled anti-miR treatment (control) with a z score < -2.0 (Fig. 2). There were also LNA miRs in our library that increased cardiomyocyte size, but since the goal of this screen was to identify potential target miRs or potential target pathways for therapeutical purposes, we did not elaborate on the pro-hypertrophic subset of LNA miR inhibitors. Instead, we selected the LNA miRs based on the extent to which they had inhibited hypertrophy and the degree of conservation between mouse and human.

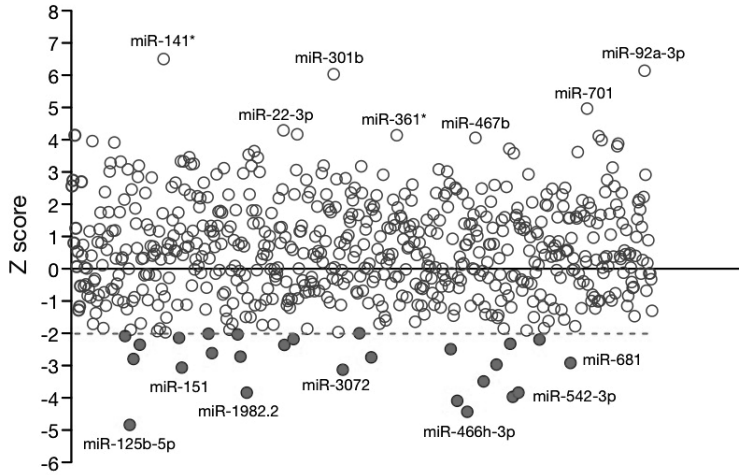

Figure 2. Identification of eccentrimiRs. Z score of all LNA miR measurements, calculated as $z = (x_i - x)/s_x$, where x_i is the raw measurement on the i^{th} compound (LNA), x and s_x are the mean and the standard deviation, respectively, of all measurements including scrambled control within the plate. Shown in red are microRNAs that inhibit CT-1 induced hypertrophy when inhibited by indicated LNA molecules.

Fig. 3 displays the fluorescent images of the candidates with the smallest z-score that had the strongest effect on inhibition of hypertrophy and are completely conserved in human. The larger the value of *z*, the less probable the experimental result is due to chance. Using miR inhibitor molecules that are designed to specifically inactivate endogenous miRs, increased the validity of the effects observed. Anti-miR-125b-5p, anti-miR-532-3p, anti-miR-542-3p, and anti-miR-151-5p all showed significant inhibition of CT-1-induced eccentric hypertrophy. Since our goal was to identify miRs that are involved in eccentric hypertrophy specifically, we compared our results to the results of a previously published screen done in cardiomyocytes that were stimulated with phenylephrine (PE) to induce concentric hypertrophy.[15] Comparing the results of that study with our data, we can conclude that our top 4 microRNA candidates; miR-125b-5p, miR-542-3p, miR-151-5p and

miR-532-3p are specific inducers of eccentric hypertrophy since those microRNAs did not significantly induce α-adrenergic-mediated hypertrophy and miR-151-5p stimulation even resulted in an anti-concentric hypertrophy phenotype.[15] Thus, this suggests that our top candidates are specifically involved in eccentric remodeling pathways rather then concentric hypertrophy mechanisms.

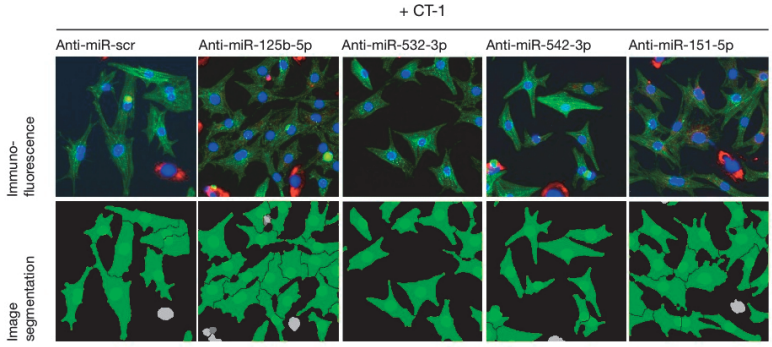

Figure 3. EccentrimiR inhibition protects against CT-1-induced eccentric cardiomyocyte hypertrophy. Microscopy images (upper panel) and image reconstruction (lower panel) of NRCM after CT-1 stimulation treated with scrambled anti-miR or antimirs against indicated microRNAs.

We systematically identified miRs essential for NRCM eccentric remodeling using a synthetic miR LNA library of mouse origin. Next, we set out to further explore the target genes of our 4 candidate miRs miR-125b-5p, miR-542-3p, miR-151-5p and miR-532-3p to check for involvement in common pathways and processes. Prediction of miR target genes is still a challenging process and these processes usually result in an excessive number of putative target genes.[16] Since the algorithms for miR target prediction provide distinct targets, we used the input of 4 different databases: miRWalk, miRanda, RNA22 and Targetscan and only included the target genes predicted by 3 out of 4 or all 4 algorithms. For each miR, the top putative target genes were analyzed using GeneCodis. This web-based application integrates different sources of information to finding groups of genes with similar biological meaning. The enrichment analysis is essential in the interpretation of high-throughput experiments and provides clues for common pathways that our top 4 miRs are regulating in relation to CT-1-induced eccentric remodeling. When analyzing for Biological Processes (BP) the tool revealed the enrichment for genes involved in 'regulation of transcription, DNA-dependent', 'transport', 'transcription, DNA-dependent', and 'metabolic process' as main categories (Fig. 4).

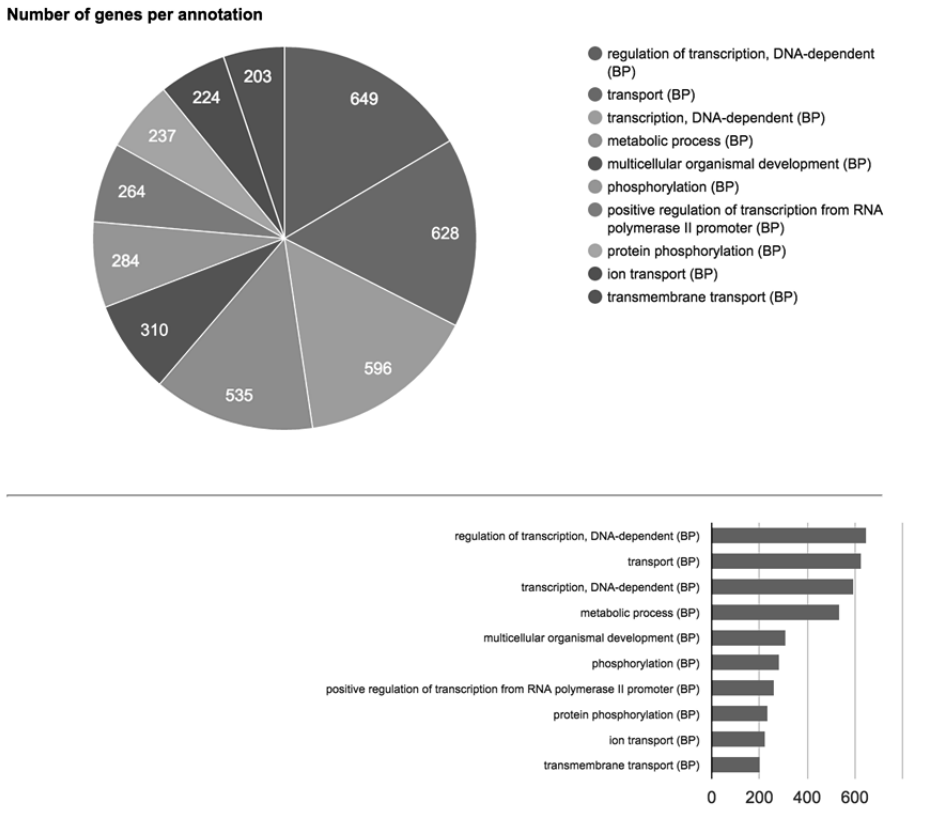

Figure 4. Singular Enrichment Analysis of GO Biological Process. Graphs showing results for all putative target genes predicted by 3 or all 4 databases used (miRWalk, miRanda, RNA22 and Targetscan). The pie chart (upper) and bar graph (lower) show some selected categories significantly enriched.

Functional analysis of the gene involvement in the Kyoto Encyclopedia of Genes and Genomes (KEGG) pathways revealed enrichment for genes belonging to 'Pathways in cancer', MAPK-signaling pathway', 'Endocytosis', and 'Regulation of actin cytoskeleton' as top categories (Fig. 5).

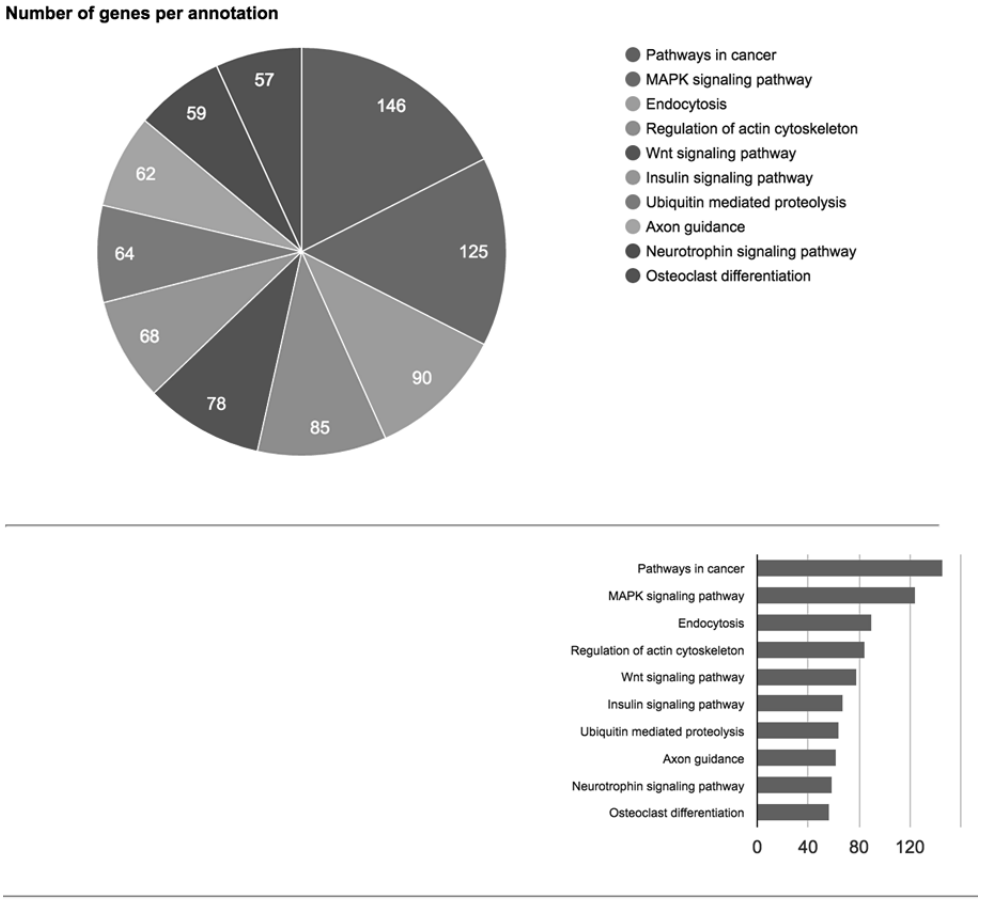

Figure 5. Singular Enrichment Analysis of KEGG pathways. Graphs showing results for all predicted target genes predicted by 3 or all 4 databases used (miRWalk, miRanda, RNA22 and Targetscan). The pie chart (upper) and bar graph (lower) show some specific categories significantly enriched.

Discussion

Different hypertrophic phenotypes can be distinguished based on the geometry of the heart and individual cardiomyocytes. Concentric pathological hypertrophy is considered to be initially compensatory and occurs usually secondary to pressure overload as in clinical conditions such as aortic stenosis or high blood pressure.[17] Concentric hypertrophy can progress to eccentric hypertrophy and dilation with associated systolic heart failure, as observed in animal models with long-term pressure overload stress due to aortic banding. However, the underlying mechanisms for this transition remain poorly understood.

After establishing that CT-1 leads specifically to dilatation of the heart (Chapter 4), we used CT-1 as the stimulating agent to induce hypertrophy and set out to determine the molecular mechanisms specifically underlying eccentric cardiac hypertrophy. To that end, microRNA inhibitors were used as tools in a high throughput screening approach to unravel specific molecular pathways involved in eccentric remodeling of the heart. CT-1 stimulation of neonatal cardiomyocytes resulted consistently in a 1.5 fold increase in cell size. The advantage of our automated setup is that a very large number of microRNAs could be screened simultaneously, and the automated microscopy-based analysis of cell size ruled out potential human bias in analyzing the screening results. This assay was perfectly able to discriminate between cardiomyocytes and non-cardiomyocytes and included a higher number of cells analyzed per condition (±800) as compared to conventional approaches that involve manual quantification.

In total 711 LNA microRNA inhibitors were tested for their ability to alter CT-1-induced eccentric hypertrophy in isolated primary neonatal cardiomyocytes. A similar massive phenotypic screening method to detect changes in cardiomyocyte cell size has been previously described for α-adrenergic-induced concentric hypertrophy.[15] That study used automated microscopy and an edge detection algorithm in order to achieve a high reproducibility using cardiomyocyte size as a key parameter. Quantitative analysis of candidate microRNA expression levels in primary cardiomyocytes revealed a low correlation level of the phenotypic effects of individual candidates and their expression level, indicating that focusing on the most strongly expressed and deregulated microRNAs risks to neglect other disease-relevant miRs. The presumption that high endogenous miR expression levels correlate with high activity was not true in regards to pro-hypertrophic potential.[15] In the present study, rather than using expression levels as a selection criterion, we used phenotypic cell size measurements as a read out.

To circumvent artificial experimental-induced false positives, we utilized a library of LNA miR inhibitors that target the endogenous miR population rather than introducing overexpression of miRs that might normally not even be present in the cardiomyocyte. The top 4 miRs identified in our screen that that are specific inducers of eccentric hypertrophy are miR-542-3p, miR-151-5p, miR-532-3p and miR-125b-5p.

To get more insight in what pathways these miRs could be involved, we used miR target prediction tool software databases to identify potential target genes and pathways. Main pathways ways predicted include pathways in cancer. Indeed, several reports implicate miR-542-3p in cancer progression. MiR-542-3p was shown to suppress tumor cell invasion via targeting the AKT pathway in human astrocytoma.[18] MiR-542-3p directly targets integrin-linked kinase (ILK) thereby inhibiting colon cancer cell proliferation and invasion.[19] Moreover, miR-542-3p directly targets surviving, and overexpression of miR-542-3p induced G1 and G2/M arrest in multiple cancer cell lines, including lung cancer, breast cancer, and cervical

cancer.[20,21] The tumor-suppressive function of miR-542-3p largely results from its synergistic effect on simultaneous modulation of multiple targets. Besides its known role as a tumor repressor, miR-542-3p also directly targets bone morphogenetic protein 7 (BMP-7), suppressing osteoblast cell proliferation and differentiation and thereby inhibiting bone formation. Silencing of miR-542-3p led to increased bone formation, bone strength and improved trabecular microarchitecture in sham and ovariectomized (Ovx) mice.[22]
MiR-151 is often co-expressed with its host gene focal adhesion kinase (FAK). Mir-151-5p directly targets RhoGDIA, a putative metastasis suppressor in hepatocellular carcinoma, thereby enhancing cell motility and tumor spreading.[23,24] MiR-151-5p can also directly bind to the 3'-UTR of FXYD1 (coding gene of phospholemman, PLM) and inhibit its expression, altering vulnerability to ventricular arrhythmias in response to acute myocardial ischemia in estrogen-deprived rats.[25]
Another miR, miR-532-3p was shown to directly target apoptosis repressor with caspase recruitment domain (ARC), thereby regulating mitochondrial fission in doxorubicin (DOX) cardiotoxicity. MiR-532-3p was not involved in DOX-induced apoptosis in cancer cells.[26]
The last microRNA, miR-125b-5p is known as a tumor suppressor and several reports show its role in cell proliferation, differentiation, and apoptosis in multiple cell types.[27-31] MiR-125b promotes apoptosis by directly targeting Mcl-1, Bcl-w and interleukin (IL)-6R.[32] MiR-125b can regulate cell differentiation through direct repression of the core binding factor β (CBFβ) in hematopoietic malignancies.[33] MiR-125b expression in breast cancer cells suppresses proliferation and induces G1 cell-cycle arrest.[34,35] In lens epithelial cell, miR-125b was shown to directly target p53.[36] Also, miR-125b-5p was found to directly target 5-Lipoxygenase (5-LO), the key enzyme in leukotriene biosynthesis. Leukotrienes are mediators of the innate immune system and inflammatory processes.[37] In relation to the heart, miR-125b was shown to regulate of human embryonic stem cell (hESC) differentiation in general, and the development of hESC-derived mesoderm and cardiac muscle in particular.[38] Overexpression of miR-125b protected mice against myocardial ischemia/reperfusion injury via targeting of p53 and TRAF6.[39] Furthermore, miR-125b is necessary for the induction of fibroblast-to-myofibroblast transition by functionally targeting apelin, a critical repressor of fibrogenesis, and inhibits p53 to induce fibroblast proliferation.[40]

Those miRs are hardly studied in relation to cardiovascular disease. Predicted involvement in MAPK-signaling pathways is no surprise, since the known downstream pathways of CT-1 signaling involve MAPK effectors. The predicted involvement in regulation of transcription could be related to activation of transcription factors involved in eccentric hypertrophy, as concentric hypertrophy does also require activation of transcription.

Additional validation of this screen is required. There are no molecular markers known to be specific for eccentric remodeling, therefore we could not use qPCR to validate our screen in the way it is done for measuring concentric hypertrophy

response. In concentric hypertrophy, measuring “fetal” gene markers like atrial natriuretic factor gene expression, a hallmark of the hypertrophy-associated gene expression program, can be used to determine the induction of the pathological hypertrophy. To validate the effect on eccentric hypertrophy in vivo, mice receiving CT-1 by osmotic minipumps could be injected with antagomir against these miRs and the level of eccentric remodeling could be established by echocardiography and evaluation of histologic sections of the hearts. Since CT-1 induces an increase in cardiomyocyte cell length rather than an increase in width, measuring cell area might not be optimal. However, the MetaXpress software we used is not capable of measuring y/x ratio in individual cells in an automated setup. Furthermore, the amount of fibroblast in certain wells was so high, that we had to exclude half of the images per well for analysis. Although this is in line with literature, only 800 cells per condition could be analyzed due to abundant fibroblast proliferation.[41] High intense fibroblast immunofluorescence staining interfered with the edge-detecting capacity of the algorithm, making the analysis process more labor intensive due to manually checking of all analyzed pictures.

This assay led to the identification of microRNA candidates, specifically involved in eccentric hypertrophic pathways that do not play a role in processes leading to concentric hypertrophy. Further *in vivo* validation will remain crucial in order to establish more molecular insight into the pathways specifically involved in dilatation. Identifying the target genes of those miRs that are affected in eccentric hypertrophy will provide more insight in the pathways that are activated specifically in eccentric remodeling. In the future, this could help to accomplish better patient stratification and development of personalized therapies aimed to specifically repress eccentric remodeling.

References

1 Drazner, M. H. The progression of hypertensive heart disease. *Circulation* **123**, 327-334, doi:10.1161/CIRCULATIONAHA.108.845792 (2011).

2 Gladka, M. M., da Costa Martins, P. A. & De Windt, L. J. Small changes can make a big difference - microRNA regulation of cardiac hypertrophy. *Journal of molecular and cellular cardiology* **52**, 74-82, doi:10.1016/j.yjmcc.2011.09.015 (2012).

3 Kumarswamy, R. & Thum, T. Non-coding RNAs in cardiac remodeling and heart failure. *Circulation research* **113**, 676-689, doi:10.1161/CIRCRESAHA.113.300226 (2013).

4 de Simone, G. *et al.* Evaluation of concentric left ventricular geometry in humans: evidence for age-related systematic underestimation. *Hypertension* **45**, 64-68, doi:10.1161/01.HYP.0000150108.37527.57 (2005).

5 Ganau, A. *et al.* Patterns of left ventricular hypertrophy and geometric remodeling in essential hypertension. *Journal of the American College of Cardiology* **19**, 1550-1558 (1992).

6 Dorn, G. W., 2nd, Robbins, J. & Sugden, P. H. Phenotyping hypertrophy: eschew obfuscation. *Circulation research* **92**, 1171-1175, doi:10.1161/01.RES.0000077012.11088.BC (2003).

7 Sehgal, S. & Drazner, M. H. Left ventricular geometry: does shape matter? *American heart journal* **153**, 153-155, doi:10.1016/j.ahj.2006.10.026 (2007).

8 Lorell, B. H. & Carabello, B. A. Left ventricular hypertrophy: pathogenesis, detection, and prognosis. *Circulation* **102**, 470-479 (2000).

9 Gaasch, W. H. & Zile, M. R. Left ventricular structural remodeling in health and disease: with special emphasis on volume, mass, and geometry. *Journal of the American College of Cardiology* **58**, 1733-1740, doi:10.1016/j.jacc.2011.07.022 (2011).

10 Opie, L. H., Commerford, P. J., Gersh, B. J. & Pfeffer, M. A. Controversies in ventricular remodelling. *Lancet* **367**, 356-367, doi:10.1016/S0140-6736(06)68074-4 (2006).

11 Wollert, K. C. *et al.* Cardiotrophin-1 activates a distinct form of cardiac muscle cell hypertrophy. Assembly of sarcomeric units in series VIA gp130/leukemia inhibitory factor receptor-dependent pathways. *The Journal of biological chemistry* **271**, 9535-9545 (1996).

12 Pennica, D. *et al.* Expression cloning of cardiotrophin 1, a cytokine that induces cardiac myocyte hypertrophy. *Proceedings of the National Academy of Sciences of the United States of America* **92**, 1142-1146 (1995).

13 De Windt, L. J., Lim, H. W., Haq, S., Force, T. & Molkentin, J. D. Calcineurin promotes protein kinase C and c-Jun NH2-terminal kinase activation in the heart. Cross-talk between cardiac hypertrophic signaling pathways. *The Journal of biological chemistry* **275**, 13571-13579 (2000).

14 Malo, N., Hanley, J. A., Cerquozzi, S., Pelletier, J. & Nadon, R. Statistical practice in high-throughput screening data analysis. *Nat Biotechnol* **24**, 167-175, doi:10.1038/nbt1186 (2006).

15 Jentzsch, C. *et al.* A phenotypic screen to identify hypertrophy-modulating microRNAs in primary cardiomyocytes. *Journal of molecular and cellular cardiology* **52**, 13-20, doi:10.1016/j.yjmcc.2011.07.010 (2012).

16 Sethupathy, P., Megraw, M. & Hatzigeorgiou, A. G. A guide through present computational approaches for the identification of mammalian microRNA targets. *Nat Methods* **3**, 881-886, doi:10.1038/nmeth954 (2006).

17 Frey, N. & Olson, E. N. Cardiac hypertrophy: the good, the bad, and the ugly. *Annual review of physiology* **65**, 45-79, doi:10.1146/annurev.physiol.65.092101.142243 (2003).

18 Cai, J. *et al.* MicroRNA-542-3p Suppresses Tumor Cell Invasion via Targeting AKT Pathway in Human Astrocytoma. *The Journal of biological chemistry* **290**, 24678-24688, doi:10.1074/jbc.M115.649004 (2015).

19 Oneyama, C. *et al.* MicroRNA-mediated upregulation of integrin-linked kinase promotes Src-induced tumor progression. *Oncogene* **31**, 1623-1635, doi:10.1038/onc.2011.367 (2012).

20 Yoon, S. *et al.* Induction of growth arrest by miR-542-3p that targets survivin. *FEBS Lett* **584**, 4048-4052, doi:10.1016/j.febslet.2010.08.025 (2010).

21 Althoff, K. *et al.* miR-542-3p exerts tumor suppressive functions in neuroblastoma by downregulating Survivin. *Int J Cancer* **136**, 1308-1320, doi:10.1002/ijc.29091 (2015).
22 Kureel, J. *et al.* miR-542-3p suppresses osteoblast cell proliferation and differentiation, targets BMP-7 signaling and inhibits bone formation. *Cell Death Dis* **5**, e1050, doi:10.1038/cddis.2014.4 (2014).
23 Ding, J. *et al.* Gain of miR-151 on chromosome 8q24.3 facilitates tumour cell migration and spreading through downregulating RhoGDIA. *Nat Cell Biol* **12**, 390-399, doi:10.1038/ncb2039 (2010).
24 Luedde, T. MicroRNA-151 and its hosting gene FAK (focal adhesion kinase) regulate tumor cell migration and spreading of hepatocellular carcinoma. *Hepatology* **52**, 1164-1166, doi:10.1002/hep.23854 (2010).
25 Zhang, Y. *et al.* Downregulation of miR-151-5p contributes to increased susceptibility to arrhythmogenesis during myocardial infarction with estrogen deprivation. *PLoS One* **8**, e72985, doi:10.1371/journal.pone.0072985 (2013).
26 Wang, J. X. *et al.* MicroRNA-532-3p regulates mitochondrial fission through targeting apoptosis repressor with caspase recruitment domain in doxorubicin cardiotoxicity. *Cell Death Dis* **6**, e1677, doi:10.1038/cddis.2015.41 (2015).
27 Le, M. T. *et al.* MicroRNA-125b is a novel negative regulator of p53. *Genes Dev* **23**, 862-876, doi:10.1101/gad.1767609 (2009).
28 Le, M. T. *et al.* MicroRNA-125b promotes neuronal differentiation in human cells by repressing multiple targets. *Mol Cell Biol* **29**, 5290-5305, doi:10.1128/MCB.01694-08 (2009).
29 Lee, Y. S., Kim, H. K., Chung, S., Kim, K. S. & Dutta, A. Depletion of human micro-RNA miR-125b reveals that it is critical for the proliferation of differentiated cells but not for the down-regulation of putative targets during differentiation. *The Journal of biological chemistry* **280**, 16635-16641, doi:10.1074/jbc.M412247200 (2005).
30 Scott, G. K. *et al.* Coordinate suppression of ERBB2 and ERBB3 by enforced expression of micro-RNA miR-125a or miR-125b. *The Journal of biological chemistry* **282**, 1479-1486, doi:10.1074/jbc.M609383200 (2007).
31 Mizuno, Y. *et al.* miR-125b inhibits osteoblastic differentiation by down-regulation of cell proliferation. *Biochem Biophys Res Commun* **368**, 267-272, doi:10.1016/j.bbrc.2008.01.073 (2008).
32 Gong, J. *et al.* MicroRNA-125b promotes apoptosis by regulating the expression of Mcl-1, Bcl-w and IL-6R. *Oncogene* **32**, 3071-3079, doi:10.1038/onc.2012.318 (2013).
33 Lin, K. Y. *et al.* miR-125b, a target of CDX2, regulates cell differentiation through repression of the core binding factor in hematopoietic malignancies. *The Journal of biological chemistry* **286**, 38253-38263, doi:10.1074/jbc.M111.269670 (2011).
34 Zhang, Y. *et al.* miR-125b is methylated and functions as a tumor suppressor by regulating the ETS1 proto-oncogene in human invasive breast cancer. *Cancer Res* **71**, 3552-3562, doi:10.1158/0008-5472.CAN-10-2435 (2011).
35 Zhou, M. *et al.* MicroRNA-125b confers the resistance of breast cancer cells to paclitaxel through suppression of pro-apoptotic Bcl-2 antagonist killer 1 (Bak1) expression. *The Journal of biological chemistry* **285**, 21496-21507, doi:10.1074/jbc.M109.083337 (2010).
36 Qin, Y. *et al.* MicroRNA-125b inhibits lens epithelial cell apoptosis by targeting p53 in age-related cataract. *Biochim Biophys Acta* **1842**, 2439-2447, doi:10.1016/j.bbadis.2014.10.002 (2014).
37 Busch, S. *et al.* 5-lipoxygenase is a direct target of miR-19a-3p and miR-125b-5p. *J Immunol* **194**, 1646-1653, doi:10.4049/jimmunol.1402163 (2015).
38 Wong, S. S. *et al.* miR-125b promotes early germ layer specification through Lin28/let-7d and preferential differentiation of mesoderm in human embryonic stem cells. *PLoS One* **7**, e36121, doi:10.1371/journal.pone.0036121 (2012).
39 Wang, X. *et al.* MicroRNA-125b protects against myocardial ischaemia/reperfusion injury via targeting p53-mediated apoptotic signalling and TRAF6. *Cardiovasc Res* **102**, 385-395, doi:10.1093/cvr/cvu044 (2014).

40 Nagpal, V. *et al.* MiR-125b is Critical for Fibroblast-to-Myofibroblast Transition and Cardiac Fibrosis. *Circulation*, doi:10.1161/CIRCULATIONAHA.115.018174 (2015).

41 Freed, D. H. *et al.* Cardiotrophin-1: expression in experimental myocardial infarction and potential role in post-MI wound healing. *Molecular and cellular biochemistry* **254**, 247-256 (2003).

CHAPTER 6

Long non-coding RNA Bigheart plays a direct role in regulating cardiomyocyte hypertrophic remodeling by affecting RNA splicing

Virginie Kinet[1]*, Frank Rühle[3]*, Ellen Dirkx[1], Leonne E. Philippen[1], Julie Halkein[1], Serve Olieslagers[1], Paula A. da Costa Martins[1,4], Monika Stoll[2,3,5]* and Leon J. de Windt[1]

[1]Department of Cardiology and [2]Biochemistry, CARIM School for Cardiovascular Diseases, Faculty of Health, Medicine and Life Sciences, Maastricht University, The Netherlands; [3]Department of Genetic Epidemiology, University of Muenster, Muenster, Germany; [4]Department of Physiology and Cardiothoracic Surgery, University of Porto, Porto, Portugal; [5]The Netherlands Maastricht Centre for Systems Biology (MaCSBio), Maastricht University.

* These authors contributed equally to this work

Abstract

Background

Long noncoding RNAs (lncRNAs) are an emerging class of epigenetic regulators with important functions in cardiac development and disease. Here, we sought to identify and functionally characterize lncRNAs implicated in murine heart failure development.

Methods and Results

We profiled lncRNAs in non-ischemic, failing hearts of two classical mouse models, a sustained transverse aortic constriction model and mice harboring a cardiac-specific calcineurin transgene, and discovered ~3.400 differentially expressed lncRNAs in the failing murine heart. RNA interference (RNAi) was employed to silence *Bigheart* and demonstrate its requirement for agonist-induced cardiomyocyte hypertrophy. One of the verified interaction partners of Bigheart is MOV10, a putative RNA helicase that is involved in pre-mRNA processing and RNA splicing. GO analysis implicated MOV10 in both diastolic and systolic blood pressure, hypertension and coronary artery calcification, linking it directly to pressure overload-induced heart diseases.

Conclusions

We have identified differentially expressed lncRNAs in the failing murine heart and characterized previously unexplored lncRNA Bigheart to be functionally involved in heart failure development. GO analysis suggest a central role for Bigheart in RNA splicing that shed new lights how modulation of the cardiac epigenetic landscape shapes cardiac signaling and transcriptional processes in heart failure.

Introduction

A variety of cardiovascular diseases, such as hypertension and myocardial infarction provoke pathological remodeling of the myocardium, vulnerability to sudden death and heart failure (HF), representing the primary cause of hospitalization and death in Europe.[1] Whereas common acquired forms of HF have genomic disease mechanisms underlying the progressive adverse remodeling of the myocardium, inherited cardiomyopathies have defined monogenetic disease causing mutations in genes encoding various structural components of the heart muscle. Despite the wide variety in disease-causing insults, HF therapy still follows a generic, 'one-size-fits-all' approach, ignoring the inter-individual differences caused by underlying genetic susceptibility, age, gender or stages of disease.[2,3] While current pharmacotherapy (β-blockers, ACE-inhibitors) and device-based therapies show effectiveness in prolonging survival in subsets of HF patients,[4] there is currently no therapy that directly treats the underlying molecular disease mechanism, rendering HF a prevalent unmet medical need that receives a largely palliative clinical treatment.

At the cellular level, a complex signaling network of transcription factors, co-regulators and various regulatory RNA species orchestrate the morphological changes of the cardiomyocytes as a response to biomechanical stress leading to pathological hypertrophy.[5] Although combinatorial transcription factor binding at proximal promoters is important and well characterized, the discovery of regulatory long noncoding RNA species (lncRNAs) has added a new layer of complexity to our understanding of transcriptional processes in heart disease. LncRNAs are RNA transcripts arbitrarily determined to be longer than 200 nucleotides and exert diverse biological functions independent of protein translation, including epigenetic silencing, transcription, and post-transcriptional regulation.[6] Over 9,000 genomic loci are predicted to code for these regulatory transcript subclasses in the human genome.[7,8] They exert their function both in the cytoplasm and in the nucleus and have the ability to act as decoys, sponges, scaffolds or chaperones allowing protein complexes, genes and chromosomes to be directed to appropriate RNA or DNA sequences.[6,9]

In recent years, lncRNAs have increasingly been implicated in cardiovascular development, physiology, and pathology. For example, *Braveheart* (Bvht, AK143260) is involved in cardiovascular lineage commitment[10], *TERMINATOR*, *ALIEN* and *PUNISHER* provide differentiation cues for pluripotent stem cells, cardiovascular progenitors and differentiated endothelial cells,[11] while *Fendrr* is necessary for proper development of the heart and body wall in the mouse.[12] Endothelial cell function, migration, differentiation and vessel growth are regulated by lncRNAs

MALAT1[13] and *SENCR*.[14] Cardiac-specific lncRNA *Myhrt* transcripts from the *Myh7* genomic locus protect the heart from hypertrophy and failure by antagonizing the function of *Brg1*, a chromatin-remodeling factor that is activated by stress to trigger aberrant gene expression and cardiac myopathy.[15] The lncRNA *CHRF* regulates cardiac hypertrophy by directly binding to miR-489, acting as a functional sponge to regulate anti-hypertrophic miR-489 expression and activity.[16] Moreover, genome-wide profiling of the cardiac transcriptome after myocardial infarction identified novel heart-specific lncRNAs with potential roles in both cardiac development and pathological cardiac remodeling. One of these novel lncRNAs, *Novlnc6*, modulates the expression of Nkx2.5, regulating cardiogenic differentiation, maturation, and homeostasis.[17] Additionally, GWAS identified variants in lncRNA *MIAT* as a risk factor for myocardial infarction[18], and susceptibility loci at chromosome 5q31 and 6p21 carrying the lncRNAs *SRA1* and *HCG22* have been significantly associated with dilated cardiomyopathy (DCM).[19,20] And finally, RNA sequencing was used to compare embryonic, normal adult and hypertrophied adult hearts, yielding lncRNAs *n411949* and *n413445* differentially expressed in the embryonic heart compared to normal and diseased adult hearts. These lncRNAs were functionally validated to target *Mccc1* and *Relb*, thereby regulating the NFκB pathway and availability of branched-chain amino acids for anabolic signaling in muscle respectively.[21]

Despite a steadily increasing number of reports on the functional role of single lncRNAs in cardiac disease, there exists uncertainty on the precise number of differentially expressed lncRNAs in non-ischemic pathological cardiac remodeling, in part due to the relatively poor annotation of lncRNAs. Although the number of databases containing information on lncRNAs is steadily increasing[22-27] as novel information on their functional properties and genomic location emerges, the annotation of the deposited lncRNAs has not yet reached the standards of mRNA variants. Here, we add new evidence of the existence of robust numbers of differentially expressed lncRNA species by simultaneously profiling both lncRNAs and mRNAs in hearts suffering from non-ischemic, pathological hypertrophic remodeling using two well-established mouse models of heart failure: a surgical model of transverse aorta constriction (TAC) to induce sustained cardiac pressure overload and mice with heart-restricted calcineurin overexpression. RNA interference (RNAi) was employed to silence the lncRNA *Bigheart* and demonstrate its requirement for agonist-induced cardiomyocyte hypertrophy. Furthermore, functional interaction analysis and gene ontology (GO) analysis of Bigheart was performed using the NPInter database, revealing Bigheart's role in mRNA processing. Taken together, Bigheart is directly implicated in adverse cardiac remodeling and provides new molecular cues underlying heart failure.

Methods

Animal models and transthoracic echocardiography

We used adult (8-10 week old) calcineurin transgenic mice in a B6CBAF1/J background expressing an activated mutant of calcineurin in the postnatal heart under control of the 5.5 kb murine *Myh6* promoter (MHC-CnA),[28] and corresponding B6CBAF1/J wildtype mice (Charles River Laboratories). Hearts were removed, rinsed in ice-cold phosphate buffered saline, atria removed, snap-frozen in liquid nitrogen and stored in liquid nitrogen until use. Adult BL6CBAF1 mice (12-16 week old) underwent transverse aortic constriction (TAC) by subjecting the aorta to a defined 27 gauge constriction between the first and second truncus of the aortic arch as described previously in detail.[29,30] At 4 weeks of TAC surgery, animals were sacrificed, hearts removed, rinsed in ice-cold phosphate buffered saline, atria removed, snap-frozen in liquid nitrogen and stored in liquid nitrogen until use. For Doppler-echocardiography, mice were shaved and lightly anaesthetized with isoflurane (mean 1% in oxygen) and allowed to breathe spontaneously via a nasal cone. Non-invasive, echocardiographic parameters were measured using a digital cardiac ultrasound platform (SONOS 5500, Philips) with a 15 MHz linear scanner (M- and B-mode), and a 12 MHz short focal length-phased array transducer (pw- and cw-Doppler) applied parasternally to the shaved chest wall. Doppler was used to calculate the pressure gradient between the proximal and distal sites of the transverse aortic constriction and only mice with a pressure gradient > 50 mm Hg were included. At 4 weeks post-banding, fractional shortening and ejection fraction were reduced to 50% of corresponding values of sham-operated, indicating severely reduced systolic cardiac function. All animal studies were performed in accordance with local institutional guidelines and regulations.

Primary neonatal rat cardiomyocytes cultures and siRNA transfections

Cardiomyocyte cultures were isolated by enzymatic dissociation of 1 day-old neonatal rat hearts as described previously in detail.[31] Cells were seeded in 10-cm dishes for RNA isolation or in 6-well plates to perform immunocytochemistry. One day after plating the neonatal rat cardiomyocytes were transfected with inhibitors (Dicer Substrate Duplex RNAs, IDT) of specific lncRNA transcripts (10nM) using Oligofectamin (Invitrogen). After 24 hours, cardiomyocyte hypertrophy was induced by phenylephrine (PE, 10 µM) stimulation for an additional 24h, as described previously.[32] For visualization of cardiomyocyte size and sarcomeric organization, cells were washed with ice cold PBS, fixed with 4% PFA (for 10 min) and stained for α2-actinin (ACTN2; 1:500; Sigma) followed by a phalloidin Texas Red- conjugated antibody (1:800; Molecular Probes). Nuclear staining was performed with

VECTASHIELD Mounting Medium containing 4',6-diamidino-2-phenylindole (DAPI; Vector Laboratories).

RNA isolation and quantitative real time-PCR

Total (1µg) RNA from mouse cardiac tissues or rat cardiomyocyte cells was isolated using TRIzol reagent (Invitrogen) and cDNA was generated using M-MLV Reverse Transcriptase (Promega). For real time RT-PCR, fluorescence detection was performed using SYBR Green on a BioRad iCycler (Biorad). Transcript quantities were compared using the relative Ct method, and normalized to endogenous GAPDH levels.

Histological analysis and (immunofluorescence) microscopy.

Hearts were arrested in diastole, perfusion fixed with 4% paraformaldehyde/PBS solution, embedded in paraffin and sectioned at 4 µm. Paraffin sections were stained with hematoxylin and eosine (H&E) for routine histological analysis; Sirius Red for the detection of fibrillar collagen; and FITC-labelled antibody against wheat-germ- agglutinin (WGA) to visualize and quantify the myocyte cross-sectional area (1:100 Sigma Aldrich). Slides were visualized using a Zeiss Axioskop 2Plus with an AxioCamHRc. Cell surface areas were determined using ImageJ - imaging software (http://rsb.info.nih.gov/ij/).

Microarray analysis of lncRNA and mRNA expression

Total RNA was isolated from three hearts of each condition (wildtype, MyHC-CnA, sham, TAC), quantified by a NanoDrop ND-1000 and RNA integrity was additionally assessed by standard denaturing agarose gel electrophoresis. For microarray analysis, an Arraystar Mouse LncRNA Expression Microarray V2.0 was used. The sample preparation and microarray hybridization were performed based on the manufacturer's standard protocols with minor modifications. Briefly, mRNA was purified from total RNA after removal of rRNA (mRNA-ONLY™ Eukaryotic mRNA Isolation Kit, Epicentre). Then, each sample was amplified and transcribed into fluorescent cRNA along the entire length of the transcripts without 3' bias utilizing a random priming method. The labeled cRNAs were hybridized onto the Mouse lncRNA Array v2.0 (8 x 60K, Arraystar). After having washed the slides, the arrays were scanned by an Agilent Scanner G2505C. Agilent Feature Extraction software (version 11.0.1.1) was used to analyze the acquired array images. Quantile normalization and subsequent data processing were performed using the GeneSpring GX v12.0 software package (Agilent Technologies).

GO analysis

Gene ontology (GO) analysis was performed for RP11-654A16.3 (human Bigheart, NONCODE ID NONHSAG018057.2) with NPInter software (www.bioinfo.org/NPInter).

Statistical and bioinformatical analyses

The expression values of lncRNAs and mRNAs are presented as mean ± standard error of the mean (SEM). Statistical analyses were performed using the R programming interface and consisted of ANOVA when group differences were detected, or Student's *t*-test when comparing two experimental groups. Adjustment for multiple testing was performed by applying Bonferroni's Multiple Comparison Test or controlling the false discovery rate (FDR), respectively. Differences were considered significant when $P<0.05$ and fold change between groups >= 2 or <= 0.5, respectively. Hierarchical clustering and heatmap illustrations were performed using the "gplots"-package to show the distinguishable expression patterns of lncRNA and mRNA subsets among samples. Correlation of expression values of lncRNAs and nearby mRNAs is calculated by Pearson correlation coefficient as implemented in R. P-values of correlation tests have been adjusted for multiple testing by FDR with respect to all 74134 possible pairs of lncRNAs and nearby mRNAs represented on the Mouse lncRNA Array v2.0 (8 x 60K, Arraystar). "Nearby" is defined as the genomic distance of < 300 kb.

For the validation of lncRNA, results are presented as mean ± standard error of the mean.[33] Statistical analyses were performed using Prism software (GraphPad Software Inc.), and consisted of ANOVA followed by Bonferroni's Multiple Comparison Test when group differences were detected at the 5% significance level, or Student's *t*-test when comparing two experimental groups. Differences were considered significant when $P<0.05$.

Results

Identification of cardiac hypertrophy associated lncRNAs

We performed a mouse combined lncRNA/mRNA array on total RNA isolated from hearts from two well-established models of pathological murine cardiac hypertrophy and failure. The first model is a transgenic mouse model overexpressing calcineurin driven by the heart-specific alpha-myosin heavy chain promotor (MHC-CnA). The second model consists of mice that underwent transverse aortic constriction (TAC) surgery resulting in sustained cardiac pressure overload, which evoked pathological hypertrophic remodeling after 4 weeks. Both histological and molecular biological analyses were performed to phenotypically characterize all animals used in this study. As expected, both hearts from mice that underwent TAC surgery and from MHC-CnA mice displayed pathological cardiac hypertrophic remodeling indicated by an increase in cardiomyocyte size, fibrosis, and re-activation of hypertrophic fetal genes encoding the natriuretic peptides atrial natriuretic factor (*Nppa*), brain natriuretic factor (*Nppb*) and β-myosin heavy chain (*Myh7*) (**Suppl Figure 1a, b**).

Hierarchical clustering was employed to differentiate the lncRNA expression patterns in wild-type (WT) or MHC-CnA murine hearts, and sham-operated and TAC-operated murine hearts. Among the 19.704 lncRNAs probed on this microarray, 1.325 lncRNAs were differentially expressed specifically in the group which received TAC surgery, graphically represented in a heat map representation (**Figure 1a**). Furthermore, 581 lncRNAs were exclusively differentially expressed in the MHC-CnA mice (**Figure 1b,e**). A total of 2.003 lncRNAs were significantly upregulated and 1.410 lncRNAs were significantly downregulated in both pathological hypertrophy models compared to the control (WT) group (**Figure 1c**). Volcano plot analyses of the microarray data used a cut-off value of 2.0 fold up- or downregulation compared to WT hearts (x-axis) and an indication of *p*-value of 0.05 (y-axis). Statistically significant, differentially expressed lncRNAs with more than 2.0 fold change are indicated by the red dots (**Figure 1d, e**).

Visualization of the data in a Venn diagram demonstrated that a total of 1.619 lncRNAs were upregulated in TAC hearts, 1.139 lncRNAs showed an increased expression in MHC-CnA hearts, while 755 lncRNAs were commonly increased in expression in both models for pathological hypertrophy compared to the WT group (**Figure 2a**). Among the lncRNAs that were significantly decreased in hypertrophic hearts, 461 were specifically downregulated in TAC hearts, 197 lncRNAs showed decreased expression levels only in MHC-CnA hearts and 752 lncRNAs were commonly downregulated in both TAC and MHC-CnA hearts compared to WT hearts (**Figure 2a**). The top-hundred most severely upregulated or downregulated lncRNAs

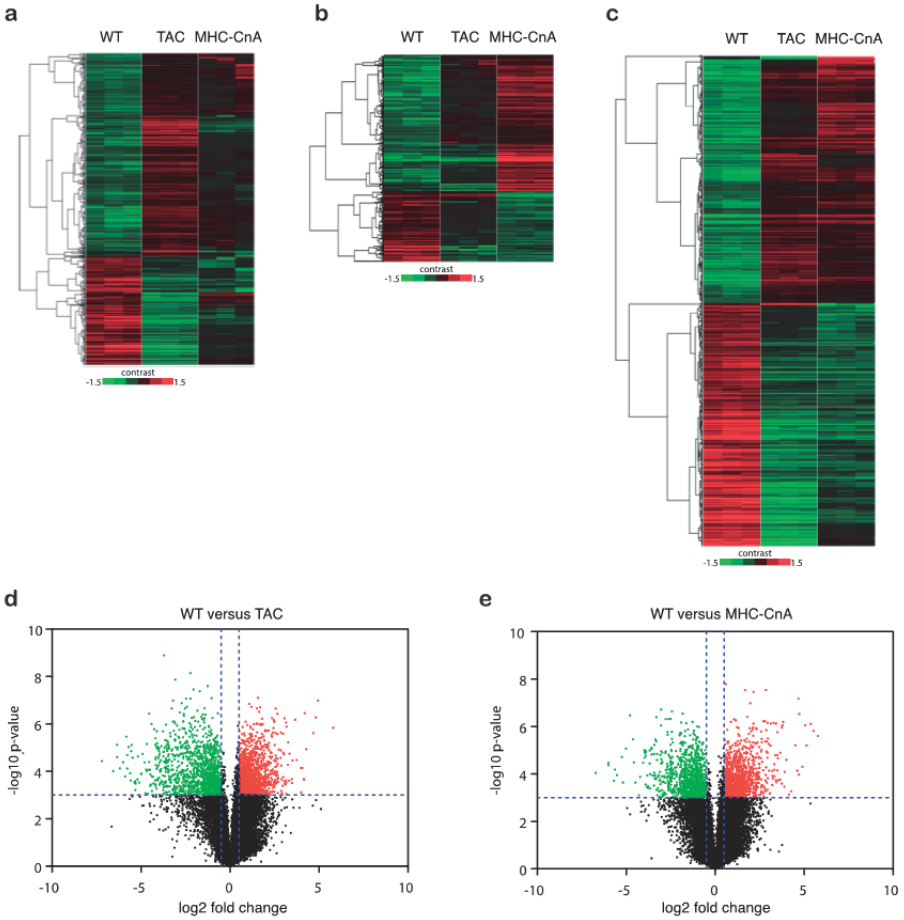

Figure 1. **Profiling of long noncoding RNAs in two animal models of heart failure**. **(a)** Heat map representation of differentially expressed LncRNAs from the microarray data between hearts from specifically WT and TAC groups. Genes significantly (*p < 0.05*) up- or downregulated in the TAC group are marked in red and green, respectively**. (b)** Heat map representation of differentially expressed LncRNAs from the microarray data between hearts from specifically WT and MHC-CnA groups. Genes significantly (*p < 0.05*) up- or downregulated in MHC-CnA mice are marked in red and green, respectively**. (c)** Heat map representation of all differentially expressed LncRNAs from the microarray data between WT, TAC and MHC-CnA hearts. **(d)** Volcano plot analysis of the microarray data on the differentially expressed lncRNAs between WT and TAC groups. The vertical lines correspond to a 2.0 fold up and down regulation while the horizontal line represents a *p*-value of 0.05. The red dots to the left and to the right of the vertical lines indicate more than 2.0 fold change and represent the differentially expressed LncRNAs with statistical significance. Statistical significance was defined as fold change ≥ 2.0 and *p*-value ≤ 0.05 between WT and TAC groups. **(e)** Volcano plot analysis of the microarray data on the differentially expressed lncRNAs between WT and MHC-CnA groups. The vertical lines correspond to a 2.0 fold up and down regulation while the horizontal line represents a *p*-value of 0.05. The red dots to the left and to the right of the vertical lines indicate more than 2.0 fold change and represent the differentially expressed LncRNAs with statistical significance. Statistical significance was defined as fold change ≥ 2.0 and *p*-value ≤ 0.05 between WT and MHC-CnA groups.

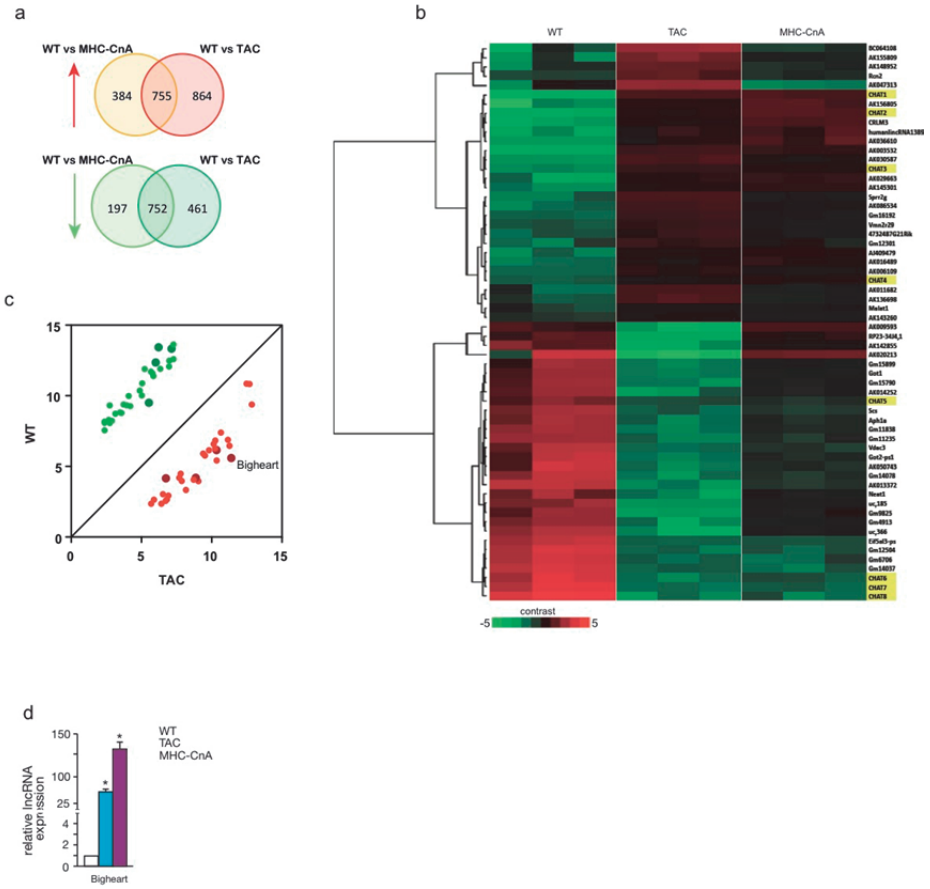

Figure 2. **Experimental validation of microarray analysis. (a)** Venn diagram presentation of the amount of lncRNAs differentially expressed in WT, TAC and MHC-CnA hearts. **(b)** Heat map presentation of a selection of the top candidates similarly expressed in both TAC and MHC-CnA hearts versus WT hearts. **(c)** Scatter plot of the top candidates presented in (b) in WT versus TAC hearts. **(d)** Real-time PCR analysis of relative abundance of *Bigheart (uc009hiz.1;ak014683;Bigheart)* in hearts from WT, MHC-CnA and mice subjected to TAC $*p < 0.05$, $**p < 0.005$, $***p < 0.0005$, $^{\#}p < 0.0001$ vs wild type group (error bars are s.e.m.).

in WT versus TAC and WT versus MHC-CnA are presented in tabular format (**Table 1-4**).

Next, we focused on the 755 lncRNAs that showed common increased expression in both hypertrophic models. Among the 30 most strongly increased lncRNA transcripts, *Braveheart* (*Bvht*) and *MALAT1* appeared (**Figure 2b**). We then selected lncRNA candidates that showed a similar differential expression pattern in both hypertrophy models and were not studied in this context before. Among these cardiac hypertrophy associated long noncoding transcripts, *AK014683* (Ensembl ID

4833412C05Rik, or *Bigheart*) was selected because it showed 5-15 fold differences with WT hearts (**Figure 2b, c**). The expression levels of *Bigheart* were validated by RT-qPCR in WT, TAC and MHC-CnA hearts, confirming its dramatic differentially expression patterns originally detected by the microarray platform (**Figure 2d**). Interestingly, a recent publication by Ye et al. showed that the expression levels of Bigheart in the cardiac muscle were increased after both TAC-induced hypertrophic remodeling as after induction of myocardial infarction in mice.[34]

Taken together, these data demonstrate that nearly two thousand lncRNAs display differential expression upon pressure overload-induced cardiac remodeling and dysfunction. Also, a large number of differentially expressed lncRNAs showed common aberrant expression in two established mouse models of non-ischemic forms of heart failure. Expression levels of lncRNA Bigheart were significantly increased in TAC and MHC-CnA mouse hearts.

A functional role of *Bigheart* in cardiomyocyte hypertrophy

Despite a steady increase in reports on the functional involvement of single lncRNAs, the functional implication of the vast majority of dysregulated lncRNAs in the heart remains virtually unexplored territory. Bigheart has been first described by Ye et al. showing that Bigheart levels were increased after TAC surgery in mice, as well as in mouse hearts after myocardial infarction. Interestingly, in their hnRNP U knockout mouse hearts, which develop lethal dilated cardiomyopathy and multiple defects in cardiac mRNA splicing, Bigheart was persistently expressed. hnRNP U deletion in the heart lead to accumulation of an alternatively spliced Bigheart isoform with an internal exon 2 skipped. The aberrant splicing of Bigheart pre-mRNA only occurred in the mutant mouse hearts.[34] However, the functional role of Bigheart in the diseased myocardium is still unknown. To evaluate whether Bigheart is directly able to influence cardiomyocyte hypertrophy, an obvious functional alteration in pressure overload-induced remodeling, neonatal rat cardiomyocytes were transfected with specific siRNA species to silence Bigheart specifically in the rat genome. RNAi against Bigheart resulted in a pronounced downregulation of 90% of Bigheart levels compared to cells transfected with a scrambled siRNA control (**Figure 3a**). Next, neonatal rat cardiomyocytes, transfected with either scrambled siRNA or a *Bigheart*-specific siRNA, were treated with the prohypertrophic agonist α1-adrenergic agonist phenylephrine.[35] To monitor changes in cell size, cardiomyocytes were stained for sarcomeric α-actinin and cell surface areas were determined. Repression of the *Bigheart*, which showed increased expression in TAC or MHC-CnA hearts compared to WT hearts (**Figure 2d**), resulted in a clear and significant reduction of PE-induced cardiomyocyte hypertrophy (**Figure 3a, b**).

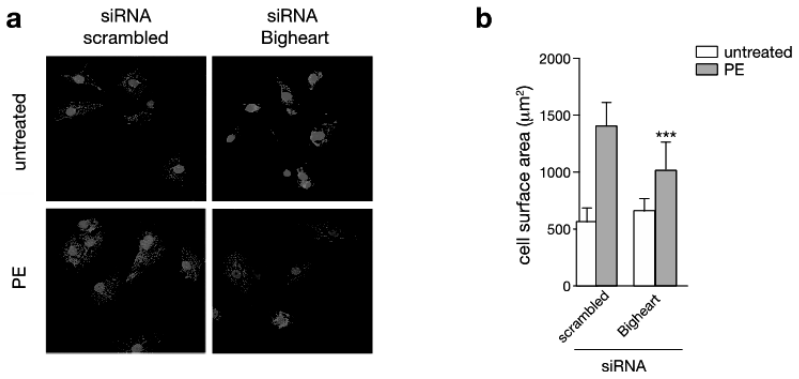

Figure 3. RNAi-mediated silencing reveals selected lncRNAs as necessary mediators of cardiac remodeling. (a) Confocal microscopy images of neonatal rat cardiomyocytes untreated or treated with PE, and transfected with siRNA against Bigheart or scrambled control. Nuclei were visualized with DAPI (blue) and stained with antibody against α-actinin [36]. **(b)** Quantification of cell surface area in conditions in **(a)**.

Taken together, these results indicate that Bigheart is responsive to RNAi silencing, and has endogenous pro-hypertrophic properties in neonatal cardiomyocytes.

Bigheart DNA sequence is partly conserved between mouse and human

Next, used bioinformatics tools to get a better understanding of the mechanism by which Bigheart regulates cardiac hypertrophy. Mouse Bigheart has 2 transcripts: 4833412C05Rik-001 of 1083bp long and 4833412C05Rik-003 of 850 bp in length (**Figure 4a**) located on chromosome 7: 67,784,538-67,803,496, reverse strand. Its human orthologue consist of one transcript, RP11-654A16.3-001, that is 588 bp in length. Sequence alignment between human Bigheart and the mouse counterpart revealed that large parts of the sequence are completely conserved among those species (**Figure 4b**). Many lncRNAs do not show the same pattern of high interspecies conservation as protein-coding genes. When they do, it's often an indication of functionality. On the other hand, conservation could be found in functional interactions with proteins or other RNAs, as opposed to the conservation of the specific nucleotide sequence.

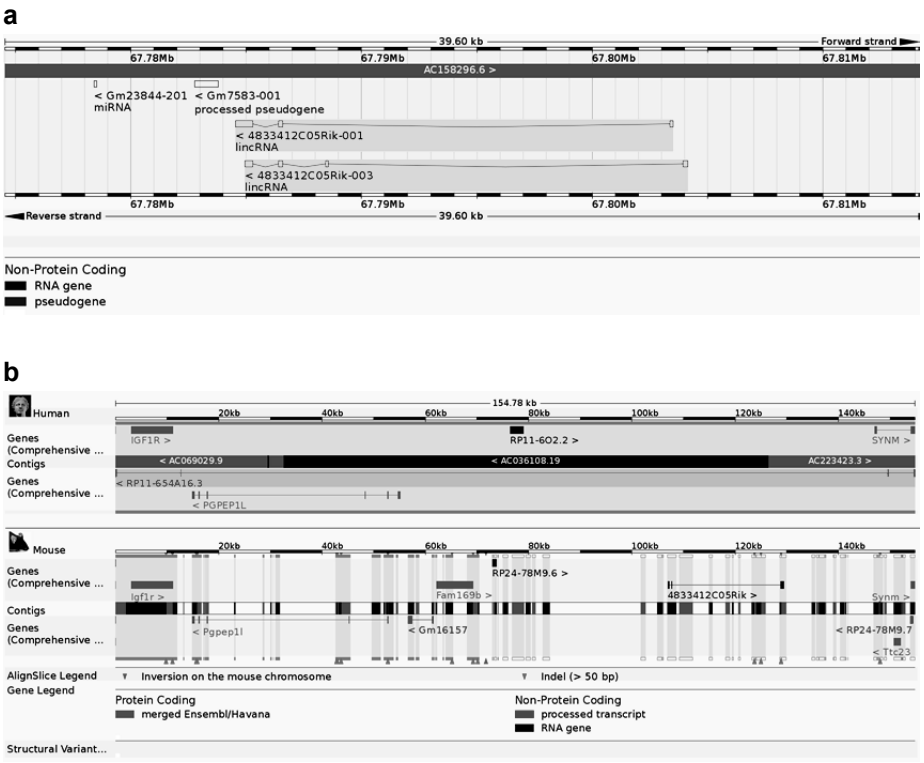

Figure 4. Location of Bigheart. (a) Image of chromosomal location with different transcripts for mouse Bigheart **(b)** Alignment image of human Bigheart [20] and mouse Bigheart (lower). Orange regions are completely conserved. Pictures from Ensembl database.

Bigheart targets MOV10, a RISC complex RNA helicase

Here we performed gene ontology (GO) analysis for RP11-654A16.3 (human Bigheart, NONCODE ID NONHSAG018057.2) with NPInter software (www.bioinfo.org/NPInter). This analysis revealed that human Bigheart was significantly associated with 10 biological processes (**Tabel 5**). Interestingly, many of these pathways indicate that Bigheart plays a role in mRNA processing events, which is consistent with the earlier publication of Ye et al. showing hnRNP U, an upstream regulator of Bigheart, is required for normal cardiac mRNA splicing.[34]

Tabel 5. GO pathway analysis of RP11-654A16.3 (NPInter software).

#ncName	GO term	The description of GO term
NONHSAG018057	GO:0006397	mRNA processing
NONHSAG018057	GO:0006366	transcription from RNA polymerase II promoter
NONHSAG018057	GO:0060011	Sertoli cell proliferation
NONHSAG018057	GO:0006369	termination of RNA polymerase II transcription
NONHSAG018057	GO:0006378	mRNA polyadenylation
NONHSAG018057	GO:0006379	mRNA cleavage
NONHSAG018057	GO:0031124	mRNA 3'-end processing
NONHSAG018057	GO:0090305	nucleic acid phosphodiester bond hydrolysis
NONHSAG018057	GO:0019054	modulation by virus of host cellular process
NONHSAG018057	GO:0046778	modification by virus of host mRNA processing

Moreover, interaction analysis with NPInter software revealed several interacting partners of Bigheart (**Tabel 6**). NPInter documents functional interactions (primarily physical interactions) between noncoding RNAs (except tRNAs and rRNAs) and proteins, RNAs and DNAs, which are experimentally verified. Among those genes, MOV10 is involved in pre-mRNA processing (**Tabel 6**). Further experimentally verified analysis revealed that MOV10 plays a significant role in both diastolic and systolic blood pressure, hypertension and coronary artery calcification, linking it directly to pressure overload-induced heart diseases.

Tabel 6. Functional interaction between RP11-654A16.3 and other molecules (NPInter software).

#interID	ncName	prName	interDescription	experiment	pubmed
ncRI-3059447	RP11-654A16.3	LIN28B	PAR-CLIP reproducibly identifies thousands of human RNAs directly bound by LIN28B	PAR-CLIP	23770886
ncRI-3059448	RP11-654A16.3	ADAR1	Genomic analysis of ADAR1 binding	CLIP-Seq	25751603
ncRI-3059449	RP11-654A16.3	WDR33	PAR-CLIP showed that WDR33 binds in and very close to the AAUAAA signal	PAR-CLIP	25301781
ncRI-3118969	RP11-654A16.3	CPSF7	We performed PAR-CLIP experiments for 3' end processing factors;CLIPseq data were analysed by CLIPdb	PAR-CLIP	22813749
ncRI-3124339	RP11-654A16.3	CPSF6	We performed PAR-CLIP experiments for 3' end processing factors;CLIPseq data were analysed by CLIPdb	PAR-CLIP	22813749
ncRI-3128166	RP11-654A16.3	CSTF2	We performed PAR-CLIP experiments for 3' end processing factors;CLIPseq data were analysed by CLIPdb	PAR-CLIP	22813749

#interID	ncName	prName	interDescription	experiment	pubmed
ncRI-3140171	RP11-654A16.3	FMR1	FMR1 targets distinct mRNA sequence elements to regulate protein expression;CLIPseq data were analysed by CLIPdb	PAR-CLIP	23235829
ncRI-3143903	RP11-654A16.3	CSTF2	We mapped CstF64-RNA interactions at the transcriptome level;CLIPseq data were analysed by CLIPdb	iCLIP	23112178
ncRI-3146441	RP11-654A16.3	YTHDF2	By using crosslinking and immunoprecipitation, we have identified over 4000 substrate RNA of YTHDF2;CLIPseq data were analysed by CLIPdb	PAR-CLIP	23453015;2
ncRI-3148202	RP11-654A16.3	HNRNPC	Quantitative iCLIP reveals genome-wide competition of hnRNP C and U2AF65;CLIPseq data were analysed by CLIPdb	iCLIP	23374342
ncRI-3149884	RP11-654A16.3	TIA1	iCLIP predicts the dual splicing effects of TIA-RNA interactions;CLIPseq data were analysed by CLIPdb	iCLIP	21048981
ncRI-3150223	RP11-654A16.3	TIAL1	iCLIP predicts the dual splicing effects of TIA-RNA interactions;CLIPseq data were analysed by CLIPdb	iCLIP	21048981
ncRI-3150783	RP11-654A16.3	TDP-43	CLIP-Seq of human brain and neuroblastoma sample to characterisethe RNA targets and position-dependent splicing regulation by TDP-43;CLIPseq data were analysed by CLIPdb	iCLIP	21358640
ncRI-3153417	RP11-654A16.3	TARBP2	Identify TARBP2 binding sites on endogenous RNA.	HITS-CLIP	25043050
ncRI-3160432	RP11-654A16.3	RBM6	CLIP-Seq analysis of RBM5, RBM6 and RBM10, with 2 biological replicates and one non-specific control for each protein.	CLIP-Seq	24332178
ncRI-3170791	RP11-654A16.3	RBM10	CLIP-Seq analysis of RBM5, RBM6 and RBM10, with 2 biological replicates and one non-specific control for each protein.	CLIP-Seq	24332178
ncRI-3180599	**RP11-654A16.3**	**MOV10**	**we demonstrate that MOV10 has an ATP-dependent 5 to 3 in vitro RNA unwinding activity and determine the RNA-binding sites of MOV10 and its helicase mutants using PAR-CLIP.**	**PAR-CLIP**	**24726324**
ncRI-3190789	RP11-654A16.3	UPF1	PAR-CLIP of UPF1 reveals that MOV10 and UPF1 bind to RNA in close proximity.	PAR-CLIP	24726324
ncRI-3209155	RP11-654A16.3	HNRNPA2B1	Nuclear HNRNPA2B1 HITS-CLIP.	HITS-CLIP	NA
ncRI-3241547	RP11-654A16.3	Fus/Tls	CLIP of Fus/Tls in adult human brain.	CLIP-Seq	23023293

Tabel 7. Functional interaction between RP11-654A16.3 and other molecules (NPInter software).

REPORTED GENE(S)	CHR_ID	CHR_POS	DISEASE/TRAIT	SNPS	P-VALUE	PUBMEDID
MOV10	1	112673921	Blood pressure	rs2932538	0.000008	21909110
MOV10	1	112673921	Diastolic blood pressure	rs2932538	1E-09	21909115
MOV10	1	112673921	Hypertension	rs2932538	0.0000003	21909115
MOV10	1	112673921	Systolic blood pressure	rs2932538	1E-09	21909115
MOV10	1	112646431	Systolic blood pressure	rs10745332	3E-09	25249183
MOV10	1	112646431	Diastolic blood pressure	rs10745332	0.00000008	25249183
MOV10	1	112646431	Hypertension	rs10745332	3E-09	25249183
WDR33	2	127745011	Coronary artery calcification	rs17015535	0.000006	23870195

Taken together, bioinformatics analyses of interaction partners and GO pathways aid in the identification of mechanisms by which lncRNAs can influence adverse cardiac remodeling. Here we revealed new mechanistic insights in the role of Bigheart in heart failure, that were previously not known.

Discussion

The Encyclopedia of DNA Elements project revealed that more than 97% of genomic DNA is actively transcribed in various species of RNA, with only a very small proportion of mammalian genomes encoding protein-coding genes that yield messenger RNA transcripts.[7,8] Small ncRNAs, most notably microRNAs (18-22 nucleotides long), have been extensively studied and implicated as key players in several human pathologies, including cardiovascular diseases.[37] However, much less is known about the biology and functions of lncRNAs in the cardiovascular system. Despite a steady increase in reports on the involvement of single lncRNAs, the functional implication of the vast majority of dysregulated lncRNAs in heart remains virtually unexplored territory. Although recent studies performed lncRNA profiling in models of cardiac differentiation, cardiac disease and cardiac angiogenesis,[17,21,38,39] the discipline covering lncRNAs in cardiovascular diseases remains preliminary in nature and often address different diseases entities.

In the current study, we profiled lncRNAs in non-ischemic, failing hearts of two classical mouse models, a sustained transverse aortic constriction model and mice harboring a cardiac-specific calcineurin transgene, and discovered ~3.400 differentially expressed lncRNAs in the failing murine heart. We chose the Arraystar

platform for lncRNA and mRNA profiling since it provided the most reliable resource for lncRNA and mRNA profiling in a single experiment. Furthermore, next generation sequencing [7] applications and bioinformatics routines are not equally well established, and annotation of novel, putative lncRNAs remains a challenge. Among identified lncRNAs, we detected *Braveheart*, a critical regulator of cardiac cell fate,[10] and *MALAT1*, a regulator of endothelial cell function and vessel growth.[13] Apart from these known lncRNAs, we identified the differentially expressed lncRNA Bigheart that was previously shown to be upregulated in heart disease models, but it's function in the context of heart disease or downstream mechanism has not been described before. In the current study, we explored the functional role of *Bigheart*. *Bigheart* was significantly upregulated in cardiac hypertrophic remodeling. In line, RNAi-mediated knockdown of *Bigheart* transcripts remarkably decreased agonist-induced hypertrophic effects, suggesting its direct functional requirement in this process.

To obtain mechanistic insight in the potential lncRNA-mediated molecular mechanisms underlying cardiac remodeling, we took advantage of the NPInter database that documents functional interactions between noncoding RNAs and proteins, RNAs and DNAs based on experimentally verified results. GO-analysis-based bioinformatics revealed that Bigheart in involved in mRNA processing (**Tabel 5**). Indeed, one of the verified interaction partners of Bigheart is MOV10, a putative RNA helicase that is involved in pre-mRNA processing (**Tabel 6**). GO analysis implicated MOV10 in both diastolic and systolic blood pressure, hypertension and coronary artery calcification, linking it directly to pressure overload-induced heart diseases. A genome-wide association study of systolic and diastolic blood pressure, shows that MOV10 is associated with blood pressure and hypertension.[40,41] Bigheart was previously implicated in a cardiac-specific heterogeneous nuclear ribonucleoprotein U (hnRNP U) knockout model of cardiac disease. Loss of hnRNP U expression in cardiomyocytes results in impaired sarcomere contractility and cardiac function, and mice deficient in hnRNP U expression in the heart develop a severe DCM phenotype. HnRNP U protein is required for normal pre-mRNA splicing and postnatal heart development and function. RNA sequencing of hnRNP U-deficient hearts showed activation of lncRNA Bigheart. Loss of hnRNP U resulted in context-dependent splicing defects, since mixed splicing activities (skipping and inclusion) were observed. HnRNP U mutant hearts showed increased Bigheart levels. In addition, Bigheart is expressed as two alternatively spliced isoforms in hnRNP U mutant cells. Deletion of hnRNP U resulted in persistent expression of Bigheart in the heart, and the accumulation of an alternatively spliced Bigheart isoform with an internal exon 2 skipped.[34] HnRNP U has binds specifically to lncRNAs and plays a role in chromosome organization.[34] Moreover, hnRNP U protein is required for

chromosomal localization of Xist RNA in normal X chromosome inactivation[42] and interacts with lncRNA Firre that is located on the X chromosome and is essential for maintaining or establishing higher-order nuclear architecture.[43] Since hnRNP U acts upstream of Bigheart and is involved in cardiac pre-mRNA splicing events, it is likely that Bigheart also plays a direct role in the RNA splicing process, presumably via interaction with the RNA helicase MOV10. Introns are spliced from pre-mRNAs by the spliceosome of eukaryotic cells. RNA helicases are key regulators of splicing. They are involved in promoting conformational rearrangements and ensure that only appropriate substrates proceed through the splicing reactions.

RNA helicases are key regulators of gene expression that act by remodeling RNA secondary structures and RNA-protein interactions. MOV10 has an ATP-dependent 5' to 3' in vitro RNA unwinding activity. Moreover, MOV10 interacts directly with UPF1, the key component of the nonsense-mediated mRNA decay pathway. Knockdown of MOV10 resulted in increased mRNA half-lives of MOV10-bound as well as UPF1-regulated transcripts, indicating that MOV10 helicase activity promotes mRNA degradation of its target mRNAs and UPF1-regulated transcripts.[44]

Accumulating evidence shows that alternative mRNA splicing affects a broad spectrum of cardiac genes during normal development as well as pathological progress of heart diseases.[45-48] In patients with myotonic dystrophy type 1 abnormal splicing of *SCN5A* (the gene encoding the Na^+ channel subunit expressed in the human heart) lead to the life-threatening heart rhythm disorder Brugada syndrome.[49] Another study used the Affymetrix Exon array to evaluate mRNA splicing in left ventricular myocardial RNA from controls and patients with ischemic cardiomyopathy. They observed that mRNA splicing is broadly altered in human heart disease and that patterns of aberrant RNA splicing in four sarcomeric genes accurately assign samples to control or disease classes, suggesting distinct changes in mRNA splicing between groups. The ratio of minor to major splice variants of TNNT2, MYH7, and FLNC classified independent test samples as control or disease with >98% accuracy.[50] Another example is the central fructose-metabolizing enzyme ketohexokinase, which is shown to be regulated during pathological cardiac hypertrophy through the splicing factor SF3B1.[51] Although RNA splicing is a major contributor to total transcriptome complexity, the functional role and regulation of splicing in heart failure remain poorly understood. The discovery of pro-hypertrophic lncRNA Bigheart that is implicated in cardiac splicing, might shed a new light on the regulation of splicing in heart disease. Further validation to confirm that MOV10 is responsible for the Bigheart-mediated effect on cardiac hypertrophy is still required.

Although lncRNA research is a relatively new field, approaches to therapeutically target dysregulated lncRNA transcripts are already being pursued by *in vivo* inhibition with small interfering RNAs or GapmeRs, a therapeutics field inspired by the success of microRNA therapeutics.[52] Indeed, *MALAT1* inhibition produced a promigratory response and increased basal sprouting and migration, whereas proliferation of endothelial cells was inhibited, reducing blood flow recovery and capillary density after hindlimb ischemia.[13] Further functional characterization of lncRNAs will enhance our understanding of the molecular mechanisms underlying pathological cardiac remodeling and could open a new field for therapeutic strategies for heart failure patients.

Acknowledgements

We gratefully acknowledge Giuliano G. Stirparo (Milan) for bioinformatics support and members of the De Windt laboratory for technical support and helpful discussions. E.D. is supported by a VENI award 916-150-16 from the Netherlands Organization for Health Research and Development (ZonMW), P.D.C.M. is supported by a MEERVOUD grant from The Netherlands Organisation for Scientific Research (NWO). L.D.W. acknowledges support from the *Netherlands CardioVascular Research Initiative*: the Dutch Heart Foundation, Dutch Federation of University Medical Centers, ZonMW and the Royal Netherlands Academy of Sciences. L.D.W. was further supported by grant 311549 from the European Research Council [6] and a VICI award 918-156-47 from NWO.

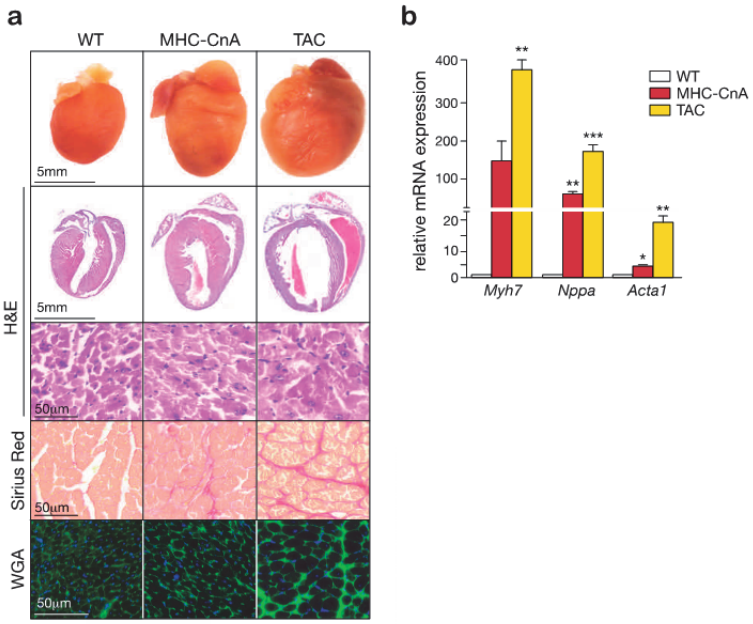

Supplemental Figure 1. Profiling of long non coding RNAs in two animal models of heart failure. (a) Representative images of whole hearts (top panels), haematoxylin & eosin (H&E)- stained sections of four-chamber view (second panel), high magnification H&E-stained sections (third panel), Sirius Red stained sections (fourth panel) and wheat germ agglutinin (WGA)-stained (fifth panel) histological sections of hearts from wild type (WT), calcineurin transgenic mice (MHC-CnA) and transverse aortic constriction (TAC) pressure overloaded. **(b)** Real-time PCR analysis of relative transcript abundance for the fetal marker genes *Myh7, Nppa*, and *Acta1* in hearts from wild type (WT), calcineurin transgenic mice (MHC-CnA) and mice subjected to transverse aortic constriction (TAC) $*P < 0.05$, $**P < 0.005$ vs wild type group (error bars are s.e.m.).

References

1 Packer, M. *et al.* Effect of carvedilol on survival in severe chronic heart failure. *N Engl J Med* **344**, 1651-1658 (2001).

2 Benjamin, I. J. & Schneider, M. D. Learning from failure: congestive heart failure in the postgenomic age. *J Clin Invest* **115**, 495-499 (2005).

3 Creemers, E. E., Wilde, A. A. & Pinto, Y. M. Heart failure: advances through genomics. *Nat Rev Genet* **12**, 357-362 (2011).

4 Lang, C. C. & Struthers, A. D. Targeting the renin-angiotensin-aldosterone system in heart failure. *Nat Rev Cardiol* **10**, 125-134 (2013).

5 Philippen, L. E., Dirkx, E., da Costa-Martins, P. A. & De Windt, L. J. Non-coding RNA in control of gene regulatory programs in cardiac development and disease. *J Mol Cell Cardiol* (2015).

6 Mercer, T. R., Dinger, M. E. & Mattick, J. S. Long non-coding RNAs: insights into functions. *Nat Rev Genet* **10**, 155-159 (2009).

7 Carninci, P. *et al.* The transcriptional landscape of the mammalian genome. *Science* **309**, 1559-1563 (2005).

8 Consortium, E. P. An integrated encyclopedia of DNA elements in the human genome. *Nature* **489**, 57-74 (2012).

9 Batista, P. J. & Chang, H. Y. Long noncoding RNAs: cellular address codes in development and disease. *Cell* **152**, 1298-1307 (2013).

10 Klattenhoff, C. A. *et al.* Braveheart, a long noncoding RNA required for cardiovascular lineage commitment. *Cell* **152**, 570-583 (2013).

11 Kurian, L. *et al.* Identification of novel long noncoding RNAs underlying vertebrate cardiovascular development. *Circulation* **131**, 1278-1290 (2015).

12 Grote, P. *et al.* The tissue-specific lncRNA Fendrr is an essential regulator of heart and body wall development in the mouse. *Developmental cell* **24**, 206-214 (2013).

13 Michalik, K. M. *et al.* Long noncoding RNA MALAT1 regulates endothelial cell function and vessel growth. *Circulation research* **114**, 1389-1397 (2014).

14 Bell, R. D. *et al.* Identification and initial functional characterization of a human vascular cell-enriched long noncoding RNA. *Arteriosclerosis, thrombosis, and vascular biology* **34**, 1249-1259 (2014).

15 Han, P. *et al.* A long noncoding RNA protects the heart from pathological hypertrophy. *Nature* **514**, 102-106 (2014).

16 Wang, K. *et al.* The long noncoding RNA CHRF regulates cardiac hypertrophy by targeting miR-489. *Circulation research* **114**, 1377-1388 (2014).

17 Ounzain, S. *et al.* Genome-wide profiling of the cardiac transcriptome after myocardial infarction identifies novel heart-specific long non-coding RNAs. *Eur Heart J* (2014).

18 Ishii, N. *et al.* Identification of a novel non-coding RNA, MIAT, that confers risk of myocardial infarction. *Journal of human genetics* **51**, 1087-1099 (2006).

19 Friedrichs, F. *et al.* HBEGF, SRA1, and IK: Three cosegregating genes as determinants of cardiomyopathy. *Genome research* **19**, 395-403 (2009).

20 Meder, B. *et al.* A genome-wide association study identifies 6p21 as novel risk locus for dilated cardiomyopathy. *European heart journal* **35**, 1069-1077 (2014).

21 Matkovich, S. J., Edwards, J. R., Grossenheider, T. C., de Guzman Strong, C. & Dorn, G. W., 2nd. Epigenetic coordination of embryonic heart transcription by dynamically regulated long noncoding RNAs. *Proc Natl Acad Sci U S A* **111**, 12264-12269 (2014).

22 Volders, P. J. *et al.* LNCipedia: a database for annotated human lncRNA transcript sequences and structures. *Nucleic acids research* **41**, D246-251 (2013).

23 Bhartiya, D. *et al.* lncRNome: a comprehensive knowledgebase of human long noncoding RNAs. *Database : the journal of biological databases and curation* **2013**, bat034 (2013).

24 Amaral, P. P., Clark, M. B., Gascoigne, D. K., Dinger, M. E. & Mattick, J. S. lncRNAdb: a reference database for long noncoding RNAs. *Nucleic acids research* **39**, D146-151 (2011).
25 Gong, J., Liu, W., Zhang, J., Miao, X. & Guo, A. Y. lncRNASNP: a database of SNPs in lncRNAs and their potential functions in human and mouse. *Nucleic acids research* **43**, D181-186 (2015).
26 Ning, S. *et al.* SNP@lincTFBS: an integrated database of polymorphisms in human LincRNA transcription factor binding sites. *PloS one* **9**, e103851 (2014).
27 Chen, G. *et al.* LncRNADisease: a database for long-non-coding RNA-associated diseases. *Nucleic acids research* **41**, D983-986 (2013).
28 Molkentin, J. D. *et al.* A calcineurin-dependent transcriptional pathway for cardiac hypertrophy. *Cell* **93**, 215-228 (1998).
29 Rockman, H. A. *et al.* Segregation of atrial-specific and inducible expression of an atrial natriuretic factor transgene in an in vivo murine model of cardiac hypertrophy. *Proc Natl Acad Sci U S A* **88**, 8277-8281 (1991).
30 Bourajjaj, M. *et al.* NFATc2 is a necessary mediator of calcineurin-dependent cardiac hypertrophy and heart failure. *J Biol Chem* **283**, 22295-22303 (2008).
31 De Windt, L. J., Lim, H. W., Haq, S., Force, T. & Molkentin, J. D. Calcineurin promotes protein kinase C and c-Jun NH2-terminal kinase activation in the heart. Cross-talk between cardiac hypertrophic signaling pathways. *The Journal of biological chemistry* **275**, 13571-13579 (2000).
32 De Windt, L. J. *et al.* Calcineurin-mediated hypertrophy protects cardiomyocytes from apoptosis in vitro and in vivo: An apoptosis-independent model of dilated heart failure. *Circ Res* **86**, 255-263 (2000).
33 Van Berendoncks, A. M. *et al.* Functional adiponectin resistance at the level of the skeletal muscle in mild to moderate chronic heart failure. *Circ Heart Fail* **3**, 185-194 (2010).
34 Ye, J. *et al.* hnRNP U protein is required for normal pre-mRNA splicing and postnatal heart development and function. *Proceedings of the National Academy of Sciences of the United States of America* **112**, E3020-3029 (2015).
35 http://www.escardio.org/The-ESC/Initiatives/EuroHeart/2012-European-Cardiovascular-Disease-Statistics.
36 Pleger, S. T. *et al.* Cardiac AAV9-S100A1 gene therapy rescues post-ischemic heart failure in a preclinical large animal model. *Science translational medicine* **3**, 92ra64 (2011).
37 van Rooij, E. & Olson, E. N. MicroRNAs: powerful new regulators of heart disease and provocative therapeutic targets. *J Clin Invest* **117**, 2369-2376 (2007).
38 Fiedler, J. *et al.* Development of Long Noncoding RNA-Based Strategies to Modulate Tissue Vascularization. *Journal of the American College of Cardiology* **66**, 2005-2015 (2015).
39 Ounzain, S. *et al.* CARMEN, a human super enhancer-associated long noncoding RNA controlling cardiac specification, differentiation and homeostasis. *J Mol Cell Cardiol* **89**, 98-112 (2015).
40 International Consortium for Blood Pressure Genome-Wide Association, S. *et al.* Genetic variants in novel pathways influence blood pressure and cardiovascular disease risk. *Nature* **478**, 103-109 (2011).
41 Wain, L. V. *et al.* Genome-wide association study identifies six new loci influencing pulse pressure and mean arterial pressure. *Nat Genet* **43**, 1005-1011 (2011).
42 Hasegawa, Y. *et al.* The matrix protein hnRNP U is required for chromosomal localization of Xist RNA. *Dev Cell* **19**, 469-476 (2010).
43 Hacisuleyman, E. *et al.* Topological organization of multichromosomal regions by the long intergenic noncoding RNA Firre. *Nat Struct Mol Biol* **21**, 198-206 (2014).
44 Gregersen, L. H. *et al.* MOV10 Is a 5' to 3' RNA helicase contributing to UPF1 mRNA target degradation by translocation along 3' UTRs. *Mol Cell* **54**, 573-585 (2014).
45 Poon, K. L. *et al.* RNA-binding protein RBM24 is required for sarcomere assembly and heart contractility. *Cardiovasc Res* **94**, 418-427 (2012).

46 Ramchatesingh, J., Zahler, A. M., Neugebauer, K. M., Roth, M. B. & Cooper, T. A. A subset of SR proteins activates splicing of the cardiac troponin T alternative exon by direct interactions with an exonic enhancer. *Mol Cell Biol* **15**, 4898-4907 (1995).
47 Xu, X. *et al.* ASF/SF2-regulated CaMKIIdelta alternative splicing temporally reprograms excitation-contraction coupling in cardiac muscle. *Cell* **120**, 59-72 (2005).
48 Ding, J. H. *et al.* Dilated cardiomyopathy caused by tissue-specific ablation of SC35 in the heart. *EMBO J* **23**, 885-896 (2004).
49 Wahbi, K. *et al.* Brugada syndrome and abnormal splicing of SCN5A in myotonic dystrophy type 1. *Arch Cardiovasc Dis* **106**, 635-643 (2013).
50 Kong, S. W. *et al.* Heart failure-associated changes in RNA splicing of sarcomere genes. *Circ Cardiovasc Genet* **3**, 138-146 (2010).
51 Mirtschink, P. *et al.* HIF-driven SF3B1 induces KHK-C to enforce fructolysis and heart disease. *Nature* **522**, 444-449 (2015).
52 Philippen, L. E. *et al.* Antisense MicroRNA Therapeutics in Cardiovascular Disease: Quo Vadis? *Mol Ther* **23**, 1810-1818 (2015).

Table 1. WT versus TAC

Gene Symbol	logFC	p value	-log10Pval
AK003532	4.936	1.03E-07	6.987
AK155809	4.832	1.64E-03	2.786
AK030587	4.812	5.28E-07	6.278
AK020360	4.675	2.43E-06	5.614
AK156805	4.654	2.81E-03	2.552
CRLM3	4.284	1.15E-05	4.939
Lrp8	4.192	3.51E-07	6.455
humanlincRNA1389	4.161	2.22E-04	3.653
Sprr2g	4.140	2.09E-04	3.680
AK036610	4.063	7.10E-05	4.149
AK029663	3.995	7.76E-04	3.110
AK086534	3.986	7.13E-05	4.147
AK148952	3.897	3.43E-03	2.464
AK145301	3.741	3.32E-05	4.479
Gm16192	3.657	6.62E-07	6.179
AK011682	3.566	3.40E-03	2.469
Rcn2	3.506	3.43E-05	4.465
Gm12301	3.489	1.50E-03	2.823
AK136698	3.482	3.08E-04	3.512
AJ409479	3.472	2.08E-04	3.682
AK047313	3.422	3.98E-02	1.401
AK006109	3.342	1.80E-05	4.746
4732487G21Rik	3.315	2.42E-04	3.616
Vmn2r29	3.257	6.07E-06	5.217
AK016489	3.248	5.22E-05	4.282
AK041310	3.188	3.28E-03	2.484
AK143464	3.175	1.29E-06	5.889
MM9LINCRNAEXON11713-	3.156	8.83E-04	3.054
Gm12092	3.148	3.04E-04	3.517
AK005183	3.142	8.63E-07	6.064
BC030398	3.134	2.43E-04	3.614
uc.451	3.118	1.94E-02	1.713
AK015101	3.111	3.62E-04	3.442
MM9LINCRNAEXON12060+	3.091	1.28E-03	2.891
AJ409495	3.067	3.31E-04	3.480
AK042604	3.065	5.81E-07	6.236
AK002748	3.057	3.52E-03	2.454

Gene Symbol	logFC	p value	-log10Pval
AK086591	3.031	1.91E-05	4.719
AK192563	3.027	2.59E-04	3.587
AK082921	2.985	1.64E-05	4.786
AK048000	2.985	1.73E-04	3.762
AK078752	2.980	2.59E-06	5.586
AK131851	2.958	1.56E-03	2.807
AK052076	2.952	3.72E-02	1.429
D430040D24Rik	2.950	4.07E-04	3.391
4930570G19Rik	2.923	8.36E-04	3.078
GDNFR-alpha	2.912	9.54E-02	1.021
AK016944	2.886	2.16E-04	3.665
AK033935	2.881	4.32E-03	2.364
AK007126	2.874	5.69E-05	4.245
Zfp82	2.873	6.79E-04	3.168
AK137188	2.862	2.30E-06	5.637
mouselincRNA0569	2.854	1.22E-03	2.914
AK052417	2.849	1.30E-05	4.885
AK013700	2.841	2.66E-05	4.575
AK019332	2.761	6.57E-03	2.182
AK172237	2.743	1.19E-05	4.923
AK079804	2.730	7.25E-03	2.140
AK044126	2.728	5.35E-03	2.272
Sfrs14	2.706	1.90E-04	3.720
AK006677	2.705	2.75E-04	3.560
LOC100270707	2.700	8.18E-03	2.087
AK008891	2.675	1.44E-04	3.842
humanlincRNA1768	2.668	8.16E-04	3.088
Telomerase-vert.2	2.668	4.73E-05	4.325
Gm11164	2.664	3.76E-07	6.425
BC028801	2.660	2.61E-06	5.583
C030013C21Rik	2.659	2.92E-05	4.535
AK035076	2.657	2.13E-04	3.671
Gm15310	2.655	1.05E-04	3.979
AK039307	2.652	2.48E-03	2.606
AK089363	2.649	2.89E-04	3.539
BM942986	2.631	5.88E-05	4.230
AK006093	2.630	9.94E-03	2.003
AK139621	2.617	1.55E-02	1.810

Gene Symbol	logFC	p value	-log10Pval
humanlincRNA2047	2.613	2.85E-01	0.545
Gm16118	2.612	1.33E-03	2.877
AK163739	2.606	1.57E-04	3.803
Aoah	2.594	2.82E-04	3.550
Gm13334	2.593	2.75E-05	4.561
AK017368	2.588	1.65E-02	1.783
AK076843	2.583	3.75E-02	1.426
AK046653	2.583	3.28E-04	3.485
Gm15297	2.577	1.35E-02	1.869
AK034419	2.571	3.67E-05	4.436
Cdcp1	2.566	1.21E-04	3.918
AK141773	2.562	2.14E-05	4.670
AK082265	2.557	2.21E-07	6.655
BB497033	2.547	2.40E-06	5.621
Gm15541	2.544	1.25E-04	3.903
BC134356	2.543	1.35E-04	3.868
Ptn	2.542	1.83E-03	2.738
Gm16990	2.539	6.46E-05	4.190
AK033223	2.536	3.78E-05	4.423
AK076245	2.528	2.27E-04	3.643
AK084834	2.523	1.25E-03	2.903
AK081202	2.519	2.80E-04	3.552
1700003F17Rik	2.514	1.01E-04	3.997

Table 2. WT versus TAC

Gene Symbol	logFC	p value	-log10Pval
MM9LINCRNAEXON11101-	-3.923	3.12E-04	3.506
Gm12620	-3.927	1.02E-04	3.991
Gm13232	-3.936	9.02E-05	4.045
Gm6733	-3.937	1.14E-03	2.942
Gm8979	-3.956	1.75E-05	4.758
AK136146	-3.959	4.14E-05	4.383
AK036276	-3.959	9.73E-04	3.012
Gm8822	-3.959	3.68E-04	3.434
AK161725	-3.980	2.85E-02	1.546
uc.203	-3.982	1.87E-04	3.729
Kars-ps1	-3.987	1.03E-05	4.989
Gm11841	-3.989	2.18E-05	4.661
Gm5466	-4.005	1.35E-05	4.871
Gm13237	-4.016	5.49E-05	4.260
AK171173	-4.025	1.95E-04	3.710
Gm14937	-4.027	1.09E-05	4.963
Gm14269	-4.032	2.69E-05	4.571
Gm15331	-4.045	1.08E-05	4.967
Gm11839	-4.073	2.38E-04	3.624
Gm13167	-4.086	6.57E-05	4.183
Gm7308	-4.092	1.06E-05	4.973
Gm12626	-4.095	8.76E-06	5.058
AC138228.1	-4.104	6.48E-06	5.188
Gm3608	-4.104	6.99E-03	2.155
Gm13082	-4.110	2.21E-04	3.655
AK017799	-4.119	2.03E-06	5.692
Ankrd16	-4.125	7.93E-05	4.101
AK033485	-4.128	5.35E-04	3.272
Gm12623	-4.129	9.81E-06	5.009
Gm14670	-4.152	9.47E-04	3.023
mKIAA0031	-4.169	5.42E-05	4.266
Gm11448	-4.176	2.49E-05	4.604
Anp32-ps	-4.177	1.19E-03	2.924
Timm44	-4.180	3.08E-05	4.511
Gm8410	-4.183	4.20E-04	3.377
Gm6563	-4.195	4.03E-06	5.394
Gm5383	-4.196	3.54E-04	3.451

Gene Symbol	logFC	p value	-log10Pval
Rpl3l	-4.201	7.65E-06	5.117
BC030682	-4.212	2.38E-04	3.623
Gm15754	-4.260	1.67E-06	5.778
Nsun2	-4.261	2.83E-03	2.549
BC080792	-4.292	1.06E-02	1.977
Maf1	-4.303	3.24E-04	3.490
Gm15861	-4.328	1.11E-03	2.954
Gm13378	-4.331	1.70E-04	3.769
AK142657	-4.389	6.73E-04	3.172
Gm15285	-4.396	1.63E-04	3.789
Gm9308	-4.417	1.00E-06	5.999
AK142426	-4.442	5.69E-03	2.245
Gm12097	-4.461	3.58E-04	3.446
Hnrph1	-4.482	1.34E-04	3.872
RP23-273I12.2	-4.497	4.06E-04	3.391
Gm11893	-4.505	1.33E-02	1.877
Ywhae	-4.506	2.92E-03	2.535
Gm13140	-4.509	8.41E-05	4.075
Gm12647	-4.523	2.30E-03	2.639
Gm13498	-4.550	4.03E-05	4.395
RP23-147O14.4	-4.551	3.64E-07	6.439
Gm10254	-4.560	8.62E-05	4.065
humanlincRNA2192	-4.630	8.75E-04	3.058
AK166453	-4.680	7.06E-06	5.151
AK051369	-4.687	9.63E-05	4.016
AK020577	-4.712	8.26E-05	4.083
Itgb1	-4.762	8.31E-04	3.080
Gm9826	-4.802	4.21E-05	4.376
Nrbp1	-4.862	2.72E-03	2.566
uc.420	-4.920	1.82E-05	4.740
Gm15502	-4.943	2.76E-03	2.558
Ivns1abp	-4.991	1.25E-04	3.904
Scs	-4.991	1.30E-04	3.887
Gm15899	-5.067	1.17E-03	2.932
Got1	-5.101	2.95E-04	3.530
RP23-34J4.1	-5.179	2.33E-05	4.632
Aph1a	-5.207	2.18E-04	3.662
Vdac3	-5.313	3.23E-04	3.491

Gene Symbol	logFC	p value	-log10Pval
Gm15790	-5.326	2.60E-04	3.585
AK014252	-5.331	6.13E-04	3.213
Neat1	-5.340	3.10E-04	3.509
AK009593	-5.378	2.87E-04	3.543
Gm11235	-5.486	2.62E-05	4.582
Got2-ps1	-5.499	1.13E-03	2.946
Gm11838	-5.536	7.73E-06	5.112
Eif5al3-ps	-5.557	1.40E-05	4.854
Gm4913	-5.591	2.41E-04	3.618
AK142855	-5.617	1.21E-04	3.918
AK050743	-5.646	1.45E-03	2.840
uc.185	-5.709	9.35E-06	5.029
Gm6706	-5.787	2.07E-05	4.684
Gm9825	-5.788	7.58E-05	4.121
Gm14037	-5.825	3.46E-06	5.461
Gm14078	-5.889	1.63E-04	3.787
Gm12504	-6.022	4.07E-05	4.390
Qk	-6.194	7.49E-05	4.125
Gm14016	-6.346	2.49E-05	4.604
AK013372	-6.354	7.58E-06	5.120
uc.366	-6.567	9.78E-05	4.010
AK020213	-6.658	2.14E-02	1.670
Gm15466	-7.211	3.65E-05	4.438

Table 3. WT versus MHC-CnA

Gene Symbol	logFC	p value	-log10Pval
AK014683	5.777	2.47E-06	5.607
AK020360	5.524	1.52E-06	5.819
AK021043	5.367	7.67E-07	6.115
AK156805	5.357	1.76E-03	2.754
CRLM3	5.143	6.26E-06	5.203
AK006317	5.059	8.80E-07	6.056
AK036610	4.901	4.94E-05	4.306
AK013557	4.726	2.95E-07	6.531
humanlincRNA1389	4.705	1.07E-04	3.969
AK003532	4.688	6.69E-08	7.174
Gm12092	4.612	7.31E-05	4.136
Gm12295	4.503	6.17E-06	5.210
AK029663	4.272	5.41E-04	3.267
MM9LINCRNAEXON12060+	4.153	7.40E-04	3.131
AK145301	4.002	2.54E-05	4.596
AK144299	3.909	8.17E-05	4.088
Gm11476	3.886	3.44E-04	3.463
AK143464	3.819	6.35E-07	6.197
Lrp8	3.788	8.77E-07	6.057
AK079801	3.764	9.97E-02	1.001
AK042604	3.751	2.54E-04	3.595
AK030587	3.745	1.11E-06	5.956
AJ409479	3.663	1.71E-04	3.768
4930512H18Rik	3.660	1.27E-05	4.895
AK135766	3.585	1.86E-01	0.731
AK035076	3.563	1.82E-04	3.740
MM9LINCRNAEXON10137-	3.526	2.17E-05	4.663
AK016489	3.499	6.96E-05	4.157
AK007126	3.497	1.60E-05	4.795
AK137188	3.492	1.74E-06	5.759
AK136902	3.439	2.22E-04	3.653
AK084560	3.426	7.50E-07	6.125
AK016944	3.412	1.82E-04	3.740
Ppp1r1c	3.381	1.63E-05	4.788
Gm15247	3.331	6.60E-05	4.180
AK010197	3.330	3.87E-05	4.412
Gm6277	3.328	1.24E-04	3.907

Gene Symbol	logFC	p value	-log10Pval
AK031202	3.298	6.99E-07	6.156
Gm15810	3.236	1.57E-04	3.803
AK149258	3.227	1.20E-04	3.922
BC028532	3.207	7.37E-05	4.132
AK048037	3.203	2.93E-04	3.534
Gm15297	3.168	5.89E-03	2.230
AK085787	3.127	7.38E-07	6.132
A430093F15Rik	3.116	6.37E-06	5.196
B130046B21Rik	3.102	1.19E-03	2.923
Gm9962	3.100	1.58E-01	0.802
AK136666	3.083	6.49E-04	3.188
4930570G19Rik	3.058	6.68E-04	3.175
BC028660	3.027	7.29E-05	4.137
AK052417	3.013	5.47E-06	5.262
AK007034	3.000	3.71E-03	2.431
AK041310	2.997	4.34E-03	2.363
Gm12542	2.995	4.79E-03	2.320
A830039N20Rik	2.964	3.21E-06	5.493
Fxy	2.962	1.49E-04	3.828
AK084753	2.943	6.97E-07	6.156
Gm13334	2.940	2.05E-05	4.688
Gm15934	2.939	4.64E-04	3.334
AK082921	2.928	1.24E-05	4.907
AK166127	2.906	4.36E-06	5.361
AK076775	2.905	2.33E-04	3.633
AK166199	2.888	1.13E-05	4.947
AK039307	2.882	2.60E-03	2.585
Gm15079	2.867	1.42E-06	5.847
AK034630	2.857	5.27E-05	4.278
AK089560	2.846	5.28E-04	3.277
AK027968	2.846	2.89E-08	7.539
AK048000	2.840	1.87E-04	3.728
AK134233	2.835	1.11E-04	3.956
AK089171	2.824	1.93E-04	3.715
AK140174	2.817	4.14E-06	5.383
AK076843	2.809	2.63E-02	1.580
AK006109	2.802	5.94E-07	6.226
BC094434	2.796	9.70E-02	1.013

Gene Symbol	logFC	p value	-log10Pval
AK015101	2.792	5.19E-04	3.285
AK034309	2.790	2.16E-03	2.666
AK139146	2.778	3.96E-04	3.402
AK086534	2.726	3.32E-04	3.479
BC125002	2.720	1.08E-03	2.967
AK006973	2.719	8.60E-04	3.066
BB497033	2.714	5.97E-07	6.224
AK015703	2.713	9.13E-03	2.040
Gm12454	2.710	6.93E-05	4.159
AK131851	2.702	6.32E-04	3.199
AK006677	2.700	1.84E-02	1.736
AK165889	2.685	5.06E-03	2.296
AK134400	2.665	1.53E-03	2.815
AK084476	2.648	1.51E-03	2.820
AK005614	2.647	2.94E-04	3.532
AK083645	2.639	3.06E-05	4.515
Zfp82	2.635	1.56E-03	2.807
AK018131	2.630	4.63E-06	5.334
Rint1	2.627	2.99E-04	3.525
AK089363	2.622	3.07E-04	3.513
AK139402	2.619	3.31E-06	5.480
AK139621	2.617	1.58E-02	1.803
AK041628	2.603	9.62E-06	5.017
AK089956	2.599	1.71E-03	2.766
AK039478	2.598	5.89E-04	3.230

Table 4. WT versus MHC-CnA

Gene Symbol	logFC	p value	-log10Pval
AK048881	-2.962	6.87E-04	3.163
Gm7834	-2.967	1.24E-05	4.907
AK039595	-2.972	3.09E-05	4.511
CU041236.1	-2.982	2.16E-04	3.665
Plekhj1	-2.983	4.75E-04	3.323
Gm13082	-2.984	8.92E-04	3.049
Son	-2.986	2.32E-03	2.634
1110005A23Rik	-2.989	1.25E-04	3.902
Got1	-2.997	2.22E-03	2.653
Gm11581	-2.999	2.63E-03	2.580
AK077785	-3.010	6.54E-03	2.185
Gm9826	-3.020	3.51E-05	4.454
Gm3531	-3.023	3.55E-05	4.450
Gm15808	-3.033	2.38E-05	4.623
Gm6563	-3.036	1.09E-05	4.963
Gm5513	-3.037	1.91E-07	6.718
Gm8383	-3.046	9.07E-07	6.042
Gm7327	-3.058	1.13E-03	2.948
mKIAA0031	-3.078	2.71E-04	3.567
Gm9800	-3.087	3.08E-03	2.512
mouselincRNA0143	-3.088	1.55E-05	4.808
Gm15660	-3.091	5.23E-04	3.281
MM9LINCRNAEXON11754-	-3.094	1.67E-04	3.776
AK014252	-3.108	9.06E-04	3.043
Gm8402	-3.110	8.15E-05	4.089
Gm4913	-3.127	1.92E-04	3.716
Gm15790	-3.135	1.62E-03	2.790
Gm8682	-3.140	1.95E-03	2.711
BC024571	-3.161	5.29E-04	3.276
AK042131	-3.174	1.12E-04	3.950
Gm6762	-3.183	2.35E-03	2.629
Gm14269	-3.203	1.29E-04	3.890
Gm12820	-3.221	1.27E-03	2.897
AK034318	-3.228	3.97E-04	3.402
Gm16480	-3.245	4.20E-03	2.377
Gm15163	-3.247	7.89E-04	3.103
AK004273	-3.264	1.43E-05	4.844

Gene Symbol	logFC	p value	-log10Pval
AK156302	-3.267	2.59E-05	4.586
Gm13378	-3.296	4.68E-04	3.330
Gm15754	-3.307	4.14E-06	5.383
AK140265	-3.311	4.03E-07	6.395
Rshl2a	-3.316	1.53E-04	3.817
Gm13232	-3.341	1.66E-04	3.779
AK017799	-3.359	3.53E-06	5.452
Gm13237	-3.378	1.11E-04	3.953
uc.366	-3.390	1.17E-04	3.932
Gm13167	-3.393	1.54E-04	3.812
Gm9308	-3.412	5.85E-06	5.233
uc.420	-3.424	8.76E-05	4.057
uc.203	-3.434	3.06E-04	3.515
Rpl3l	-3.434	1.44E-05	4.842
AK018095	-3.465	1.20E-03	2.920
AK047372	-3.533	1.16E-04	3.934
Eif4a-ps4	-3.567	8.82E-06	5.054
Gm40	-3.572	3.55E-01	0.449
RP23-147O14.4	-3.574	1.51E-05	4.822
Gm15332	-3.585	7.81E-06	5.107
Gm15153	-3.653	4.07E-04	3.390
Kars-ps1	-3.660	1.00E-04	3.998
Maf1	-3.685	1.00E-05	4.998
Gm9386	-3.685	3.55E-05	4.449
Itgb1	-3.725	2.04E-03	2.690
Ywhae	-3.753	5.61E-03	2.251
Ivns1abp	-3.768	3.29E-04	3.483
Hnrph1	-3.776	3.80E-04	3.420
Gm12620	-3.817	1.15E-04	3.939
Aph1a	-3.826	3.67E-04	3.435
AK142426	-3.862	9.37E-03	2.028
AC138228.1	-3.890	1.09E-05	4.961
Gm12623	-3.901	1.68E-05	4.774
Gm12626	-3.902	1.21E-05	4.919
Gm11839	-3.904	2.78E-04	3.556
Gm13758	-3.918	3.05E-03	2.516
Gm11838	-3.954	1.29E-05	4.888
Gm5466	-3.965	1.11E-05	4.953

Gene Symbol	logFC	p value	-log10Pval
Got2-ps1	-3.967	3.79E-03	2.422
Gm11841	-3.970	2.05E-05	4.687
Gm15331	-3.980	9.84E-06	5.007
Gm5379	-4.040	2.11E-03	2.675
Gm11235	-4.051	3.31E-05	4.481
Gm8459	-4.139	2.28E-03	2.643
AK050743	-4.158	3.98E-03	2.400
AK033935	-4.168	1.47E-03	2.832
Scs	-4.220	1.31E-04	3.882
Vdac3	-4.286	7.80E-04	3.108
Gm14078	-4.487	2.31E-04	3.636
AK051369	-4.568	3.26E-05	4.486
Gm8979	-4.619	3.48E-06	5.459
AK013372	-4.784	3.37E-07	6.472
humanlincRNA2192	-4.787	5.07E-03	2.295
Gm15502	-4.945	2.73E-03	2.563
AK166453	-5.014	8.45E-06	5.073
BC030682	-5.187	2.30E-04	3.637
Eif5al3-ps	-5.245	1.93E-05	4.714
Qk	-5.514	1.11E-04	3.954
Gm12504	-5.641	6.51E-05	4.187
Gm6706	-5.695	1.93E-04	3.715
Gm14016	-5.990	3.47E-05	4.460
Gm14037	-6.006	4.23E-05	4.373
Gm15466	-6.722	8.99E-05	4.046

CHAPTER 7

Summary and General Discussion

State of the art of heart failure

Heart failure (HF) is a deadly and costly disease affecting 5.7 million people in the US alone, and a leading cause of hospitalization for those >65 years of age.[1] It is the leading cause of death in industrialized nations and represents an enormous economic burden to society. Pathological hypertrophy of the heart muscle is a common process among numerous types of heart diseases, including ischemic diseases, hypertension and several genetic forms of cardiomyopathies.[2] Therefore, sustained hypertrophic remodeling represents one of the major clinical predictors of heart failure in humans. Hypertrophy of the left ventricle is caused by chronic pressure overload (hypertension, aortic stenosis).[3] This can lead to decreased cardiac output due to reduced systolic fractional shortening. As described in **Chapter 1**, distinct phenotypes of hypertrophy can be distinguished based on the geometry of the heart and individual cardiomyocytes. Concentric cardiac hypertrophy displays a reduced left ventricular chamber dimension and thickening of the left ventricular free wall and septum. Eccentric hypertrophy is characterized by ventricular wall dilatation and can occur after myocardial infarction. Concentric hypertrophy can progress to eccentric hypertrophy and dilation leading to systolic heart failure.

Current standard pharmacological therapy includes the use of inhibitors of angiotensin II, β-AR antagonists, aldosterone antagonists, and diuretics.[4-6] Other modern therapies are interventional therapy (intracoronary stent implantation, balloon angioplasty, percutaneous valve repair),[7] electrophysiological therapy (implantation of cardioverter defibrillator, cardiac resynchronization treatment, ablating arrhythmic foci),[8] and surgical treatment (ventricular assist device implantation, heart transplantation).[9] Current HF therapy is primarily focused on treating symptoms and fails to directly address the key underlying intracellular signal transduction abnormalities. Despite these different forms of treatments, HF-related mortality remains high. It should be noted that so far there are no pharmacological HF drugs that target intracellular targets, as those compounds are difficult to create due to biochemical challenges (cell permeability issues etc.). Furthermore, our understanding of the deranged signaling pathways inside the cell that lead to the progress of the disease is far from complete. A better understanding of molecular mechanisms of the change in cardiac remodeling is clearly needed.

The non-coding genome

The genome is the carrier of hereditary information that defines an organism. Results from the Encyclopedia of DNA Elements (ENCODE) project indicates that at least 80% of the human genome can be transcribed, yet only less than 2% of our genome encodes proteins.[10] Accumulating evidence shows that there is a clear correlation between the functional complexity of a certain organism and the diversity of its non-coding genome. The main output of the genomes of complex organisms is genetically active but non-coding RNA (ncRNA).[11] These ncRNAs act as integral components of the molecular networks in development and disease.[12] Classification of ncRNAs is based on their length, function, biogenesis, polarity (sense or antisense), and protein-binding partners.[13] According to their size, ncRNAs are subdivided into two groups: small ncRNAs (< 200 nt) and long ncRNAs. Long ncRNAs (>200 nucleotides) are relatively stable and do not undergo major processing before carrying out their normal functions.[14] On the other hand, short ncRNAs (<200 nucleotides) are processed from longer precursors.[15]

One of the most studied short ncRNAs are microRNAs (miRs), single-stranded small RNA molecules consisting of 20-23 nucleotides that are generated from endogenous hairpin transcripts.[16] Numerous studies have identified alterations in expression levels of ncRNAs as a feature of heart failure, especially microRNAs (miRs). Therefore, considerable attention is focused on chemically targeting miR expression as a therapeutic solution for HF. In general, there are two approaches to developing miR-based therapeutics: miR antagonists and miR mimics. A new mechanism of action, the ability to function as master regulators of entire pathways and an apparent lack of adverse events in normal tissue make miR antisense inhibitors and miR mimics promising technologies for current and future therapeutics development. Ways to inhibit miR expression by antisense oligonucleotides are outlined in **Chapter 3**. For example, Regulus' drug RG-101 is a GalNAc-conjugated anti-miR targeting miR-122 for the treatment of Hepatitis C virus (HCV). Their Phase I study is successfully completed, and the first Phase II clinical data are expected to be reported by the end of 2016 (http://www.regulusrx.com). Santaris Pharma, based in Copenhagen, Denmark has miravirsen (another antisense microRNA-122 drug), in Phase II clinical trials.[17,18] Phase I studies confirmed preclinical findings results in rodents and nonhuman primates,[17,19] which showed good tolerability of the drug. A complete overview of preclinical studies applying anti-microRNA oligonucleotides to inhibit specific miRs in relevant models of HF is provided in **Chapter 3**, Table 1 (page 57).

Besides inhibiting miR expression, it is possible to induce miR expression using adeno-associated virus (AAV) vectors. Although AAV9 is not widely used for miR overexpression yet, in various cases it has proven to be beneficial to stimulate expression of a particular miR, as also described for miR-148a by AAV9 in **Chapter 4**. Intraventricular delivery of AAV vectors induced long-term (18 months) overexpression of miR-669a and improved survival of β-sarcoglycan (Sgcb)-null mice, a model for muscular dystrophy. Treated dystrophic mice displayed reduced pathological remodeling, enhanced sarcomere organization and increased systolic fractional shortening of the left ventricle.[20] Furthermore, AAV-mediated overexpression of hsa-miR-590 and hsa-miR-199a in mice, after myocardial infarction, reduced infarct size and significantly improved cardiac function because they trigger cardiomyocyte proliferation and cardiac regeneration after myocardial infarction.[21] Other reports indicate that AAV9–miR-378 attenuates cardiac hypertrophy after pressure overload because of thoracic aortic constriction.[22] In rats, AAV-mediated overexpression of miR-1 lead to a marked reduction of myocardial fibrosis, improved calcium handling, inhibition of apoptosis, and inactivation of the mitogen-activated protein kinase signaling pathways, indicating prevention of maladaptive ventricular remodeling.[23] AAV-mediated miR-overexpression studies in relevant heart failure models are summarized in **Table 1**.

Although there are no clinical trials yet for AAV-mediated overexpression of miRs, companies are developing miR mimics for therapy. Mirna Therapeutics developed a miR-34 mimic, called MRX34. MRX34 is a double-stranded RNA mimic of the tumor suppressor miR-34, which is delivered by liposome to inhibit multiple oncogenic pathways as well as to stimulate anti-tumor immune response to induce cancer cell death (www.mirnarx.com). MRX34 is currently in a Phase I clinical trial in patients with unresectable primary liver cancer, and advanced or metastatic cancer with liver involvement (ClinicalTrials.gov identifier: NCT01829971).[24] If MRX34 proves to be promising, others will soon follow.

Table 1 Overview of preclinical studies using AAV to overexpress certain miRs in relevant models of heart failure

miR	Dose/Delivery	Model	Target	Outcome	Ref
1	AAV9, single-bolus 5×10^{11} vg (viral genomes) tail-vein injection	Rat, pressure overload	Fibullin-2 (Fbln2)	Reversed cardiac hypertrophy, attenuated pathological remodeling	[23]
148a	AAV9, single-bolus $1x10^{12}$ viral genomes, tail-vein injection	Mouse, TAC	Gp130	Improved systolic function after TAC, preventing transition of concentric hypertrophy towards dilation	Ch 4
199a 590	AAV9, single-bolus 1×10^{11} vg intraperitoneally or intracardiac injection	Mouse, MI	Homer1 Hopx Clic5	Marked cardiac regeneration and almost complete recovery of cardiac functional parameters after MI	[21]
378	AAV9, 1×10^{12} genome copies, tail vein injection	Mouse, TAC	MAPK1, GRB2, KSR1, IGF1R	Attenuated thoracic aortic constriction–induced cardiac hypertrophy, improved cardiac function	[22]
669a	AAV2/9, 1×10^{9} genome copies, intraventricular puncture in neonates .	Mouse, DCM (Sgcb-null)	MyoD Agtr1a Il6 Il1b (not confirmed)	Reduced adverse remodeling, enhanced systolic fractional shortening of left ventricle in treated dystrophic mice	[20]

miR-148a as a regulator of cardiac hypertrophy

In **Chapter 4** we showed that *miR-148a* is differentially and dynamically expressed in distinct subtypes of human and mouse forms of heart failure. Concentric hypertrophy in both human and mouse hearts correlates with increased miR-148a expression, whereas dilated cardiomyopathy is accompanied by a profound decrease in *miR-148a* myocardial expression levels. In the heart, *miR-148a* directly targets glycoprotein 130 (gp130). Gp130 is a shared receptor utilized by several related cytokines, including IL-6, IL-11, IL-27, Leukemia Inhibitory Factor (LIF), Oncostatin M (OSM), and Cardiotrophin 1 (CT-1). CT-1 is a member of the IL-6 family, and CT-1-mediated gp130 activation is well known to induce eccentric hypertrophic remodeling in cardiac myocytes. *In vitro* experiments demonstrated

that overexpression of miR-148a, by delivery of precursor molecules, inhibits eccentric cardiomyocyte hypertrophy after CT-1 stimulation in neonatal rat cardiomyocytes. In line, silencing of endogenous miR-148a results in spontaneous eccentric cardiomyocyte hypertrophy. *In vivo* inhibition of miR-148a, by using a specific antagomir, caused marked impairment in cardiac function and increased fibrosis, which was associated with an increase in gp130 expression. In addition, AAV9-mediated overexpression of miR-148a provoked a resistance to pressure-overload induced cardiac contractile dysfunction and dilatation.

In recent years, many efforts have been done to unravel the different mechanisms between concentric and eccentric cardiac remodeling. How molecular dysfunction evokes different patterns of cardiac remodeling is unclear. Our results demonstrate that miR-148a can prevent the transition from concentric hypertrophy induced by pressure-overload towards eccentric hypertrophic remodeling and dilation of the left ventricle. This indicates that the different forms of hypertrophic remodeling are induced by distinct molecular programs.

A recent study from the Molkentin lab describes a tension-based model, the force-time integral of cardiomyocyte function, that distinguishes between hypertrophic versus dilated cardiomyopathy. They used an array of genetically altered mice that permit the systemic tuning of sarcomeric tension generation to assess consequences on cardiac remodeling and disease. This study focused on hereditary conditions affecting cardiac sarcomeric proteins. Well-characterized functionally opposite mutations of the calcium-sensing thin filament sarcomeric protein, cardiac troponin C (cTnC) were used that quantitatively shift calcium-binding and tension-producing features of the myofilaments at a fixed amount on either side of normal to correlate with hypertrophic remodeling of the heart. The computational model of the integral of myofilament tension development predicted HCM and DCM in mice associated with essentially any sarcomeric gene mutations. They were also able to accurately predict human cardiac phenotypes from data generated in induced-pluripotent-stem-cell-derived myocytes from familial cardiomyopathy patients.[25] Whether miR-148a is directly activated by changes in tension of the heart muscle has yet to be determined.

Phenotypic screening to identify microRNAs involved in CT-1-mediated cardiac hypertrophy

CT-1 is known for many years for its ability to induce eccentric hypertrophy in neonatal cardiomyocytes. However, few articles report whether chronic CT-1 administration leads to eccentric cardiac remodeling and altered cardiac function in vivo. López-Andrés and colleagues showed that CT-1 treatment increased left ventricular volumes, reduced fractional shortening and ejection fraction, and induced myocardial dilatation and myocardial fibrosis in Wistar rats treated with 20 µg /kg per day during 6 weeks.[26] To the best of our knowledge, our study is the first demonstration that chronic CT-1 administration leads specifically to dilation without an initial concentric hypertrophic response in mice. The finding that microRNA miR-148a directly targets Gp130, a key component of this CT-1 pathway, identifies a possible additional site of therapeutic intervention for heart failure by the class of RNA therapeutics.

Since we found that a specific miR can control the CT-1 pathway, we wanted to know if there are additional miRs that exert a similar effect. To this end, we performed a phenotypic high-throughput screen in neonatal rat cardiomyocytes stimulated with CT-1. CT-1 is a 201 amino acid protein member of the IL-6 family, that signals through a unique receptor system, consisting of leukemia inhibitory factor receptor beta (LIFRb) and a common signal transducer, the glycoprotein 130 (gp130).[27] Signal transduction via gp130 involves at least three major downstream pathways: the janus kinase/signal transducer and activator of transcription (JAK/STAT) pathway, the Ras-Raf mitogen- activated protein kinase (MAPK, MEK/ERK) signaling cascade, and the phosphatidylinositol 3-OH kinase (PI3K)/Akt pathway.[27] Multiple studies have shown that CT-1 plays a dual role in the biophysiology of the myocardium, providing protective effects on the one hand, but predisposing the heart to pathological conditions on the other hand. It was shown that CT-1 promotes neonatal cardiac myocyte survival and proliferation and is required for cardiac myocyte maturation.[28] Treatment of cardiac cells with CT-1 induced heat shock protein (hsp) 70 and hsp90 synthesis and protected these cells against subsequent exposure to severe thermal or ischaemic stress.[29] Another study showed that CT-1 can exert a protective effect against the damaging effects of simulated ischaemia/reoxygenation both when added after the simulated ischaemia at reoxygenation or when added prior to the simulated ischaemia. These protective effects were mediated by the p42/p44 MAPK pathway downstream of CT-1 activation.[30]

Aside from its protective effects, CT-1 activation is also implicated in pathological cardiac remodeling. CT-1 was originally isolated for it's capacity to induce hypertrophy in neonatal cardiac myocytes, causing eccentric hypertrophy with an increase in cell length without a significant change in cell width. Sarcomeric units were assembled in series rather than in parallel as is observed in concentric hypertrophy.[31] In humans, increased CT-1 serum levels have been observed in patients with hypertensive heart disease. CT1 is more elevated in hypertensive patients with left ventricular hypertrophy than in patients that have normal ventricular thickening.[32] Cardiac CT-1 secretion is stimulated by ventricular stretch in perfused rat hearts.[33] Also in patients with aortic stenosis plasma levels of proBNP and CT-1 were elevated and both N-terminal proBNP and CT-1 levels correlated to the maximum trans-valvular aortic pressure gradient. CT-1 was the most significant predictor of the severity of aortic stenosis.[34] Furthermore, expression levels of CT-1 were significantly increased in the failing left ventricular myocardium of patients with end-stage heart failure compared with non-failing donor hearts.[35] Plasma CT-1 levels are increased in patients with dilated cardiomyopathy (DCM) and significantly correlated with the LVmass index, indicating that CT-1 plays an important role in structural left ventricular remodeling in patients with DCM.[36] Also after myocardial infarction, CT-1 plasma levels are elevated in humans and correlate with the degree of left ventricular systolic dysfunction.[37]

CT-1 has multiple functions that can result in opposite outcomes. CT-1 can promote proliferation and survival of cardiomyocytes but also can cause cardiac hypertrophy and ventricular remodeling. Also, it is able to regulate several organ systems besides the cardiovascular system, and it activates different signaling pathways. These facts make it difficult to target CT-1 for therapeutic purposes. Directing CT-1 therapeutics to the target organ is a key challenge that requires further investigation. The different activities of CT-1 reflect the different signaling pathways that are activated by CT-1. Thus targeting a microRNA that is involved in one specific downstream pathway could tackle the dual activity issues of CT-1. Since expression of particular miRs is in most cases not organ-specific, delivery to the target organ is again key in developing a therapeutic strategy.

In **Chapter 5**, we used CT-1 as a hypertrophic stimulus on neonatal rat cardiomyocytes, and performed a high-content microscopy, high-throughput functional screen for miRs that influenced neonatal cardiomyocyte eccentric remodeling using a whole-genome miRNA library. The goal of this approach was to gain more insight in the signaling cascades and molecular mechanisms involved in

eccentric remodeling and dilatation. From our screen we identified miR-125b-5p, miR-542-3p, miR-151-5p and miR-532-3p as specific inducers of eccentric hypertrophy. None of those miRs has been studied in relation to eccentric hypertrophy and cardiovascular disease. Functional analysis of the gene involvement in the Kyoto Encyclopedia of Genes and Genomes (KEGG) pathways revealed enrichment for genes belonging to 'Pathways in cancer', MAPK-signaling pathway', 'Endocytosis', and 'Regulation of actin cytoskeleton' as top categories. Further experimental validation implicating these miRs in directly targeting genes in those pathways is still needed.

Other screens performed in cardiomyocytes have focused on identifying miRs in proliferation[21], and miRs in concentric hypertrophy[38]. As expected, our top candidates were not among the candidate miRs in aforementioned 2 screens. An alternative approach, not including miRs, to differentiate hypertrophic signaling pathways was done by quantifying the contribution of individual pathways to specific changes in shape and transcript abundance. Cardiac myocytes were stimulated with 15 hypertrophic agonists and subsequently quantified for differential regulation of 5 shape features using high-throughput microscopy and transcript levels of 12 genes using qPCR. While hypertrophy pathways are highly connected, the agonist screen revealed distinct hypertrophy phenotypic signatures for the 15 receptor agonists they tested. They reported strong correlations between Bax and connective tissue growth factor (CTGF) mRNA abundance in response to angiotensin II and between myocyte elongation and CITED4 mRNA abundance in response to Nrg1. In their model, Nrg1 stimulates myocyte elongation and CITED4 expression, LIF stimulates myocyte elongation, and CITED4 expression negatively regulates myocyte elongation. Overexpression of CITED4 does not affect elongation of unstimulated cardiac myocytes. However, overexpression of CITED4 increased cell size and induces myocyte proliferation. Increased CITED4 may therefore be beneficial to the heart by preventing high levels of myocyte elongation.[39] Although they also used CT-1 as one of the hypertrophic stimulants, no results on those experiments are described in their main report. In the supplemental data it is showed that CT-1 stimulation is followed by a significant increase in mRNA levels of IkB and VEGF, but in none of the other genes tested.

***Bigheart*: a key lncRNA in the heart**

It has become increasingly evident that besides miRs, another class of ncRNA, lncRNAs, plays a key role in cardiac physiology and pathology. An overview of lncRNAs involved in control of gene regulatory programs in cardiac development and disease is provided in **Chapter 2**. In **Chapter 6,** we profiled lncRNAs in hearts suffering from non-ischemic, pathological hypertrophic remodeling using two well-established mouse models of heart failure: a surgical model of transverse aorta constriction (TAC) to induce sustained cardiac pressure overload and mice with heart-restricted calcineurin overexpression. We then selected lncRNA candidates that showed a similar differential expression pattern in both hypertrophy models and were not studied in this context before. We selected *AK014683* (Ensembl ID *4833412C05Rik*, or *Bigheart*) because it showed 5-15 fold differences with WT hearts. Bigheart was previously described to be upregulated in heart disease models[40], but its function was still unknown. We used RNA interference (RNAi) to silence the lncRNA *Bigheart* and demonstrate its functional requirement for agonist-induced cardiomyocyte hypertrophy. GO-analysis-based bioinformatics using the NPInter database that documents experimentally verified functional interactions between noncoding RNAs and biomolecules revealed that Bigheart in involved in mRNA processing. It was previously shown that Bigheart expression is increased in a cardiac-specific heterogeneous nuclear ribonucleoprotein U (hnRNP U) knockout model of cardiac disease. Loss of hnRNP U resulted in context-dependent splicing defects, since mixed splicing activities (skipping and inclusion) were observed.[40] Indeed, our analysis using the NPInter database revealed that one of the verified interaction partners of Bigheart is MOV10, which is involved in pre-mRNA processing. Further validation to confirm that MOV10 is responsible for the Bigheart-mediated effect on cardiac hypertrophy is still required. Besides this new lncRNA *Bigheart*, our array also identified previously verified lncRNAs in heart failure. We detected *Braveheart*, a critical regulator of cardiac cell fate,[41] and *MALAT1*, a regulator of endothelial cell function and vessel growth,[42] confirming the accuracy of our results.

Not all lncRNAs are lncRNAs

Many non-coding RNA transcripts (including lncRNAs) contain multiple putative small open reading frames (ORFs) that can potentially be translated and have a coding function.[18] There is increasing evidence that short ORFs present in some ncRNAs (including lncRNAs) are actually translated into small bioactive peptides, the

abundance of which is probably greatly underestimated. The polished rice (pri) or tarsal-less (tal) gene in Drosophila was originally annotated as a lncRNA, but demonstrated to encode a series of 11– to 32– amino acid peptides that orchestrate epidermal differentiation through the control of Shavenbaby transcriptional activity.[43] Shavenbaby is a transcription factor and it was found that multiple genetic changes in the cis-regulatory region of shavenbaby caused the loss of dorsal cuticular hairs (quaternary trichomes) in larvae of Drosophila sechellia.[44]

Recently, it was discovered that a skeletal muscle-specific lncRNA encodes a conserved micropeptide. Bioinformatic analysis revealed a short 138 nucleotide ORF with the potential to encode a highly conserved 46 amino acid micropeptide, named myoregulin (MLN).[45] The MLN micropeptide is highly conserved across mammals and shows a strong structural resemblance to phospholamban (PLN) and sarcolipin (SLN), both of which directly interact with the sarco-endoplasmic reticulum Ca^{2+} adenosine triphosphatase (SERCA) in the sarcoplasmic reticulum (SR) membrane to regulate Ca^{2+} pump activity.[46,47] After an electrical stimulus of the myocyte plasma membrane, Ca^{2+} is released from the SR allowing Ca^{2+} to bind to the myofilament protein troponin C, which then switches on the contractile machinery. For relaxation to occur $[Ca^{2+}]_i$ must decline, allowing Ca^{2+} to dissociate from troponin. Ca^{2+} is pumped back into the SR by the SERCA.[48] Skeletal muscle MLN forms a single-pass transmembrane alpha helix that binds to SERCA in the SR membrane and regulates calcium handling. MLN ablation in mice significantly increased Ca2+ handling and improved exercise performance, showing that MLN is the predominant inhibitor of SERCA pump activity in adult skeletal muscle.[45] Very recently, that same group discovered a putative muscle-specific lncRNA that encodes a peptide of 34 amino acids and that they named dwarf open reading frame (DWORF).[49] DWORF is robustly expressed in heart tissue, but DWORF mRNA was downregulated in dilated hearts of calcineurin transgenic mice. DWORF was found to enhance SR Ca2+ uptake and myocyte contractility displacing the inhibitory peptides PLN, SLN, and MLN from SERCA. Peak systolic Ca2+ transient amplitude and SR Ca2+ load were significantly increased in myocytes from DWORF overexpression mice. The pacing-induced Ca2+ transient decay rate was significantly enhanced in myocytes aMHC-DWORF transgenic mice, indicating increased SERCA activity in muscle cells overexpressing DWORF. In contrast, slow skeletal muscle lacking DWORF showed delayed Ca2+ clearance and relaxation and decreased activity of SERCA.[49]

The reason why these micropeptides were missed earlier is that it is very difficult to identify functional short ORFs in RNA transcripts. As bioinformatics tools improve, more micropeptides will most likely be found and characterized.

Therapeutic potential of targeting lncRNAs

Our understanding of lncRNA biology is still in an elementary stage and much more experimental work is needed. As described in **Chapter 1**, lncRNAs can exert different functions. They can regulate expression of genes located in close proximity (cis-acting) or target distant transcriptional activators or repressors (trans-acting).[50] LncRNAs can act as molecular decoys and 'sponge' protein factors or competing endogenous RNAs (ceRNAs) for miR target sites.[51] Third, lncRNAs can act as molecular guides by directing ribonucleoprotein complexes to specific chromatin targets.[52]

In addition to miRs, lncRNAs also have demonstrated to play crucial roles during cardiac embryogenesis (summarized in **Chapter 2**) and heart failure (**Chapter 6**) and in the development of heart failure, as their expression levels were found to be dysregulated in cardiac disease (summarized in **Chapter 2**). Expectedly, researchers are developing ways to correct the abnormal expression levels of these particular lncRNAs. Functional natural antisense transcripts (NATs) typically originate opposite the sense strand of many protein-coding genes, often overlapping in part with mRNA, promoter and regulatory regions.[53] Similar to miR antisense oligonucleotides, single-stranded oligonucleotides can be synthesized to strand-specifically block the interaction of the NAT with the corresponding sense strand gene mRNA, causing transcriptional de-repression of the gene. Brain-derived neurotrophic factor (BDNF) is normally repressed by a conserved noncoding antisense RNA transcript, BDNF-AS. Inhibition of this transcript was achieved by single-stranded, 16-nucleotide gapmers consisting of three LNA-modified DNA bases at each of the ends with ten unmodified DNA bases in the middle, allowing for RNaseH cleavage. This approach resulted in upregulated BDNF mRNA, altered chromatin marks at the BDNF locus, increased protein levels and induced neuronal outgrowth and differentiation both *in vitro* and *in vivo*.[54] Similar to miR antisense oligonucleotides, it is important to introduce chemical modifications to promote metabolic stability and minimizing the length of the oligonucleotide to aid cellular uptake, while maintaining selectivity to minimize off-target activities.

Inhibition of lncRNA function by antisense oligonucleotides will face similar challenges as antisense miR oligonucleotides do (**Chapter 3**). Toxicity and off-target effects and delivery issues still have to be addressed. On the other hand, lncRNAs do open up some possibilities for strategies that are not applicable to protein targets. Targeting a specific lncRNA could upregulate an endogenous gene in a natural way. Inhibiting lncRNAs that regulate the expression of haploinsufficient genes could increase activity of the functional copy and result in normal functioning. Whereas miRs are translational repressors targeting mRNAs, lncRNAs primarily regulate chromatin in order to inhibit transcription. Furthermore, in contrast to miRs that can target hundreds of different mRNAs, cis-acting lncRNAs are gene-locus-specific. There are probably thousands of unexplored lncRNAs, whereas fewer miR species exist and those have been more comprehensively investigated. LncRNAs have been reported to show relatively low expression compared to mRNAs. If lncRNAs are indeed transcriptional repressors, this could indicate that a small number of lncRNA molecules is sufficient to demonstrate efficacy, creating a potential advantage of targeting lncRNAs at a lower dose than the standard oligonucleotides used for mRNA and miR knockdown.

Classifying lncRNAs into diverse functional classes will capacitate the design of therapeutics that possess a certain mode of action, such as the transcriptional derepression shown by antisense lncRNA oligonucleotides. Further functional genomic studies are required to establish the roles of lncRNAs. Large-scale inhibition and overexpression approaches in proper cell models, with subsequent detailed *in vitro* and *in vivo* characterization of selected functional candidates will shed more light on the complex world of lncRNAs.

References

1 Liu, L. C. *et al.* Heart failure highlights in 2012-2013. *Eur J Heart Fail* **16**, 122-132 (2014).

2 Massie, B. M. Myocardial hypertrophy and cardiac failure: a complex interrelationship. *Am J Med* **75**, 67-74 (1983).

3 Panidis, I. P. *et al.* Development and regression of left ventricular hypertrophy. *Journal of the American College of Cardiology* **3**, 1309-1320 (1984).

4 Packer, M. *et al.* The effect of carvedilol on morbidity and mortality in patients with chronic heart failure. U.S. Carvedilol Heart Failure Study Group. *The New England journal of medicine* **334**, 1349-1355 (1996).

5 Ziff, O. J., Covic, A. & Goldsmith, D. Calibrating the impact of dual RAAS blockade on the heart and the kidney - balancing risks and benefits. *Int J Clin Pract* (2016).

6 Greenberg, B. Treatment of heart failure: state of the art and prospectives. *J Cardiovasc Pharmacol* **38 Suppl 2**, S59-63 (2001).

7 de la Torre Hernandez, J. M., Diaz Fernandez, J. F., Sabate Tenas, M. & Goicolea Ruigomez, J. Update on interventional cardiology. *Rev Esp Cardiol (Engl Ed)* **66**, 282-289 (2013).

8 Todd, D. *et al.* Standards for device implantation and follow-up: personnel, equipment, and facilities: results of the European Heart Rhythm Association Survey. *Europace* **16**, 1236-1239 (2014).

9 Rojas, S. V., Hanke, J. S., Haverich, A. & Schmitto, J. D. Chronic ventricular assist device support: surgical innovation. *Curr Opin Cardiol* **31**, 308-312 (2016).

10 Djebali, S. *et al.* Landscape of transcription in human cells. *Nature* **489**, 101-108 (2012).

11 Mattick, J. S. RNA regulation: a new genetics? *Nat Rev Genet* **5**, 316-323 (2004).

12 Rinn, J. L. & Chang, H. Y. Genome regulation by long noncoding RNAs. *Annual review of biochemistry* **81**, 145-166 (2012).

13 Farazi, T. A., Juranek, S. A. & Tuschl, T. The growing catalog of small RNAs and their association with distinct Argonaute/Piwi family members. *Development* **135**, 1201-1214 (2008).

14 Ponting, C. P., Oliver, P. L. & Reik, W. Evolution and functions of long noncoding RNAs. *Cell* **136**, 629-641 (2009).

15 Brosnan, C. A. & Voinnet, O. The long and the short of noncoding RNAs. *Curr Opin Cell Biol* **21**, 416-425 (2009).

16 Kim, V. N. MicroRNA biogenesis: coordinated cropping and dicing. *Nat Rev Mol Cell Biol* **6**, 376-385 (2005).

17 Lanford, R. E. *et al.* Therapeutic silencing of microRNA-122 in primates with chronic hepatitis C virus infection. *Science* **327**, 198-201 (2010).

18 Ingolia, N. T., Lareau, L. F. & Weissman, J. S. Ribosome profiling of mouse embryonic stem cells reveals the complexity and dynamics of mammalian proteomes. *Cell* **147**, 789-802 (2011).

19 Hildebrandt-Eriksen, E. S. *et al.* A locked nucleic acid oligonucleotide targeting microRNA 122 is well-tolerated in cynomolgus monkeys. *Nucleic acid therapeutics* **22**, 152-161 (2012).

20 Quattrocelli, M. *et al.* Long-term miR-669a therapy alleviates chronic dilated cardiomyopathy in dystrophic mice. *Journal of the American Heart Association* **2**, e000284 (2013).

21 Eulalio, A. *et al.* Functional screening identifies miRNAs inducing cardiac regeneration. *Nature* **492**, 376-381 (2012).

22 Ganesan, J. *et al.* MiR-378 controls cardiac hypertrophy by combined repression of mitogen-activated protein kinase pathway factors. *Circulation* **127**, 2097-2106 (2013).

23 Karakikes, I. *et al.* Therapeutic cardiac-targeted delivery of miR-1 reverses pressure overload-induced cardiac hypertrophy and attenuates pathological remodeling. *Journal of the American Heart Association* **2**, e000078 (2013).

24 Agostini, M. & Knight, R. A. miR-34: from bench to bedside. *Oncotarget* **5**, 872-881 (2014).

25 Davis, J. *et al.* A Tension-Based Model Distinguishes Hypertrophic versus Dilated Cardiomyopathy. *Cell* **165**, 1147-1159 (2016).

26 Lopez-Andres, N. *et al.* Cardiotrophin 1 is involved in cardiac, vascular, and renal fibrosis and dysfunction. *Hypertension* **60**, 563-573 (2012).
27 Fischer, P. & Hilfiker-Kleiner, D. Survival pathways in hypertrophy and heart failure: the gp130-STAT3 axis. *Basic Res Cardiol* **102**, 279-297 (2007).
28 Sheng, Z., Pennica, D., Wood, W. I. & Chien, K. R. Cardiotrophin-1 displays early expression in the murine heart tube and promotes cardiac myocyte survival. *Development* **122**, 419-428 (1996).
29 Stephanou, A. *et al.* Cardiotrophin-1 induces heat shock protein accumulation in cultured cardiac cells and protects them from stressful stimuli. *Journal of molecular and cellular cardiology* **30**, 849-855 (1998).
30 Brar, B. K. *et al.* Cardiotrophin-1 can protect cardiac myocytes from injury when added both prior to simulated ischaemia and at reoxygenation. *Cardiovasc Res* **51**, 265-274 (2001).
31 Pennica, D. *et al.* Expression cloning of cardiotrophin 1, a cytokine that induces cardiac myocyte hypertrophy. *Proceedings of the National Academy of Sciences of the United States of America* **92**, 1142-1146 (1995).
32 Lopez, B. *et al.* Is plasma cardiotrophin-1 a marker of hypertensive heart disease? *J Hypertens* **23**, 625-632 (2005).
33 Pemberton, C. J., Raudsepp, S. D., Yandle, T. G., Cameron, V. A. & Richards, A. M. Plasma cardiotrophin-1 is elevated in human hypertension and stimulated by ventricular stretch. *Cardiovasc Res* **68**, 109-117 (2005).
34 Talwar, S. *et al.* Plasma N-terminal pro BNP and cardiotrophin-1 are elevated in aortic stenosis. *Eur J Heart Fail* **3**, 15-19 (2001).
35 Zolk, O., Ng, L. L., O'Brien, R. J., Weyand, M. & Eschenhagen, T. Augmented expression of cardiotrophin-1 in failing human hearts is accompanied by diminished glycoprotein 130 receptor protein abundance. *Circulation* **106**, 1442-1446 (2002).
36 Tsutamoto, T. *et al.* Relationship between plasma level of cardiotrophin-1 and left ventricular mass index in patients with dilated cardiomyopathy. *Journal of the American College of Cardiology* **38**, 1485-1490 (2001).
37 Talwar, S. *et al.* Plasma cardiotrophin-1 following acute myocardial infarction: relationship with left ventricular systolic dysfunction. *Clin Sci (Lond)* **102**, 9-14 (2002).
38 Jentzsch, C. *et al.* A phenotypic screen to identify hypertrophy-modulating microRNAs in primary cardiomyocytes. *Journal of molecular and cellular cardiology* **52**, 13-20 (2012).
39 Ryall, K. A., Bezzerides, V. J., Rosenzweig, A. & Saucerman, J. J. Phenotypic screen quantifying differential regulation of cardiac myocyte hypertrophy identifies CITED4 regulation of myocyte elongation. *Journal of molecular and cellular cardiology* **72**, 74-84 (2014).
40 Ye, J. *et al.* hnRNP U protein is required for normal pre-mRNA splicing and postnatal heart development and function. *Proceedings of the National Academy of Sciences of the United States of America* **112**, E3020-3029 (2015).
41 Klattenhoff, C. A. *et al.* Braveheart, a long noncoding RNA required for cardiovascular lineage commitment. *Cell* **152**, 570-583 (2013).
42 Michalik, K. M. *et al.* Long noncoding RNA MALAT1 regulates endothelial cell function and vessel growth. *Circulation research* **114**, 1389-1397 (2014).
43 Kondo, T. *et al.* Small peptides switch the transcriptional activity of Shavenbaby during Drosophila embryogenesis. *Science* **329**, 336-339 (2010).
44 Stern, D. L. & Frankel, N. The structure and evolution of cis-regulatory regions: the shavenbaby story. *Philos Trans R Soc Lond B Biol Sci* **368**, 20130028, (2013).
45 Anderson, D. M. *et al.* A micropeptide encoded by a putative long noncoding RNA regulates muscle performance. *Cell* **160**, 595-606 (2015).
46 Kranias, E. G. & Hajjar, R. J. Modulation of cardiac contractility by the phospholamban/SERCA2a regulatome. *Circulation research* **110**, 1646-1660 (2012).
47 MacLennan, D. H., Asahi, M. & Tupling, A. R. The regulation of SERCA-type pumps by phospholamban and sarcolipin. *Ann N Y Acad Sci* **986**, 472-480 (2003).

48 Bers, D. M. Cardiac excitation-contraction coupling. *Nature* **415**, 198-205 (2002).
49 Nelson, B. R. *et al.* A peptide encoded by a transcript annotated as long noncoding RNA enhances SERCA activity in muscle. *Science* **351**, 271-275 (2016).
50 Nagano, T. *et al.* The Air noncoding RNA epigenetically silences transcription by targeting G9a to chromatin. *Science* **322**, 1717-1720 (2008).
51 Cesana, M. *et al.* A long noncoding RNA controls muscle differentiation by functioning as a competing endogenous RNA. *Cell* **147**, 358-369 (2011).
52 Lee, J. T. Lessons from X-chromosome inactivation: long ncRNA as guides and tethers to the epigenome. *Genes & development* **23**, 1831-1842 (2009).
53 Katayama, S. *et al.* Antisense transcription in the mammalian transcriptome. *Science* **309**, 1564-1566 (2005).
54 Modarresi, F. *et al.* Inhibition of natural antisense transcripts in vivo results in gene-specific transcriptional upregulation. *Nature biotechnology* **30**, 453-459 (2012).

CHAPTER 8

Valorization

Cardiovascular diseases (CVDs) are the number one cause of hospitalization and death worldwide. Different CVDs include aneurysms, angina, arrhythmias, stroke, coronary artery disease (or CHD), myocardial infarction, valve problems (stenosis, regurgitation), hypertension, pulmonary heart disease, cardiomyopathy, and congestive heart failure. According to the most recent health statistics of the World Health Organization (WHO), an estimated number of 17.3 million people died from CVDs in 2008 of which 6.2 million were due to stroke and 7.3 million were due to coronary artery disease. More than 80% of the deaths occur in low- and middle-income countries, affection women and men in equal proportion.[*] In Europe, CVDs account for over 4 million deaths each year, with coronary heart disease (CHD) and stroke being the main forms. Almost half (47%) of all deaths are from CVD (52% of deaths in women and 42% of deaths in men). Just under half of all deaths from CVD in both men and women are from CHD, with stroke accounting for nearly a third of deaths in women and a quarter of deaths in men.[**]

While current pharmacological treatment strategies (e.g. β-blockers and ACE-inhibitors) have shown effectiveness in prolonging survival of heart failure patients, the prognosis of affected individuals remains poor and new therapeutic approaches for treatment of this devastating disease are still necessary. Besides the devastating effects on the quality of life of those patients (social burden), life-long treatment is expensive and increases the economic burden on society that comes with high healthcare costs.

Many risk factors are associated with CVD. Obesity[1], plasma triglyceride level[2], physical inactivity[3], elevated serum cholesterol level[4], cigarette smoking[5], hypertension[6], diabetes and glucose intolerance[7] are all primary risk factors for CVD. Metabolic syndrome is a cluster of metabolic conditions that can lead to CVD, including hypertension, abnormal cholesterol, insulin resistance, and obesity. Total blood volume and cardiac output correlate positively and proportionately with the degree of excess body weight, because of the high metabolic activity of excessive fat. The increased filling pressure and volume in obese patients often leads to development left ventricular eccentric hypertrophy and chamber dilation.[8] Body mass index in obese patients was also reported to correlate with other structural abnormalities such as left ventricular mass and wall thickness, and concentric remodeling.[9] Although some studies reported evidence of eccentric LV hypertrophy in obese patients[8,10,11], other studies of obese subjects found a predominance of concentric hypertrophy[12,13].

In this thesis we describe specific non-coding RNA species, long non-coding RNAs (lncRNAs) and microRNAs (miRs) that are involved in cardiac disease. The focus on RNA biology opens new avenues to improve our understanding of inter-cellular and inter-organic communication, increases our repertoire of available clinically useful biomarkers and innovative new medication for relevant human medical conditions.

The scientific results published in this thesis are particularly interesting for fellow researchers and pharmaceutical companies, since there is still a dire need for pharmaceutical treatment approaches. Here we identified miRs that are specifically involved in eccentric hypertrophy. The majority of current research on miRs in HF focuses on concentric hypertrophy and heart failure and it is still not clear what triggers the heart to activate pathways leading to eccentric remodeling. Further investigation of our described candidates can lead to identification of specific target molecules causing eccentric remodeling, and targeting these molecules could provide better-tailored therapy for patients. In this case our miRs would be used as tools to identify the mRNA targets that exert the effects.

Valorization of this kind of research can be the translation into patents, spin-off companies and licenses. When a therapeutic target is identified, the next step is to design a chemical or biological molecule that can target it. Efficacy, drug metabolism, pharmacokinetics and safety all have to be addressed in the pre-clinical phase. Drug metabolism and pharmacokinetics will be addressed further during clinical trial phases. Plenty of tests have to be completed before a therapeutic molecule can enter the clinical trial phases. For example, metabolism and clearance are tested by assessing stability in hepatocytes, human cytochrome P (CYP) isoforms involved and reactive intermediate formation. CYPs are the major enzymes involved in drug metabolism, accounting for about 75% of the total metabolism.[14] Regarding tissue distribution, exposure in efficacy in target tissue and major organs should be assessed, and plasma protein binding. To use our candidate miRs for therapeutic purposes, the hurdle that one miR can target dozens of mRNAs throughout the body has to be overcome. One way of circumventing targeting healthy organs is making the delivery of the miR modulator tissue-specific. Other important aspects to be addressed are human pharmacokinetics prediction and human dose prediction. Toxicology includes target assessment (physiological function, potential side effects, tissue distribution, cross-species comparison), genetic toxicity screening, and toleration studies.[***] All these and other issues have to be addressed before a drug can

proceed into phase I trials. It is evident that it still will take some time before those miRs are used as therapeutical targets in the clinic. This thesis aimed to provide a solid starting point for what miRs to pursue in the quest for molecular therapeutics for eccentric cardiac remodeling. Furthermore, we discussed the therapeutic potential of antisense oligonucleotides against miRs (Chapter 3) and briefly touched the subject of using lncRNAs as potential therapeutic targets (Chapter 7).

References

[*] World Health Organization, June 2014

[**] European Cardiovascular Disease Statistics 2012, June 2014

[***] **FDA Guidelines Guidance for Industry: Preclinical Assessment of Investigational Cellular and Gene Therapy Products, January 2016**

1 Hubert, H. B., Feinleib, M., McNamara, P. M. & Castelli, W. P. Obesity as an independent risk factor for cardiovascular disease: a 26-year follow-up of participants in the Framingham Heart Study. *Circulation* **67**, 968-977 (1983).

2 Hokanson, J. E. & Austin, M. A. Plasma triglyceride level is a risk factor for cardiovascular disease independent of high-density lipoprotein cholesterol level: a meta-analysis of population-based prospective studies. *Journal of cardiovascular risk* **3**, 213-219 (1996).

3 Powell, K. E., Thompson, P. D., Caspersen, C. J. & Kendrick, J. S. Physical activity and the incidence of coronary heart disease. *Annual review of public health* **8**, 253-287 (1987).

4 Tyroler, H. A. *et al.* Blood pressure and cholesterol as coronary heart disease risk factors. *Archives of internal medicine* **128**, 907-914 (1971).

5 Doyle, J. T., Dawber, T. R., Kannel, W. B., Heslin, A. S. & Kahn, H. A. Cigarette smoking and coronary heart disease. Combined experience of the Albany and Framingham studies. *The New England journal of medicine* **266**, 796-801 (1962).

6 Kannel, W. B., Gordon, T. & Schwartz, M. J. Systolic versus diastolic blood pressure and risk of coronary heart disease. The Framingham study. *The American journal of cardiology* **27**, 335-346 (1971).

7 Kannel, W. B. & McGee, D. L. Diabetes and glucose tolerance as risk factors for cardiovascular disease: the Framingham study. *Diabetes care* **2**, 120-126 (1979).

8 Alpert, M. A. Obesity cardiomyopathy: pathophysiology and evolution of the clinical syndrome. *The American journal of the medical sciences* **321**, 225-236 (2001).

9 Wong, C. Y. *et al.* Alterations of left ventricular myocardial characteristics associated with obesity. *Circulation* **110**, 3081-3087 (2004).

10 Messerli, F. H. *et al.* Dimorphic cardiac adaptation to obesity and arterial hypertension. *Annals of internal medicine* **99**, 757-761 (1983).

11 de Simone, G., Devereux, R. B., Roman, M. J., Alderman, M. H. & Laragh, J. H. Relation of obesity and gender to left ventricular hypertrophy in normotensive and hypertensive adults. *Hypertension* **23**, 600-606 (1994).

12 Peterson, L. R. *et al.* Alterations in left ventricular structure and function in young healthy obese women: assessment by echocardiography and tissue Doppler imaging. *Journal of the American College of Cardiology* **43**, 1399-1404 (2004).

13 Avelar, E. *et al.* Left ventricular hypertrophy in severe obesity: interactions among blood pressure, nocturnal hypoxemia, and body mass. *Hypertension* **49**, 34-39 (2007).

14 Guengerich, F. P. Cytochrome p450 and chemical toxicology. *Chem Res Toxicol* **21**, 70-83 (2008).

Acknowledgements
Curriculum Vitae
List of Publications

Acknowledgements

When I started my PhD back in Sept 2009, my mother had just passed away a few months before. As everyone can imagine, this is not the best way to start such a challenge as a PhD program. But, here I am, about to get my Dr. degree. And let me start with thanking you, Nelleke, for making me the person I am today. I still miss you every day, but although you're no longer among us, I know you are always with me.

As with all great accomplishments in life, they are rarely achieved on your own. Therefore I would like to thank everyone who has helped me over the past years to get me where I am today, even when I forget to include you in this section.

Leon, what started with a random question after a class you taught during my master's in 2008 has led to a great experience during the past years. I always admired your enthusiasm for science and your ability to come up with new and better experiments and pathways to investigate. I have learned many things from you. I'm very grateful for the support, guidance and advice during these years.

Paula, thank you for all your help and support. Working with you was a great experience. But it was not all work… Las Vegas was awesome. Even without the Chippendales.

Ellen, first a dear friend and later you became my co-promotor. You are the best mentor I could have wished for. You've always been a great support and I learned many, many things from you. Whenever I felt like everything was going not exactly as planned, your pep talks convinced me to keep going until I succeeded. I still enjoy our Skype conversations very much while being on the other end of the pond. Never a dull moment with you ☺

I also want to thank the assessment committee, Prof. M. Vooijs, Prof. J. de Boer, Prof. E. Biessen, Prof. T. Thum, and Prof. X. Wehrens for taking time to read and comment on my work. Xander, thank you for your guidance and support to improve my skills and become a more independent researcher in your lab.

Ella and Burcu, thank you for being great colleagues and wonderful friends. I'm glad I got to know you better during my last years and I enjoyed all the non-science related events we went to! Burcu, I enjoyed all the conferences we went to

together and obviously the partying until early morning. Memories of Lisbon are still very vivid. Ella, thank you for staying in touch and keeping me updated on life in the clinic once in a while!

Stephanos, dude, thanks for being an awesome roommate! Thank you for teaching me some of Greece's finest expressions that made your fellow Greeks frown upon. I hope you are doing well.

Virginie and Julie, my French-speaking roommates, it was a pleasure to work with you and I hope you are doing very well in your new jobs and personal life.

Servé, Nicole and Barbara, thank you for your technical and administrative support! Hamid, Monika, Gustavo, Antonio, Rio, and all other current and former De Windt lab members, thank you for your support and making my life as a PhD student easier and more fun.

Wouter, Rick and Kevin, thank you for always borrowing me stuff whenever we ran out again and helping me out every time I needed it. You made life in the lab way more fun!! It was great having you around!

All the great people in the cardiology department in Maastricht, especially Roel, Sandrine, and all the people I forgot thank you all for your help and great time that I had. Also, Nynke, Mick and Daniel from Physiology, thank you for helping me!

My external collaborator Natalia, thank you so much for your help and being a wonderful person. I still plan on visiting you in Pamplona some day!

Kelly, Esther, Valerie, Carola, John, Kevin, Robin, Lot, Agnes: you guys are awesome!! I'm also very grateful to all my other friends in Europe and the USA for being there and allowing me to have some precious downtime when needed. It is very much appreciated! Thank you for believing in me. I wouldn't be where I am today without you. Thank you!!

To my family in the Netherlands and the USA: thank you so much for being there for me and making this journey not as difficult as it could have been. Lei, Ruben and Stephanie, you experienced my journey from up close. Thank you for your support! Catherine, it is a blessing to have you in my life. Thank you for all your support and advice! Marijn, you showed up just in time to see the end result, thank you for being my biggest fan and always believing in me.

Curriculum Vitae

Leonne Elisabeth Philippen was born on January 17, 1986 in Valkenburg aan de Geul, The Netherlands. She attended Scholengemeenschap Sophianum in Gulpen and graduated in 2004. The same year she started her study Biomedical Sciences at Utrecht University. In 2009 she received her Master degree in Biomedical Sciences (Biology of Disease) from Utrecht University with a GPA 4.00/4.00. Her specializations were Cardiovascular Biology and Immunology. She did internships at Pathology (UMC Utrecht) and Medical Microbiology (AZM). During her Master studies she realized that cardiovascular research is where her heart belongs and her Master Thesis was written under the supervision of Dr. Leon de Windt. Right after receiving her Master diploma with *Cum Laude* honors August 2009, she started to work as a PhD student in the lab of Dr. Leon de Windt in September 2009. The results of her projects are described in this thesis. During her PhD she was invited to give several presentations during national and international conferences and in 2013 she was a finalist for the Young Investigator Award during the European Society of Cardiology Basic Science Summer School in Sophia- Antipolis, France. In Nov 2014 she started as a postdoctoral associate in Xander Wehrens' lab in Baylor College of Medicine, located in Houston Texas.

List of Publications

1. **Leonne E. Philippen**, Ellen Dirkx, Natalia López-Andrés, Nicole Bitsch, Mauro Giacca, Paula A. da Costa-Martins, Leon J. de Windt. MiR-148a directly regulates gp130-coupled signaling during dilated cardiomyopathy. In revision at EMBO Mol Med
2. **Leonne E. Philippen**, Ellen Dirkx, Nicole Bitsch, Miguel Mano, Mauro Giacca, Leon J. de Windt. Phenotypic screening to identify EccentriMIRS: microRNAs involved in eccentric cardiomyocyte hypertrophy. Manuscript in preparation
3. Virginie Kinet, Frank Rühle, Ellen Dirkx, **Leonne E. Philippen**, Giuliano G. Stirparo, Julie Halkein, Paula A. da Costa Martins, Monika Stoll, Gianluigi Condorelli, Leon J. de Windt. Long non-coding RNA species are differentially expressed and functionally implicated in cardiac hypertrophy. Submitted
4. Ann P. Quick, Qiongling Wang, **Leonne E Philippen**, David Y. Chiang, David Beavers, Guoliang Wang, Maha Khalid Julia O Reynolds, Jordan Showell, Mark D. McCauley, Arjen Scholten, Xander H. T. Wehrens. 'Striated Muscle Preferentially Expressed Protein Kinase' (SPEG) is Essential for Cardiac Function by Regulating Junctional Membrane Complex Activity. In revision at Circ Res
5. M d'Avenia M, R Citro, M De Marco, A Veronese, A Rosati, R Visone, S Leptidis, **L Philippen**, G Vitale, A Cavello, A Silverio, C Prota, P Gravina, A De Cola, E Carletti, G Coppola, S Gallo, G Provenza, E Bossone, F Piscione, M Hahne, LJ De Windt, MC Turco, V De Laurenzi. A novel miR-371a-5p-mediated pathway, leading to BAG3 upregulation in cardiomyocytes in response to epinephrine, is lost in Takotsubo cardiomyopathy. Cell Death and Disease (2015) 6, e1948;doi:10.1038/cddis.2015.280
6. **Leonne E. Philippen**, Ellen Dirkx, Jan B. M. Wit, J. Burggraaf, Leon J. De Windt, and Paula A. da Costa Martins. Antisense MicroRNA Therapeutics in Cardiovascular Disease: Quo Vadis? Molecular Therapy, 2015 (23) 12,1810-1818
7. **Leonne E. Philippen**, Ellen Dirkx, Paula A. da Costa Martins, and Leon J. De Windt. Non-coding RNA in control of gene regulatory programs in cardiac development and disease. Journal of Molecular and Cellular Cardiology, 89 (2015) 51–58
8. Ellen Dirkx*, Monika M. Gladka*, **Leonne E. Philippen**, Anne-Sophie Armand, Virginie Kinet, Stefanos Leptidis, Hamid el Azzouzi, Meriem

Bourajjaj, Servé Olieslagers, Roel van der Nagel, Roel de Weger, Nicole Bitsch, Natasja Kisters, Sandrine Seyen, Christophe Chanoine, Stephane Heymans, Paul G. Volders, Thomas Thum, Stefanie Dimmeler, Peter Cserjesi, Thomas Eschenhagen, Paula A. da Costa Martins, and Leon J. De Windt. NFAT and miR-25 cooperate to reactivate the transcription factor Hand2 in heart failure. Nature Cell Biology, 2013 Nov;15(11): 1282-93 *(*ED and MG contributed equally to this work)*

9. Robert van Domselaar, **Leonne E. Philippen**, Razi Quadir, Emmanuel J. H. J. Wiertz, J. Alain Kummer, and Niels Bovenschen. Noncytotoxic inhibition of cytomegalovirus replication through NK cell protease granzyme M-mediated cleavage of viral phosphoprotein 71. The Journal of Immunology, 2010, 185: 7605-7613.